



Using HYDRA2 to study new satellite data



Paul Menzel
University of Wisconsin-Madison
Space Science and Engineering Center (SSEC)

November 2015

HYperspectral viewer for Development of Research Applications – HYDRA2

Freely available gui-driven software

For researchers and educators

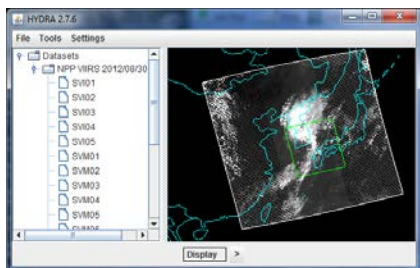
Computer platform independent

Extendable to more sensors and applications

Uses Java-based technologies

Interactive, high-performance 2D/3D animations
derived from SSEC VisAD api

On-going development effort



MODIS, AIRS,
IASI, VIIRS,
CrIS, ATMS

Developed at CIMSS by
Tom Rink

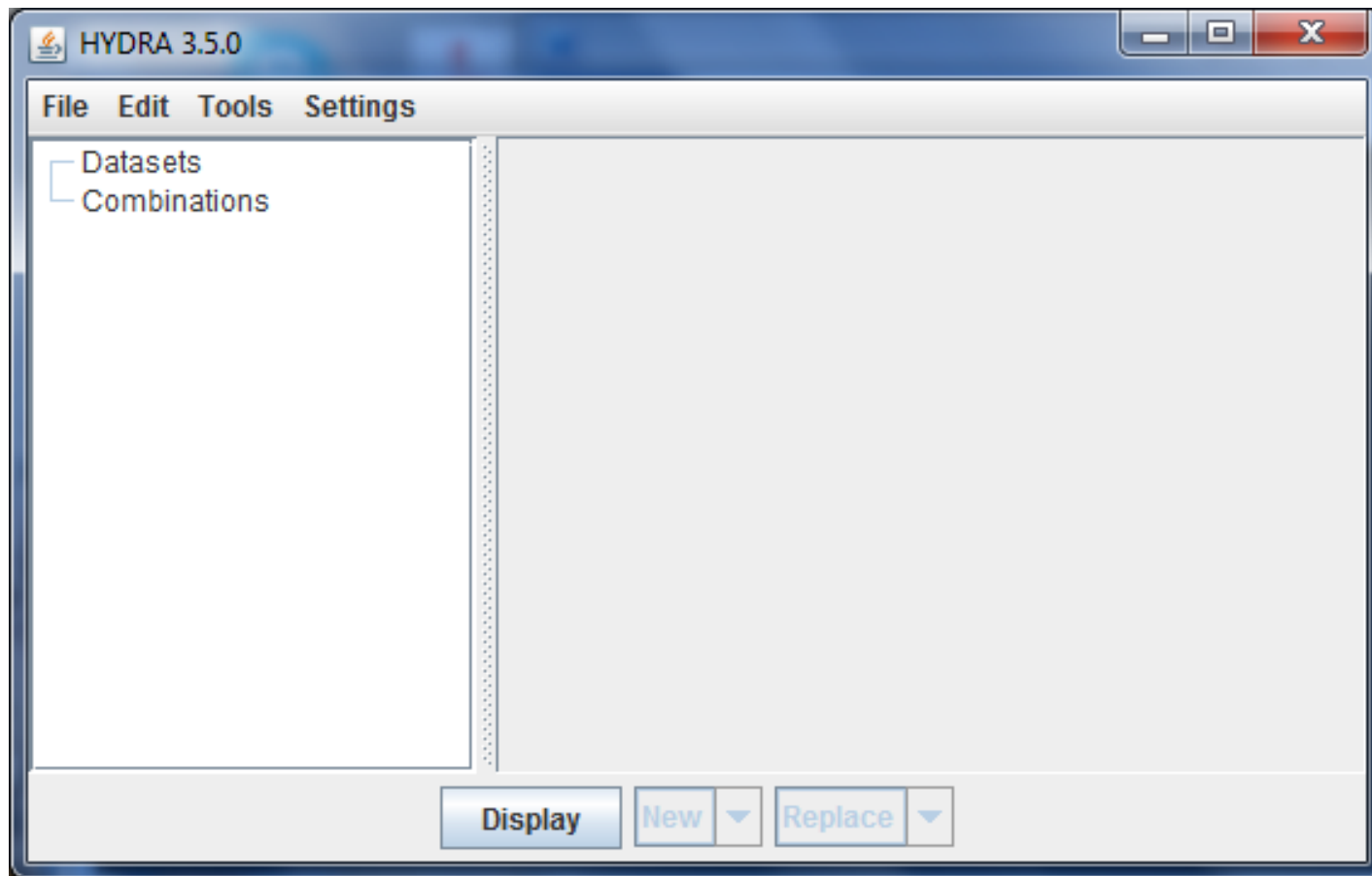
With programming
support from
Tommy Jasmin,
Ghansham Sangar
(ISRO)

With guidance from
Liam Gumley
Kathy Strabala
Paul Menzel



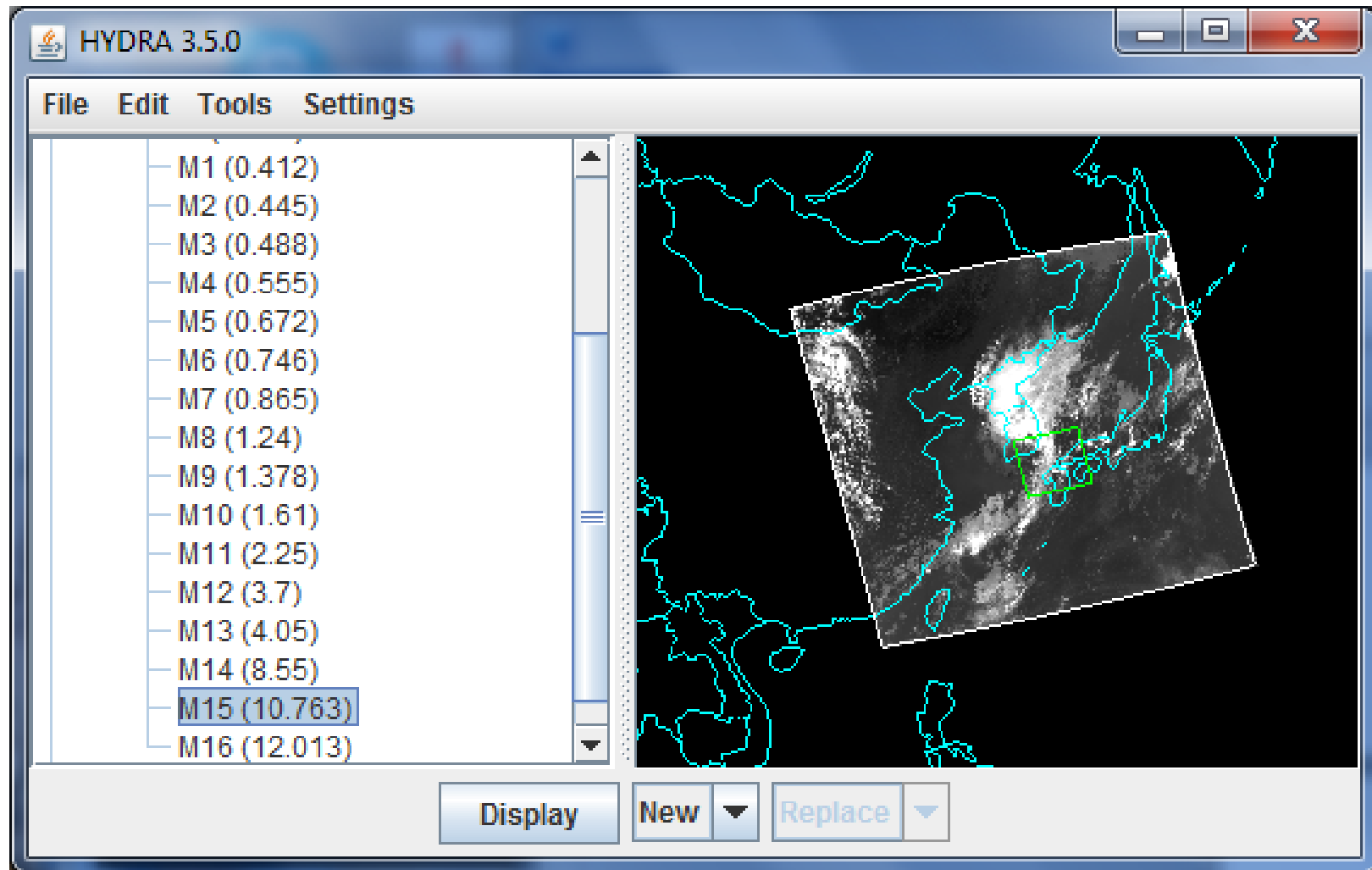
<ftp://ftp.ssec.wisc.edu/rink/HYDRA2>

Opening HYDRA2



The installers for this release can be found at <ftp://ftp.ssec.wisc.edu/rink/HYDRA2>

Selecting a File



VIIRS Examples

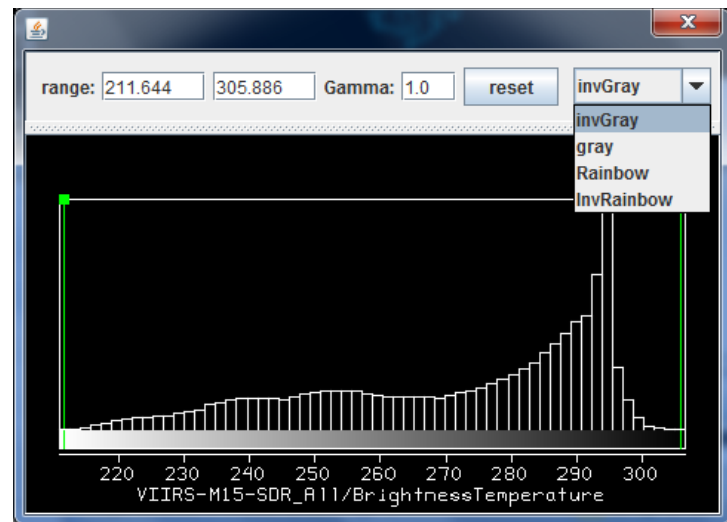
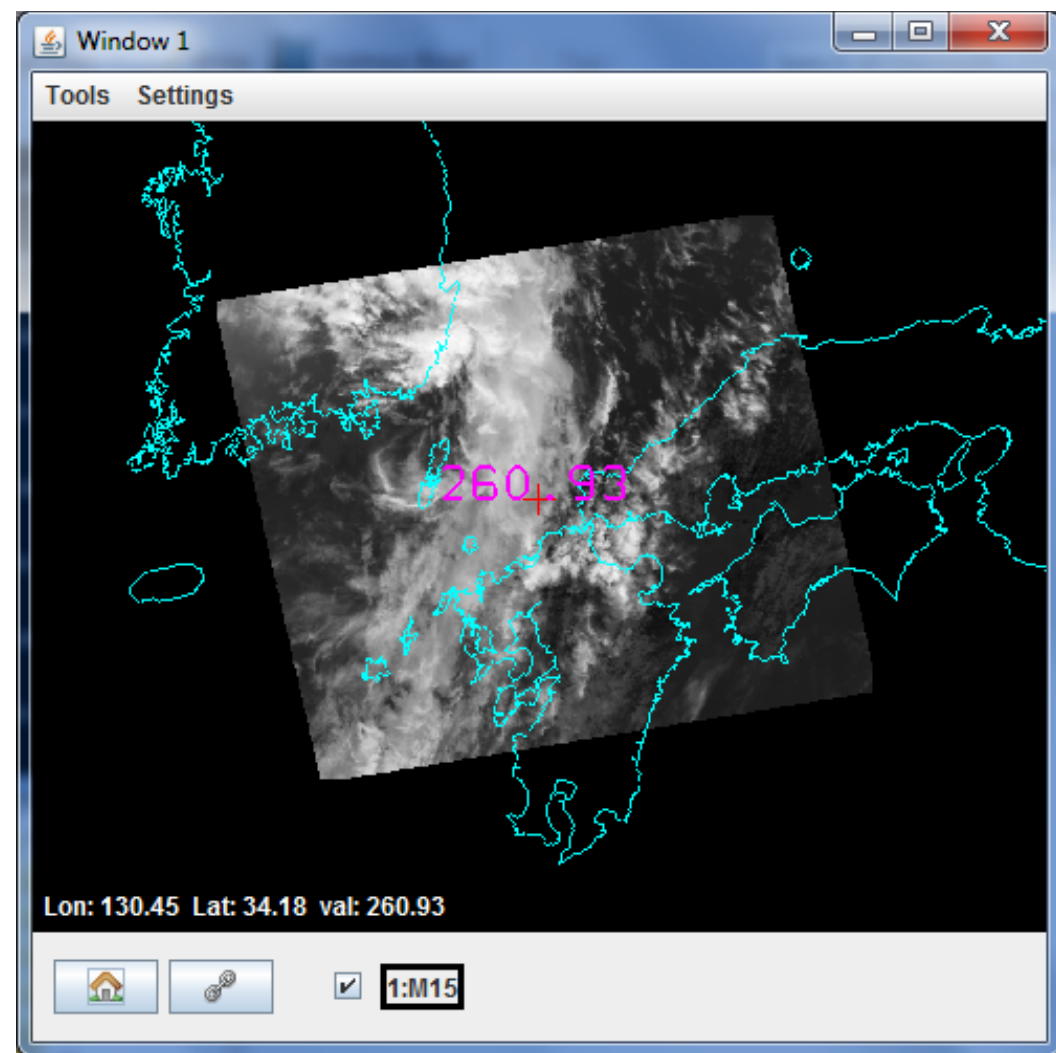
VIIRS bands and bandwidths

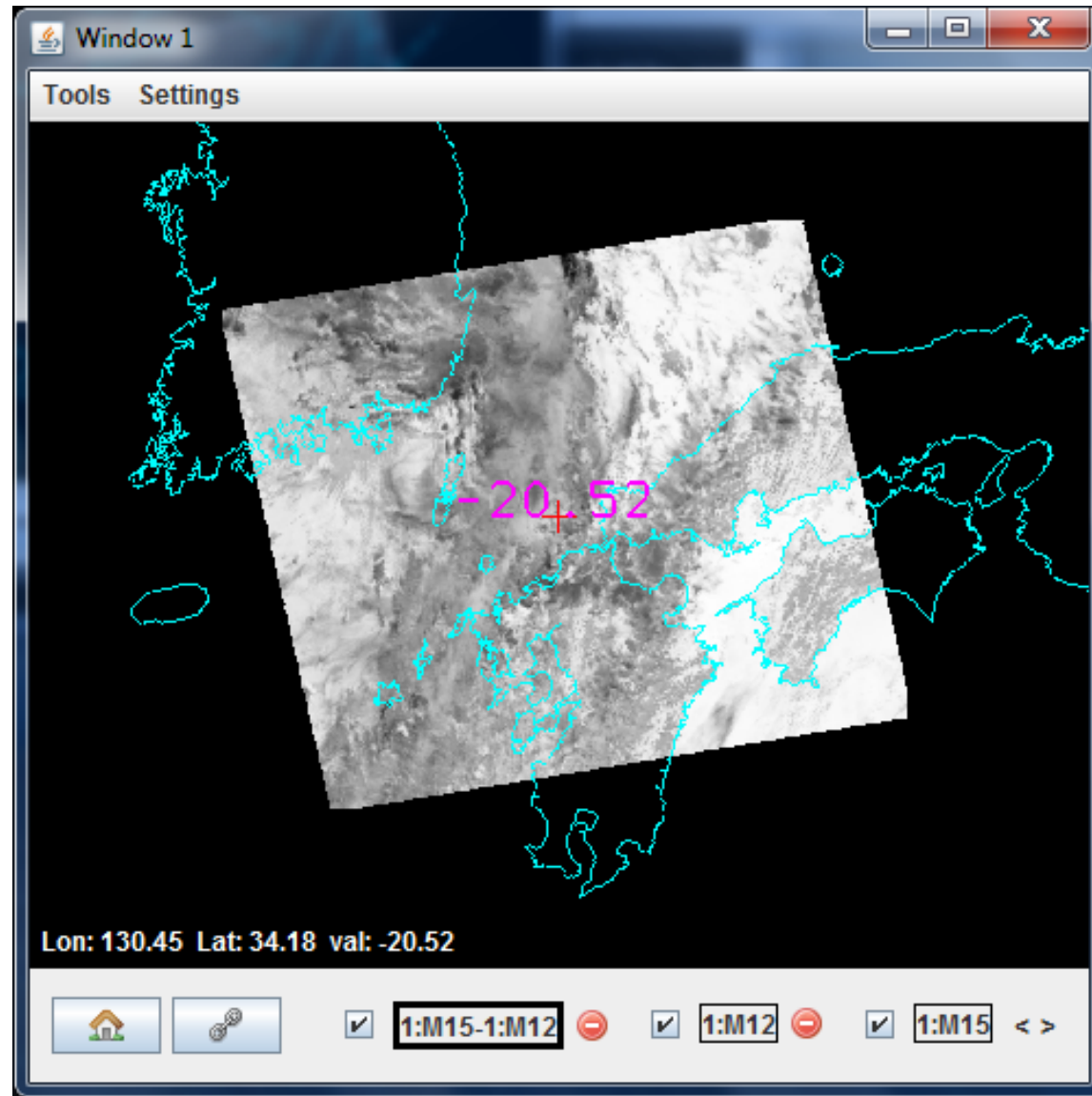
VIIRS Band	Central Wavelength (μm)	Bandwidth (μm)	Wavelength Range (μm)	Band Explanation	Spatial Resolution (m) @ nadir
M1	0.412	0.02	0.402 - 0.422	Visible/ Reflective	750 m
M2	0.445	0.018	0.436 - 0.454		
M3	0.488	0.02	0.478 - 0.488		
M4	0.555	0.02	0.545 - 0.565		
M5 (B)	0.672	0.02	0.662 - 0.682	Near IR	750 m
M6	0.746	0.015	0.739 - 0.754		
M7 (G)	0.865	0.039	0.846 - 0.885		
M8	1.240	0.020	1.23 - 1.25	Shortwave IR	750 m
M9	1.378	0.015	1.371 - 1.386		
M10 (R)	1.61	0.06	1.58 - 1.64		
M11	2.25	0.05	2.23 - 2.28	Medium-wave IR	750 m
M12	3.7	0.18	3.61 - 3.79		
M13	4.05	0.155	3.97 - 4.13		
M14	8.55	0.3	8.4 - 8.7	Longwave IR	750 m across full scan
M15	10.763	1.0	10.26 - 11.26		
M16	12.013	0.95	11.54 - 12.49		
DNB	0.7	0.4	0.5 - 0.9	Visible/ Reflective	750 m across full scan
I1 (B)	0.64	0.08	0.6 - 0.68	Visible/ Reflective	375 m
I2 (G)	0.865	0.039	0.85 - 0.88	Near IR	
I3 (R)	1.61	0.06	1.58 - 1.64	Shortwave IR	
I4	3.74	0.38	3.55 - 3.93	Medium-wave IR	
I5	11.45	1.9	10.5 - 12.4	Longwave IR	

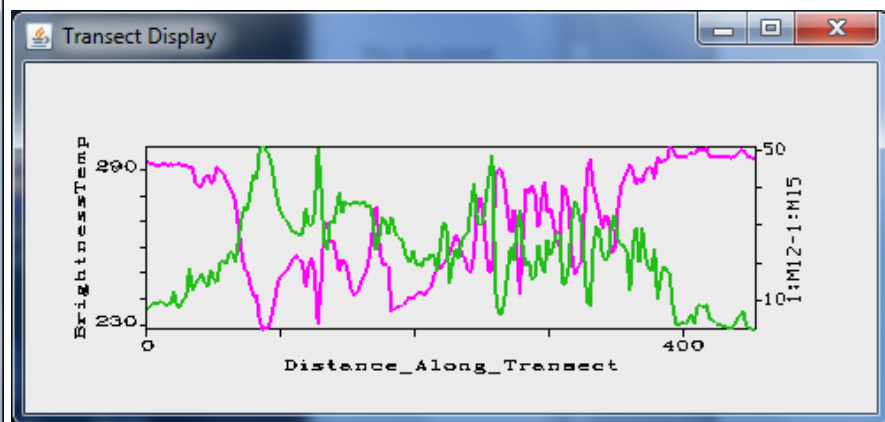
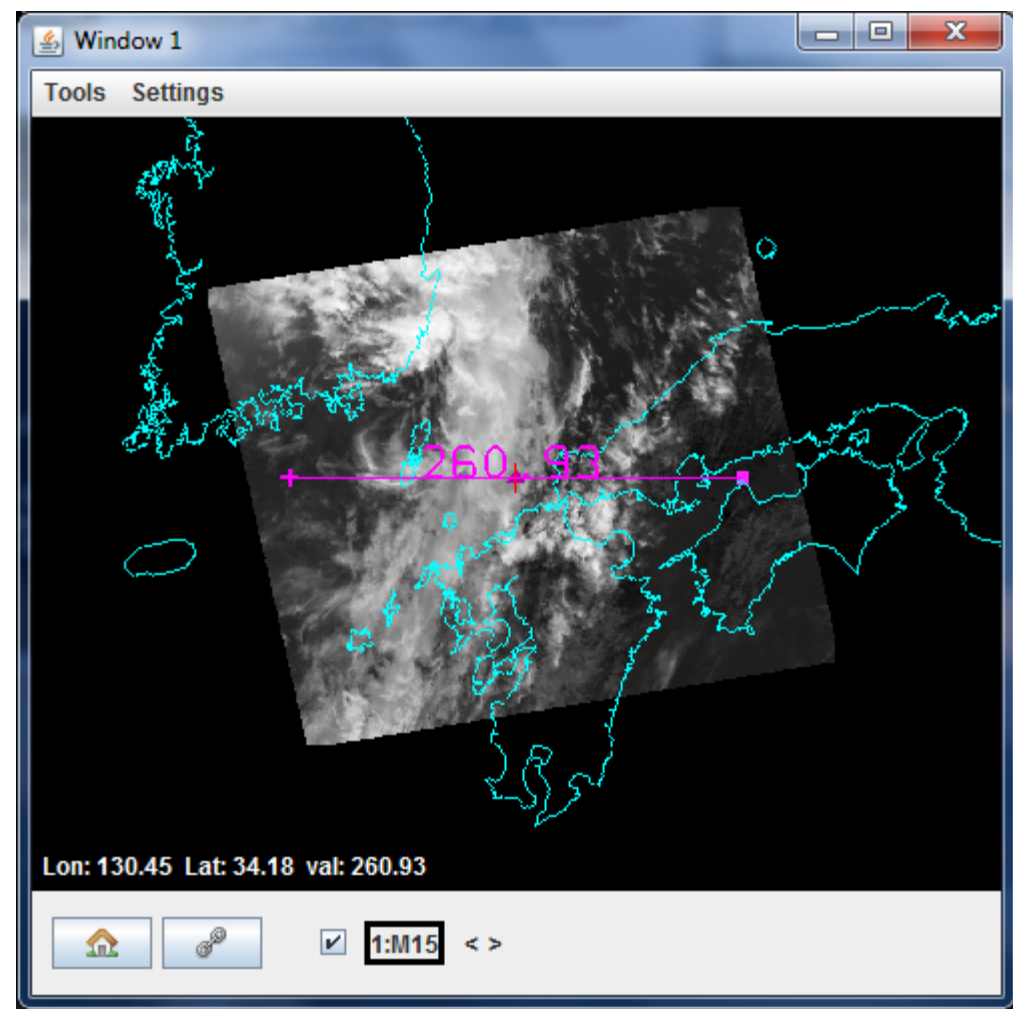
M = Moderate (750 m) resolution bands

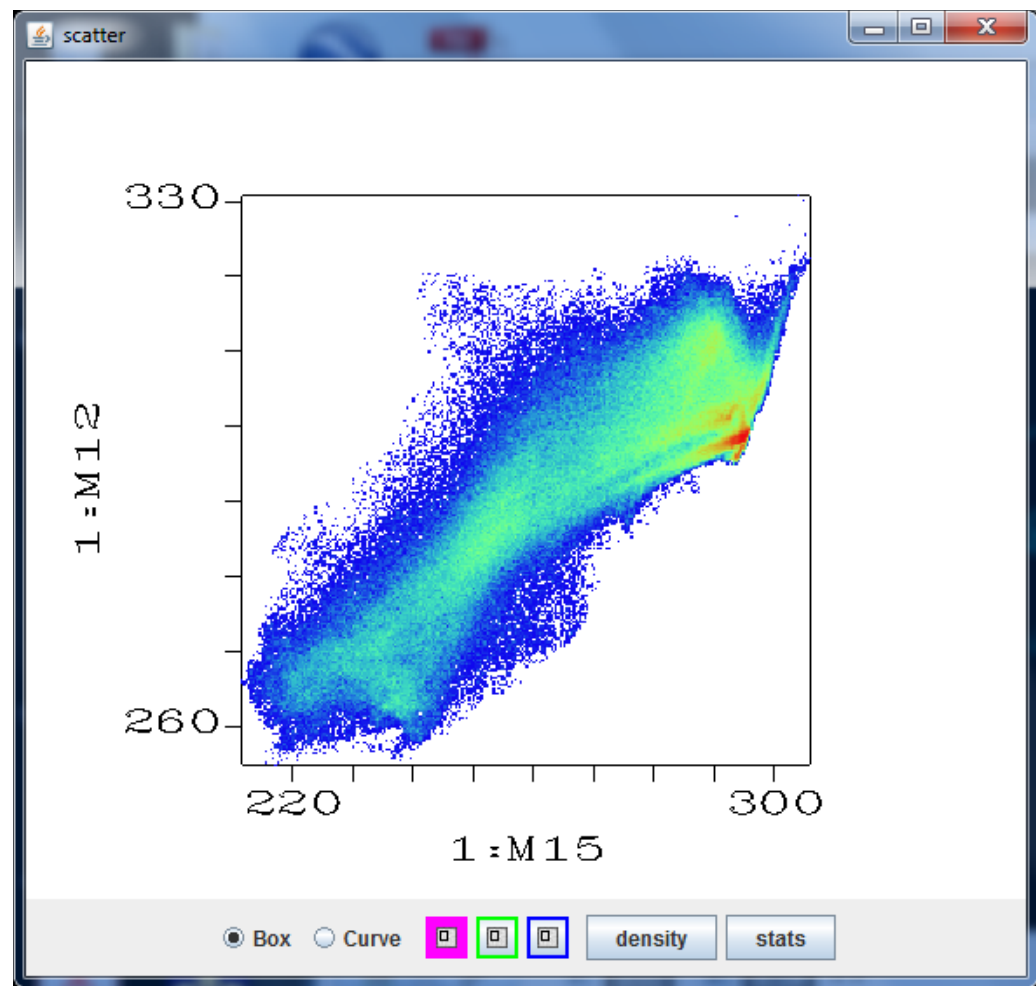
I = Imagery (375 m) resolution bands

DNB = Day-Night Band (or Near Constant Contrast (NCC) band)



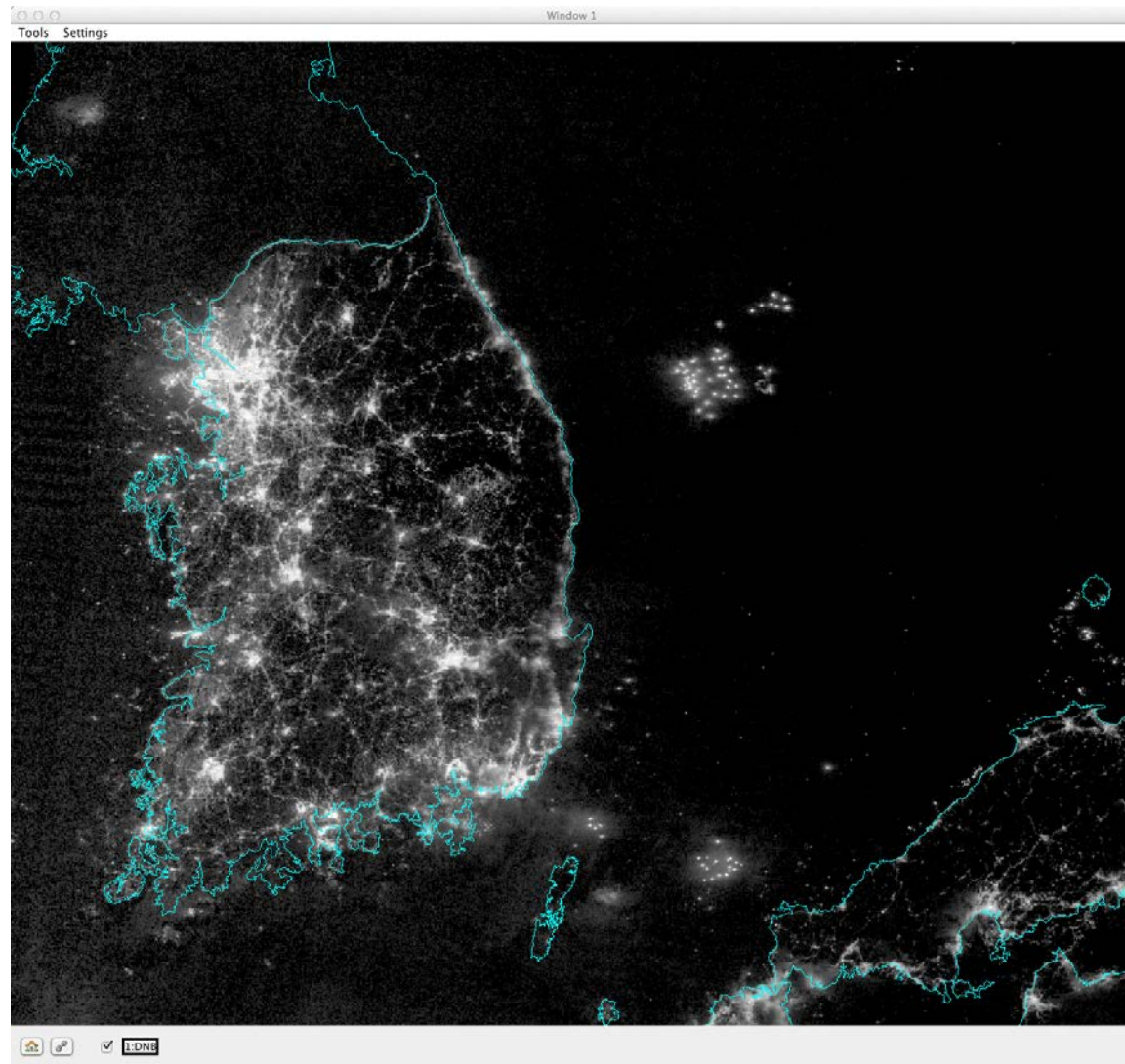


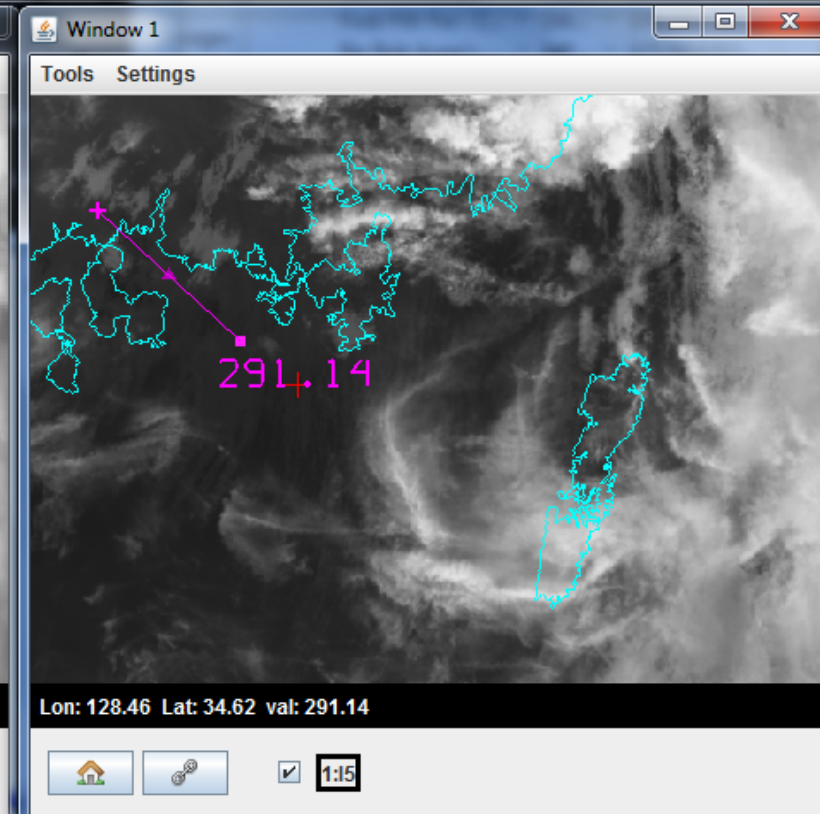
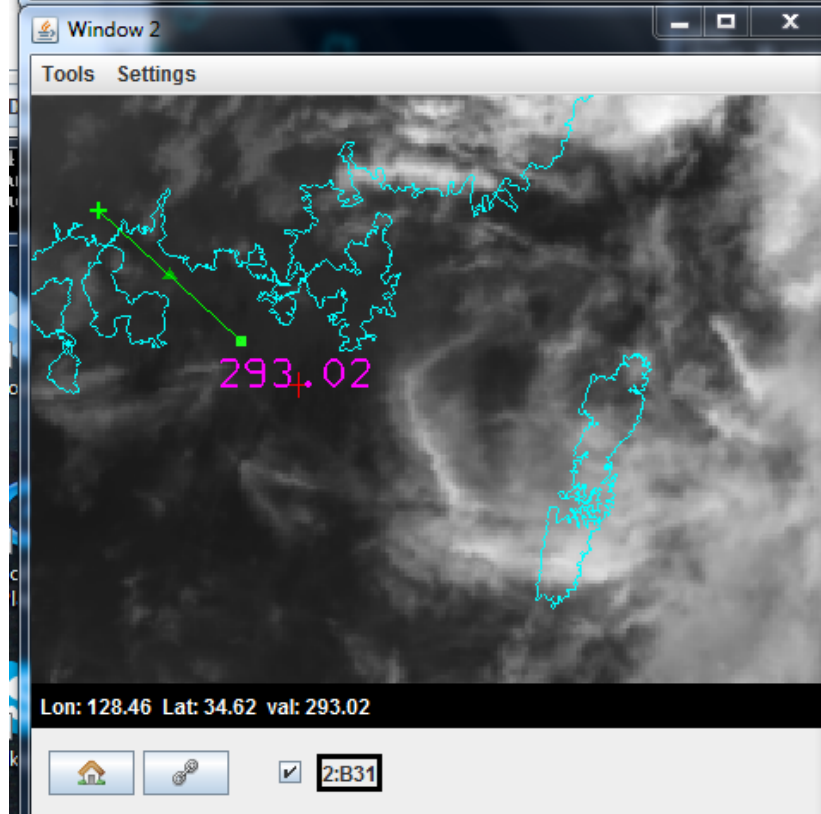
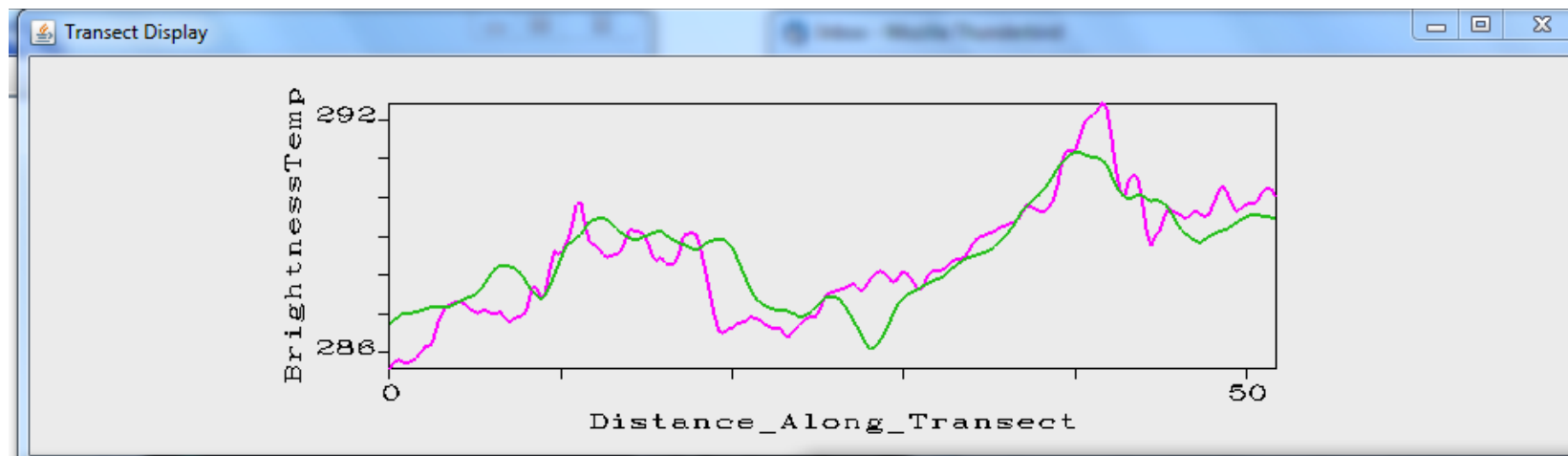


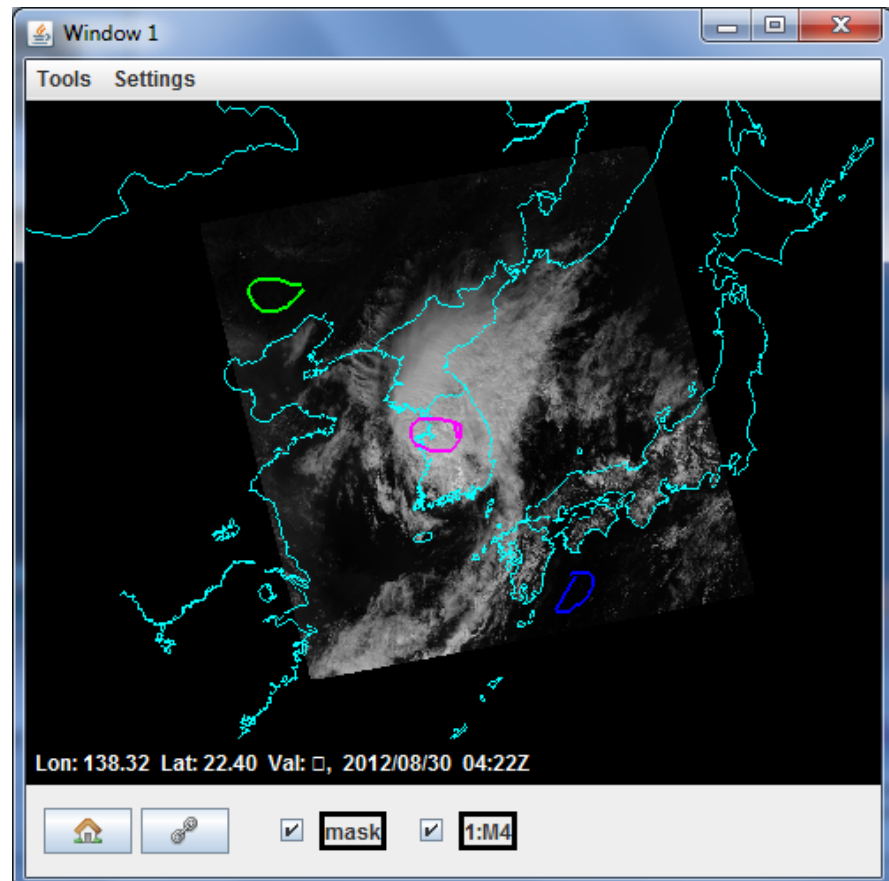
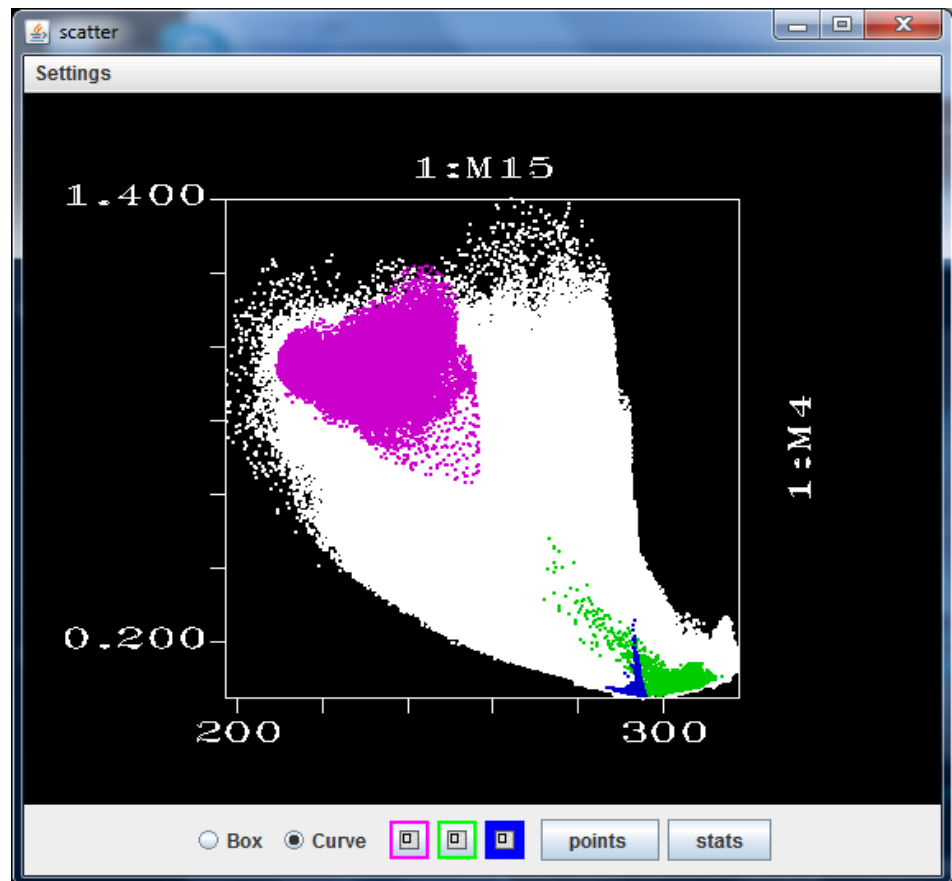


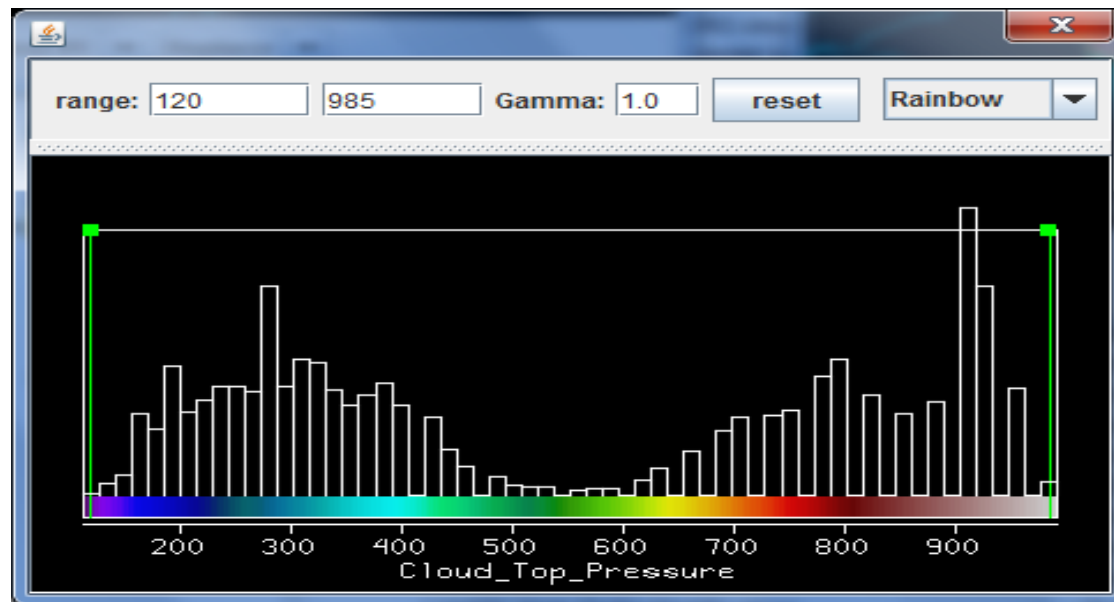
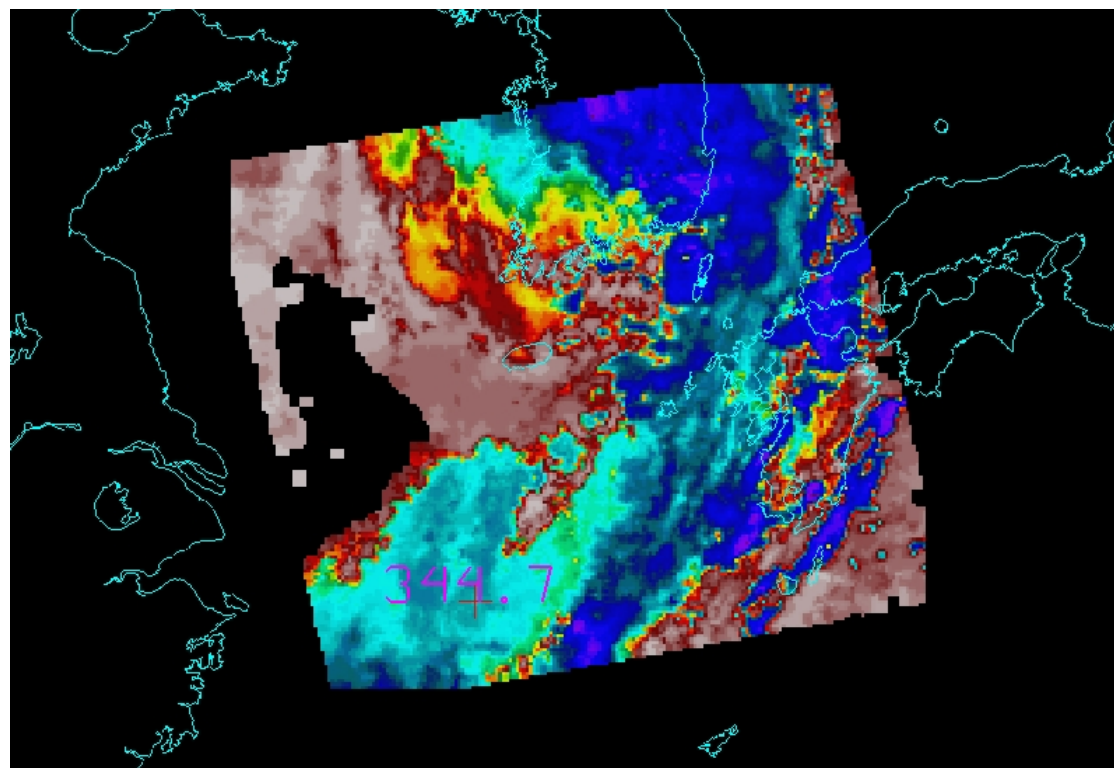
Scatter Statistics

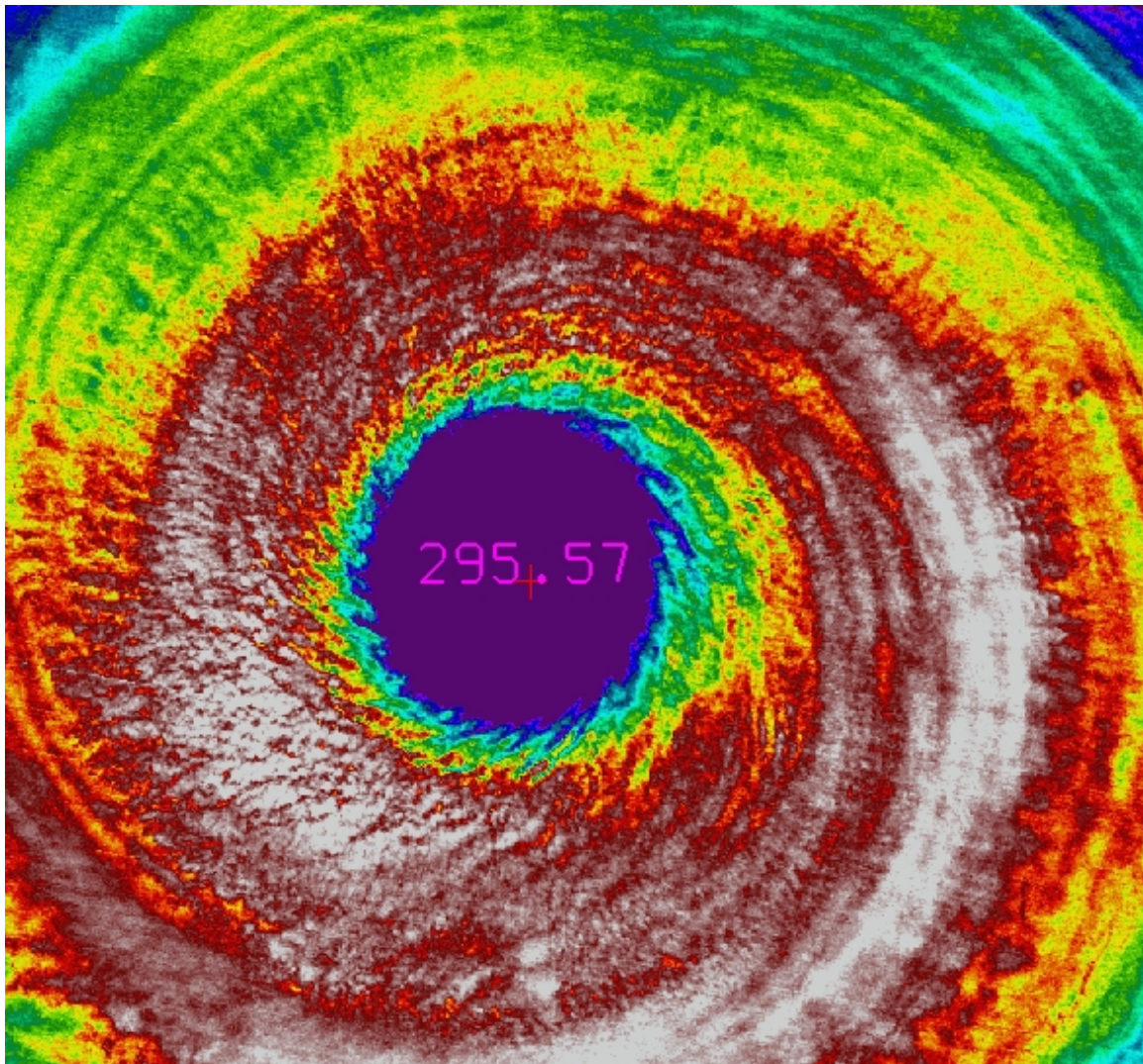
Stats Parameter	NPP VIIRS 1:M15 2012/08/30 04:22Z	NPP VIIRS 1:M12 2012/08/30 04:22Z
Maximum	305.89	330.77
Minimum	211.64	254.83
Number of points	592620	592620
Mean	272.28	294.40
Median	279.88	298.07
Variance	475.31	173.39
Kurtosis	-0.71587	-0.06323
Std Dev	21.80	13.17
Correlation	0.84746	
Difference Maximum	-1.427	
Difference Minimum	-78.91	
Difference Mean	-22.11	
Area [km ²]		

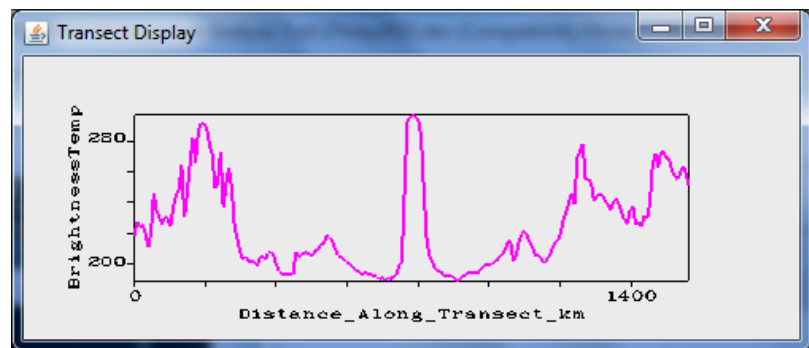
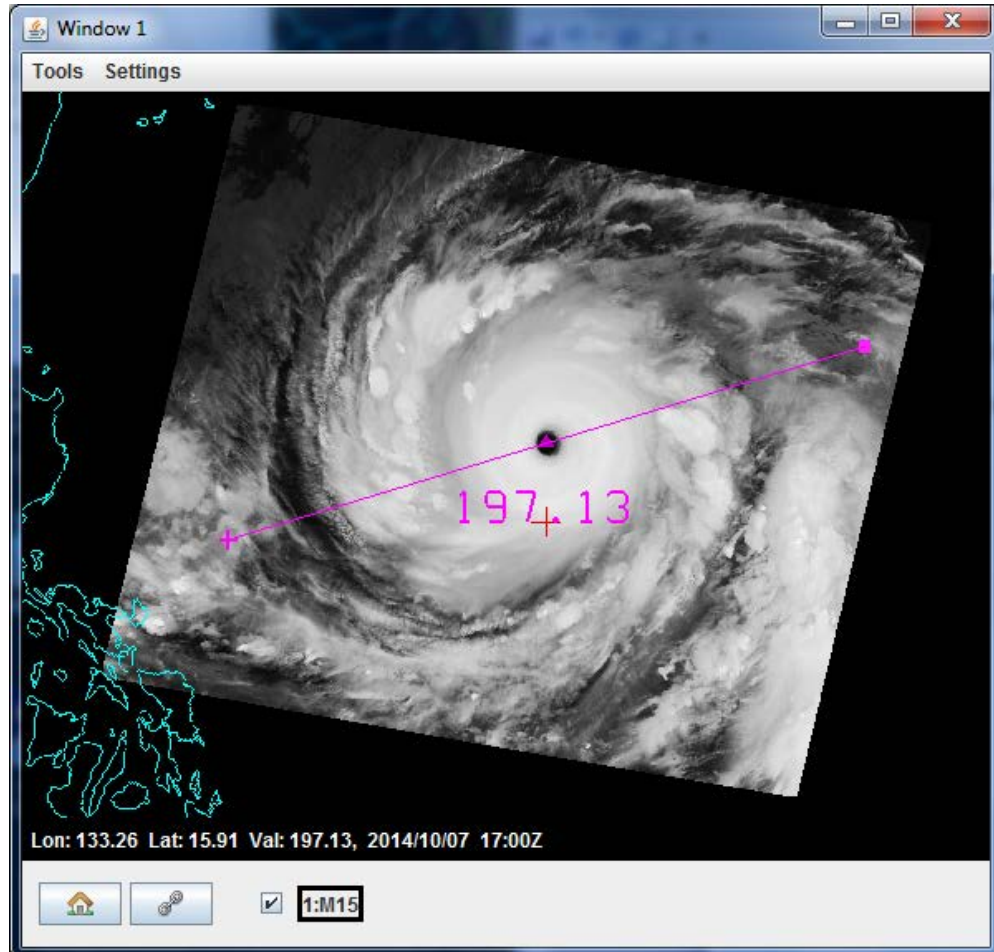


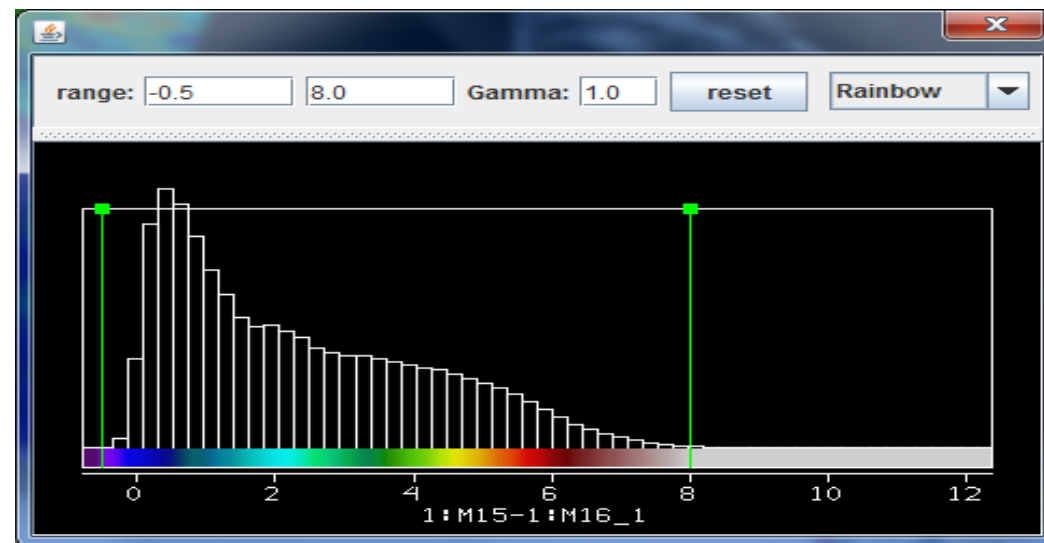
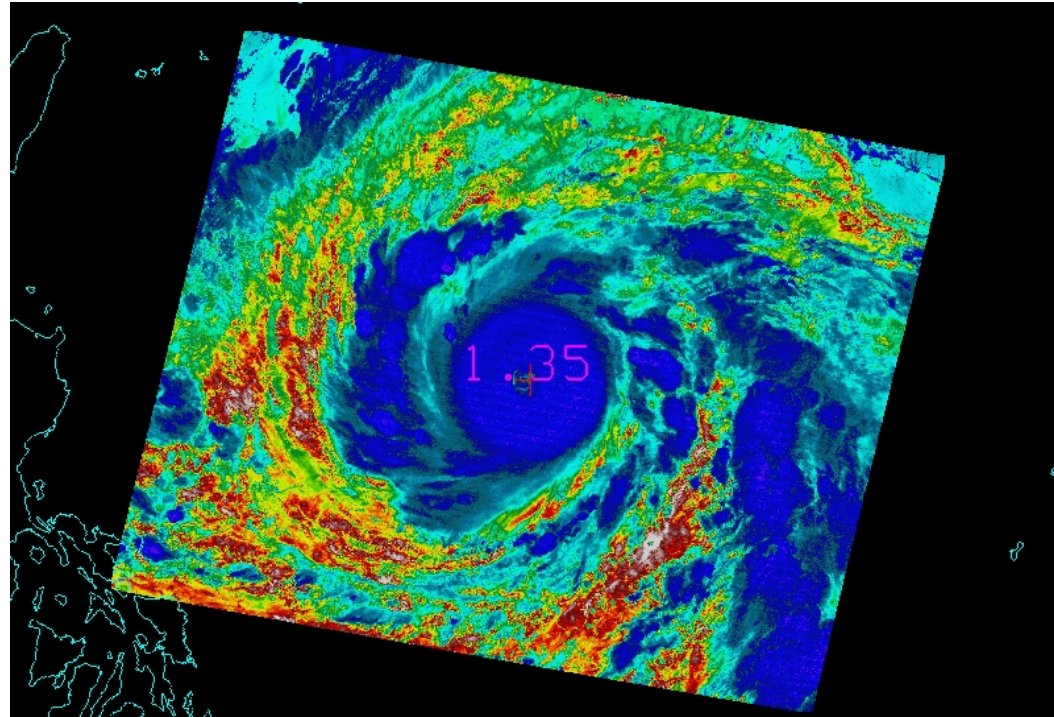






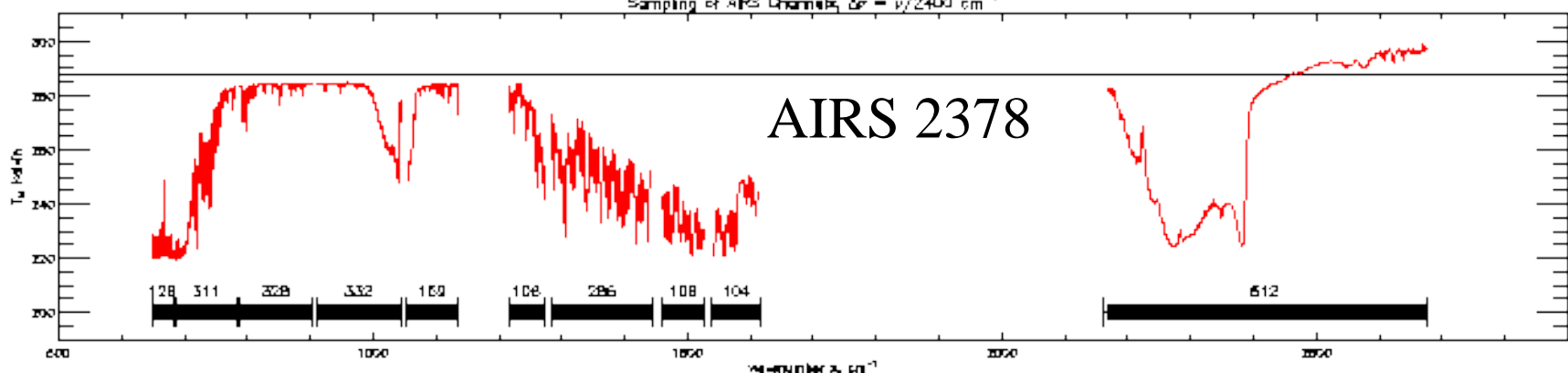




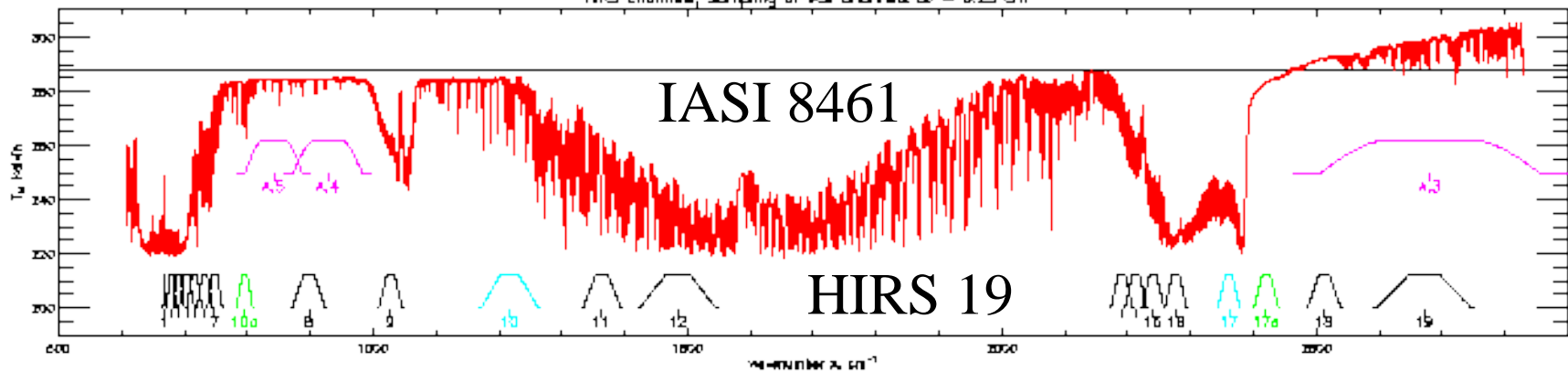


Adding CrIS and ATMS

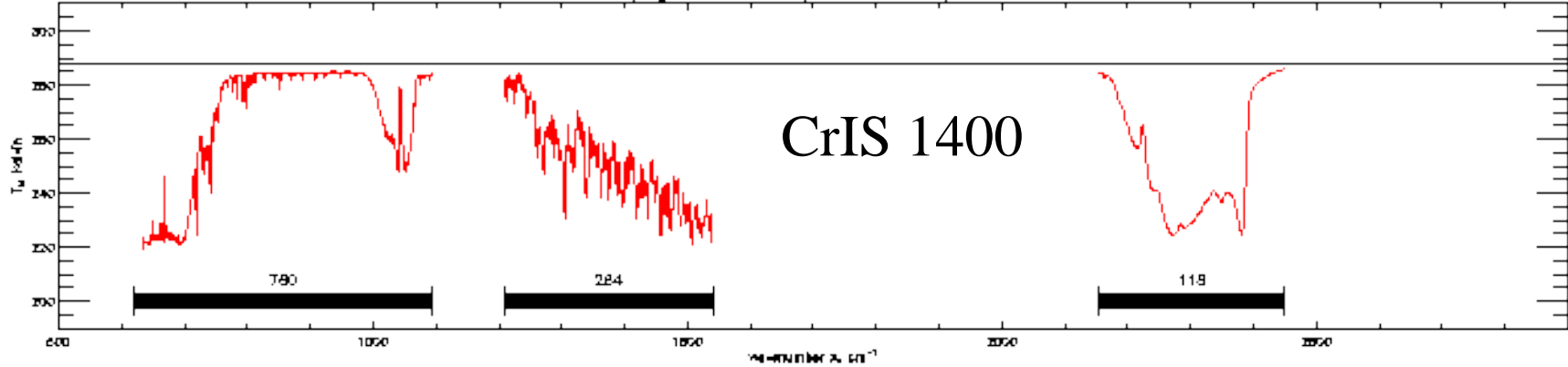
Sampling of AIRS Channels, $\Delta\nu = \nu/2400 \text{ cm}^{-1}$

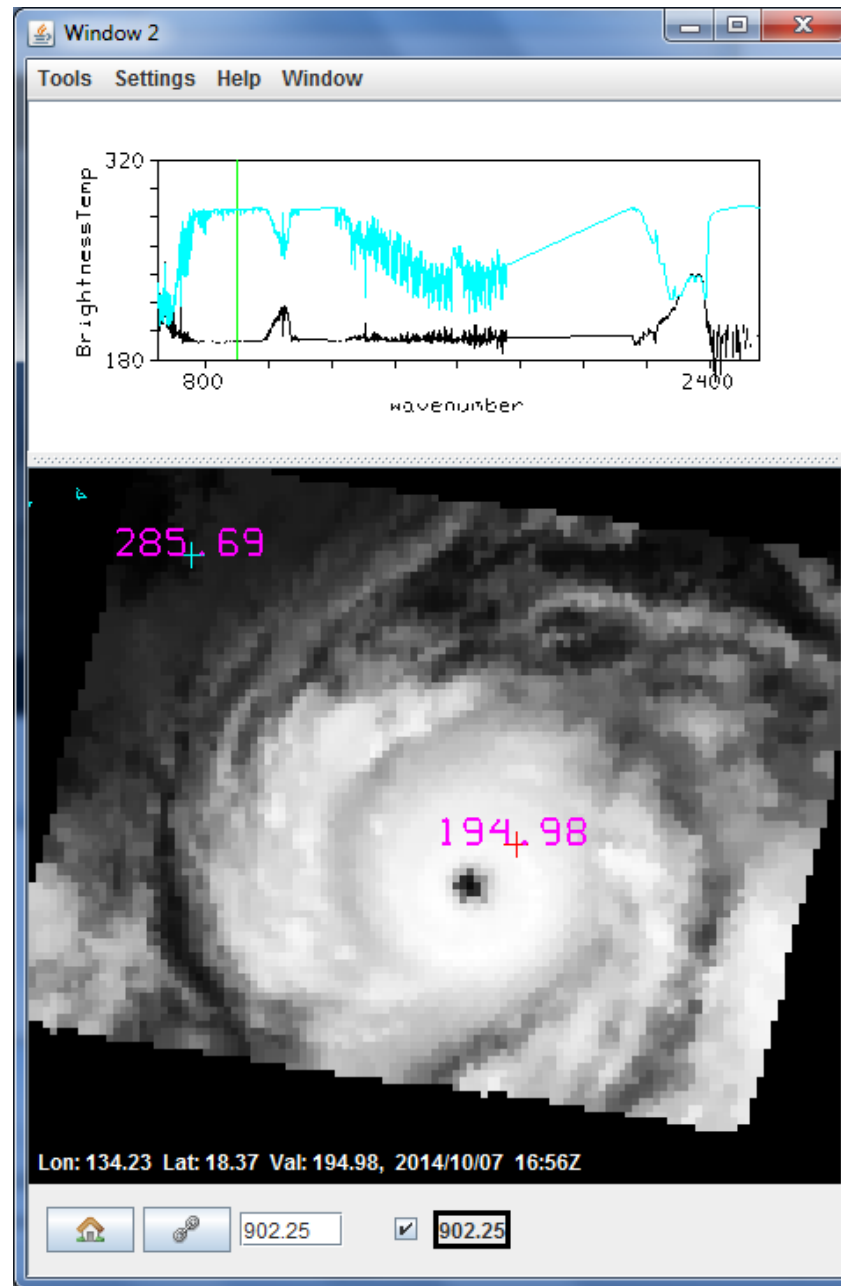


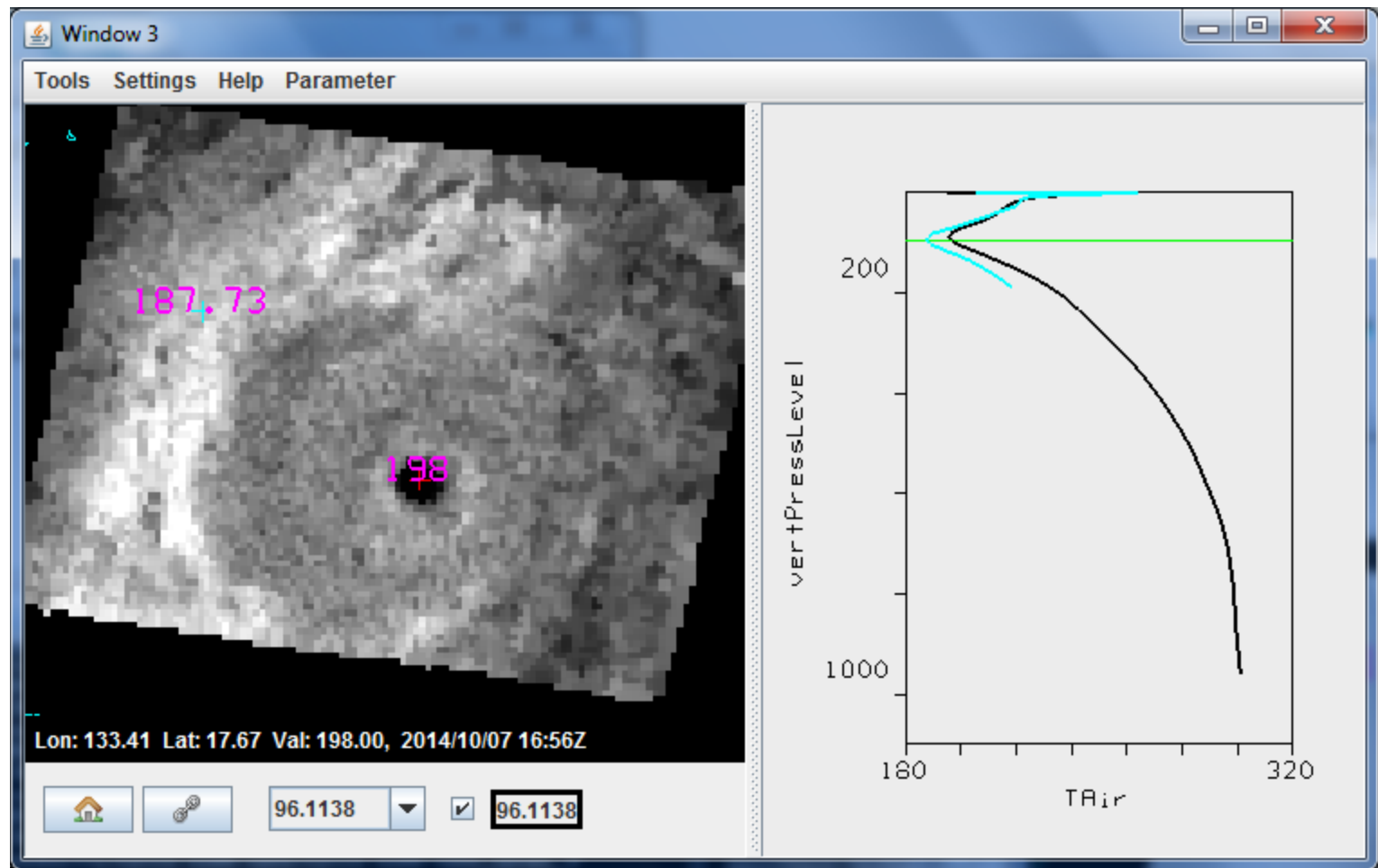
HIRS Channels, Sampling of IASI Channels, $\Delta\nu = 0.25 \text{ cm}^{-1}$

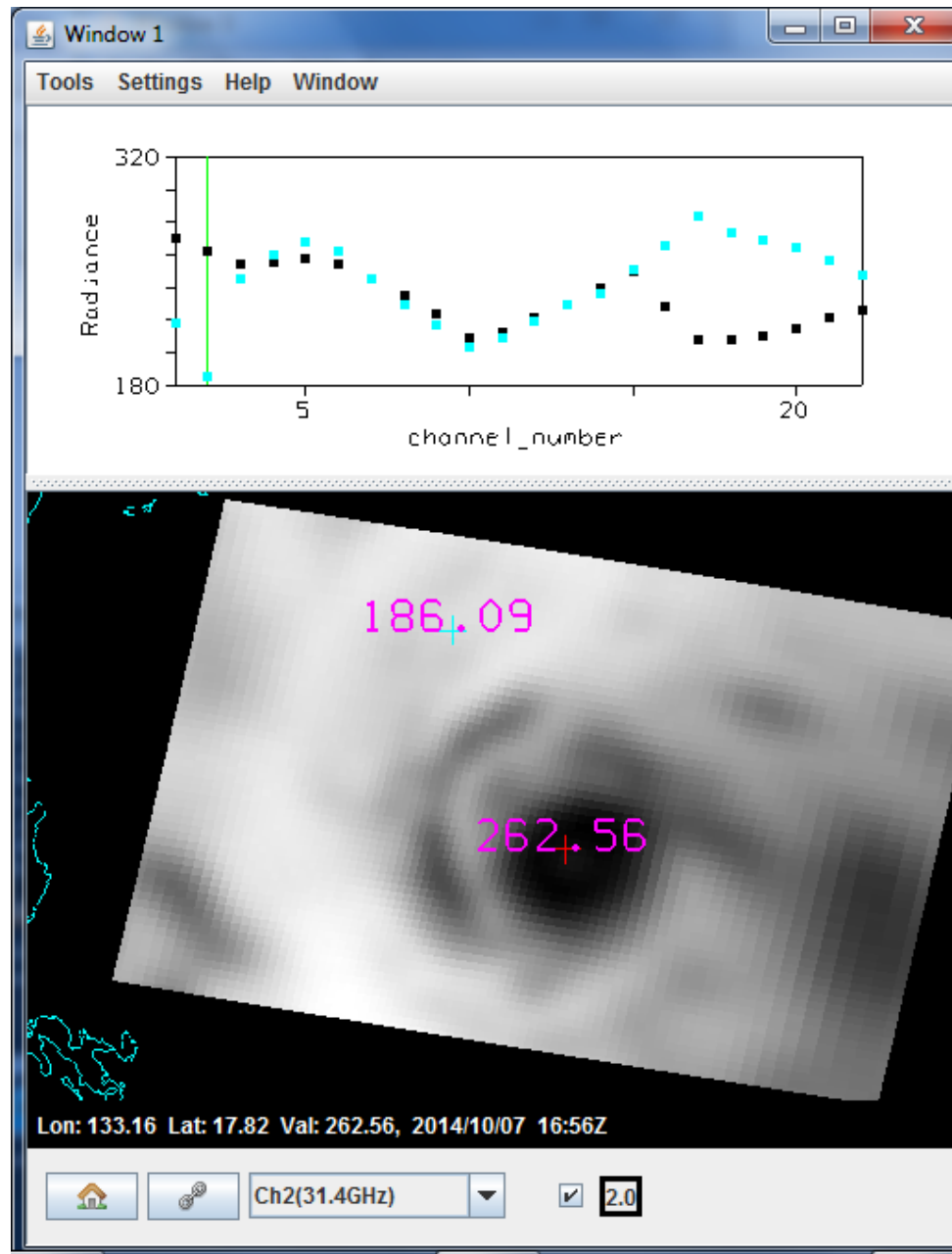


Sampling of CrIS Channels, $\Delta\nu = 0.625, 1.25, 2.50 \text{ cm}^{-1}$





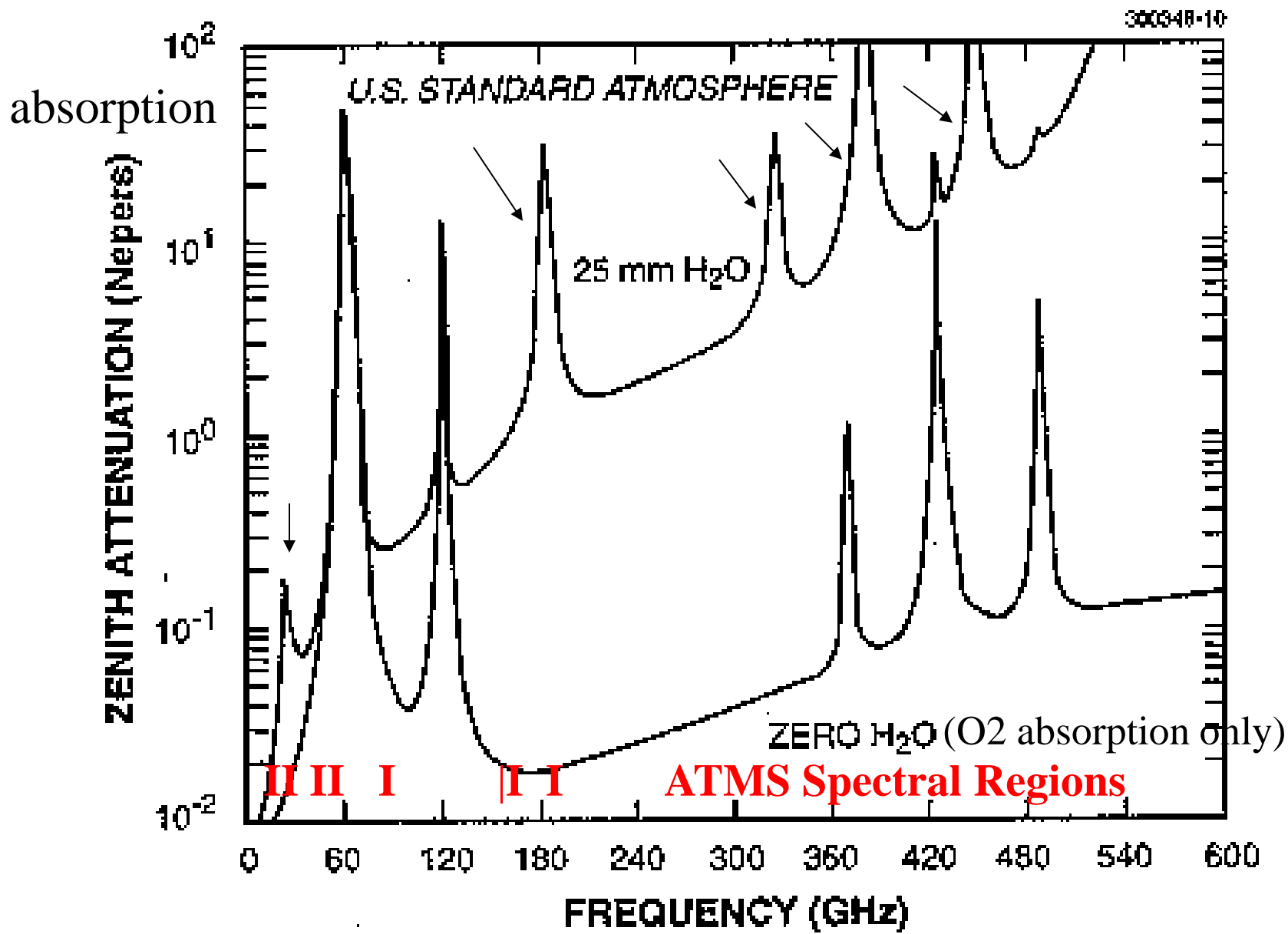


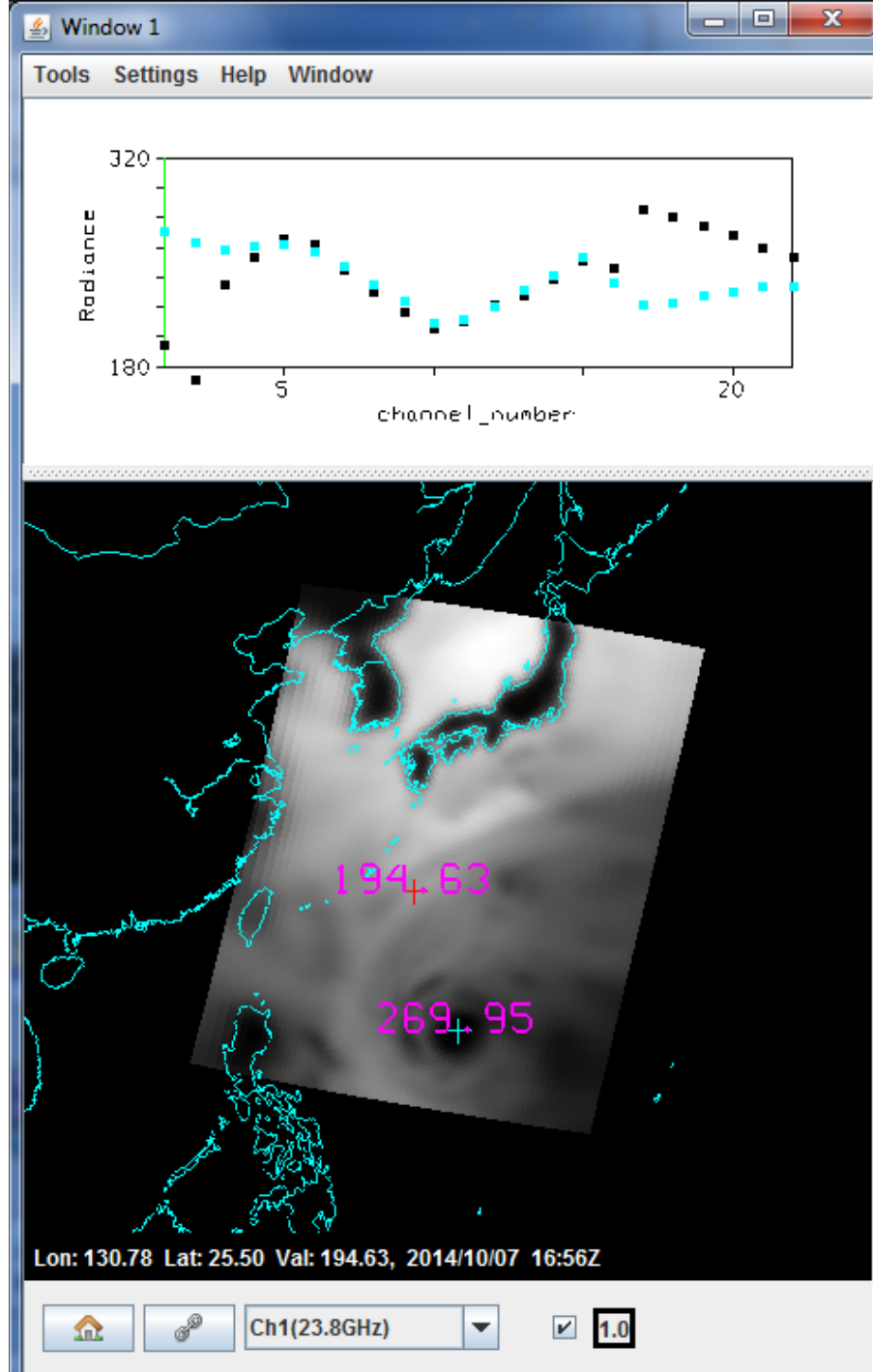
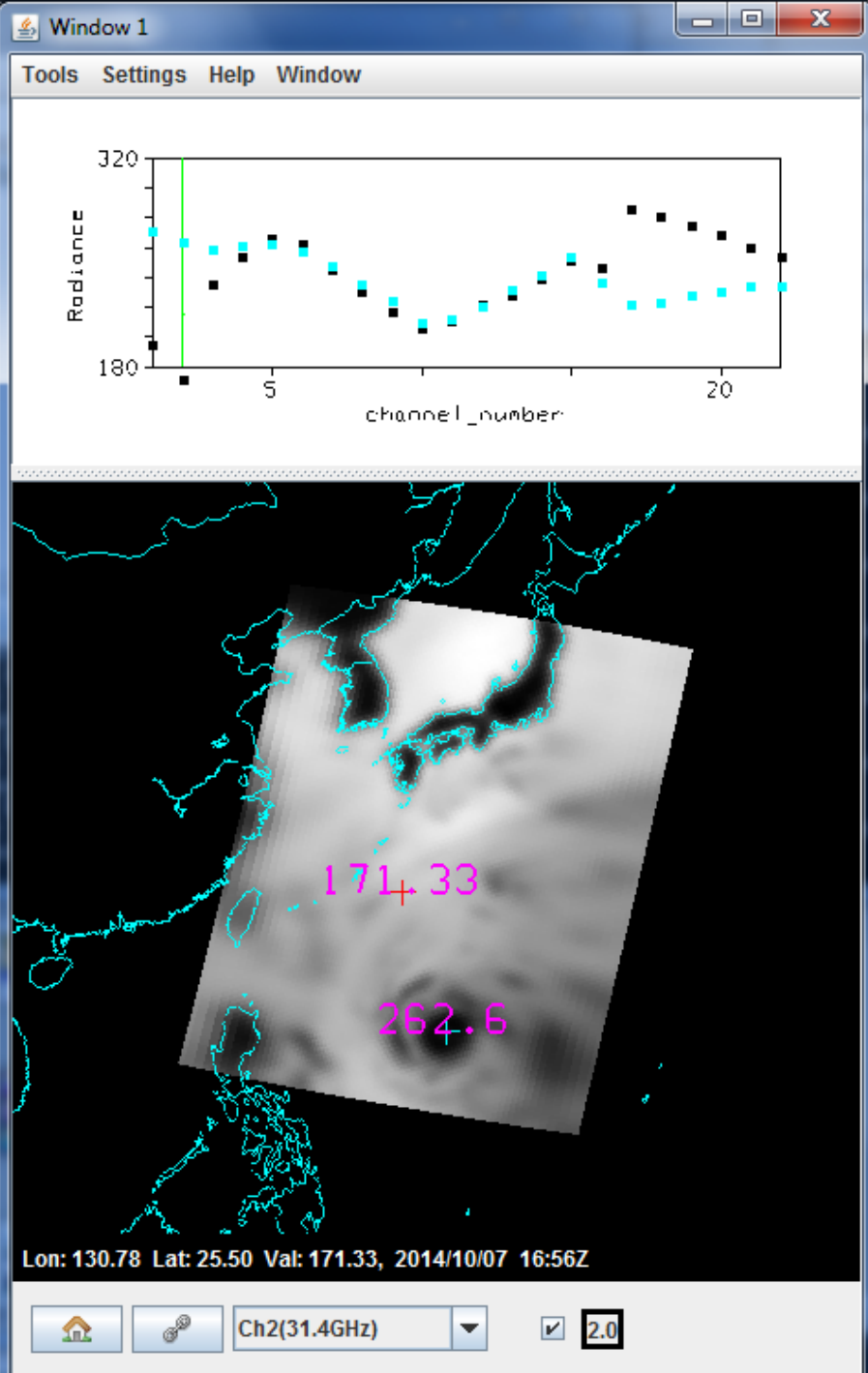


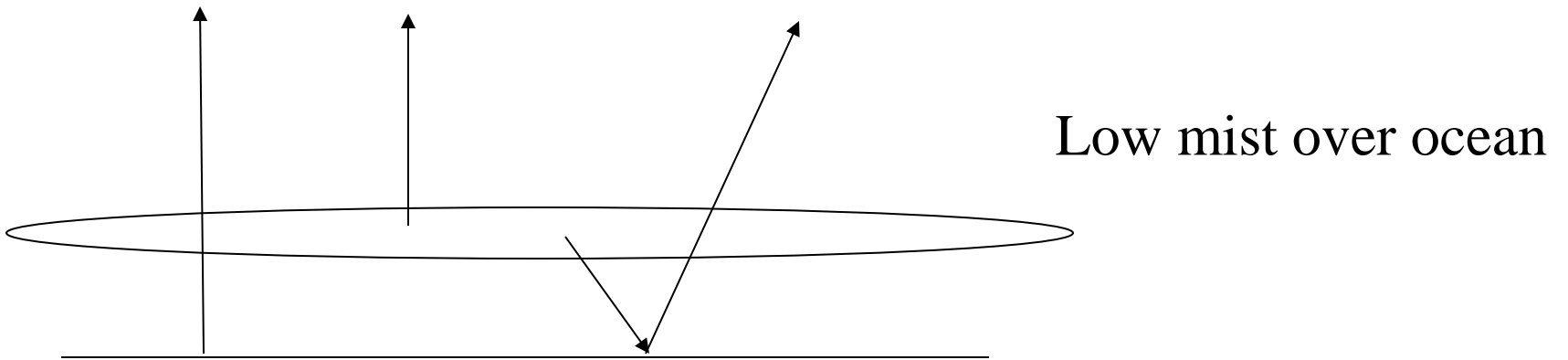
Suggested ATMS Channels

<u>Ch</u>	<u>v(GHz)</u>	<u>BW(GHz)</u>	<u>Characteristic</u>
1*	23.8	0.27	split window-water vapor 100 mm
2*	31.4	0.18	split window-water vapor 500 mm
3*	50.3	0.18	window-surface emissivity
4	51.76	0.40	window-surface emissivity
5*	52.8	0.40	surface air
6*	53.596±.115	0.17	4 km ~ 700 mb temp and precip
7*	54.4	0.40	9 km ~ 400 mb temp and precip
8*	54.94	0.40	11 km ~ 250 mb
9*	55.5	0.33	13 km ~ 180 mb
10*	57.2903	0.33	17 km ~ 90 mb
11*	57.2903 ±.217	0.078	19 km ~ 50 mb
12*	57.2903 ±.322 ±.048	0.036	25 km ~ 25 mb
13*	57.2903 ±.322 ±.022	0.016	29 km ~ 10 mb
14*	57.2903 ±.322 ±.010	0.008	32 km ~ 6 mb
15*	57.2903 ±.322 ±.004	0.03	37 km ~ 3 mb
16*	89.0	6.0	window-precip and water vapor 150 mm
17	166.31	4.0	H ₂ O 18 mm
18*	183.31±7	2.0	H ₂ O 8 mm
19	183.31±4.5	2.0	H ₂ O 4.5 mm
20*	183.31±3	1.0	H ₂ O 2.5 mm
21	183.31±1.8	1.0	H ₂ O 1.2 mm
22*	183.31±1	0.5	H ₂ O 0.5 mm

* In common with AMSU/HSB





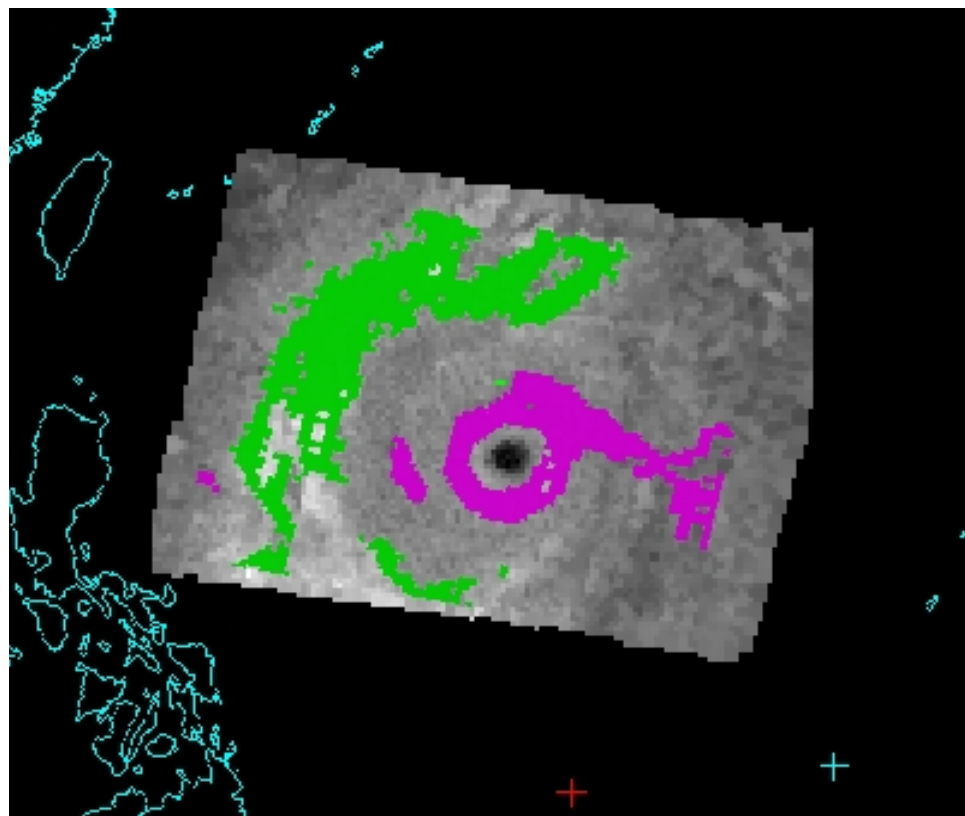
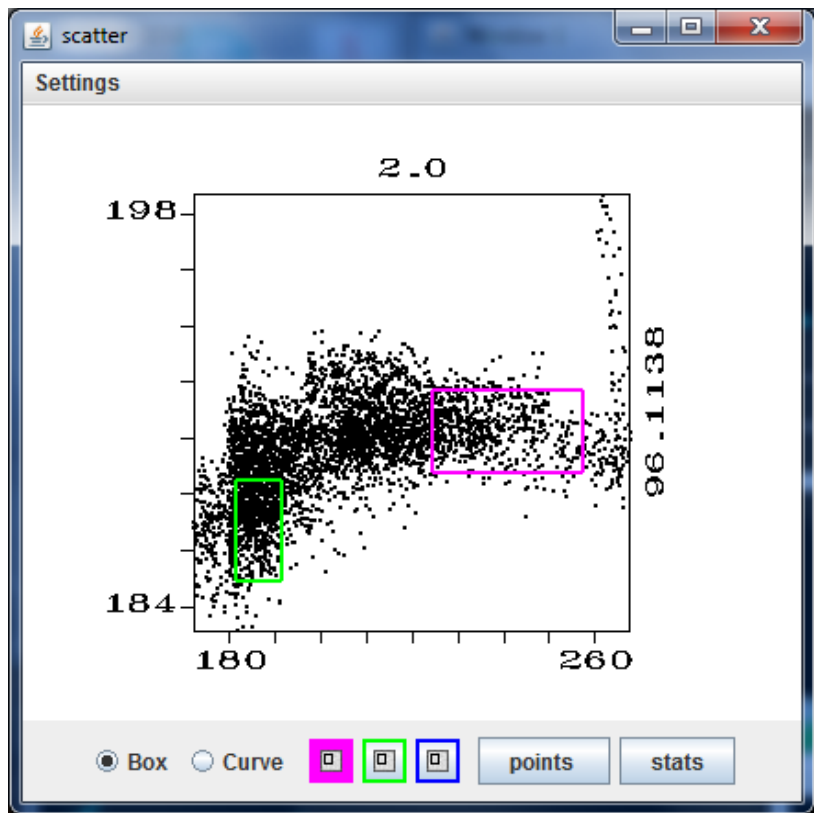


$$T_b = \varepsilon_s T_s (1 - \sigma_m) + \sigma_m T_m + \sigma_m (1 - \varepsilon_s) (1 - \sigma_m) T_m$$

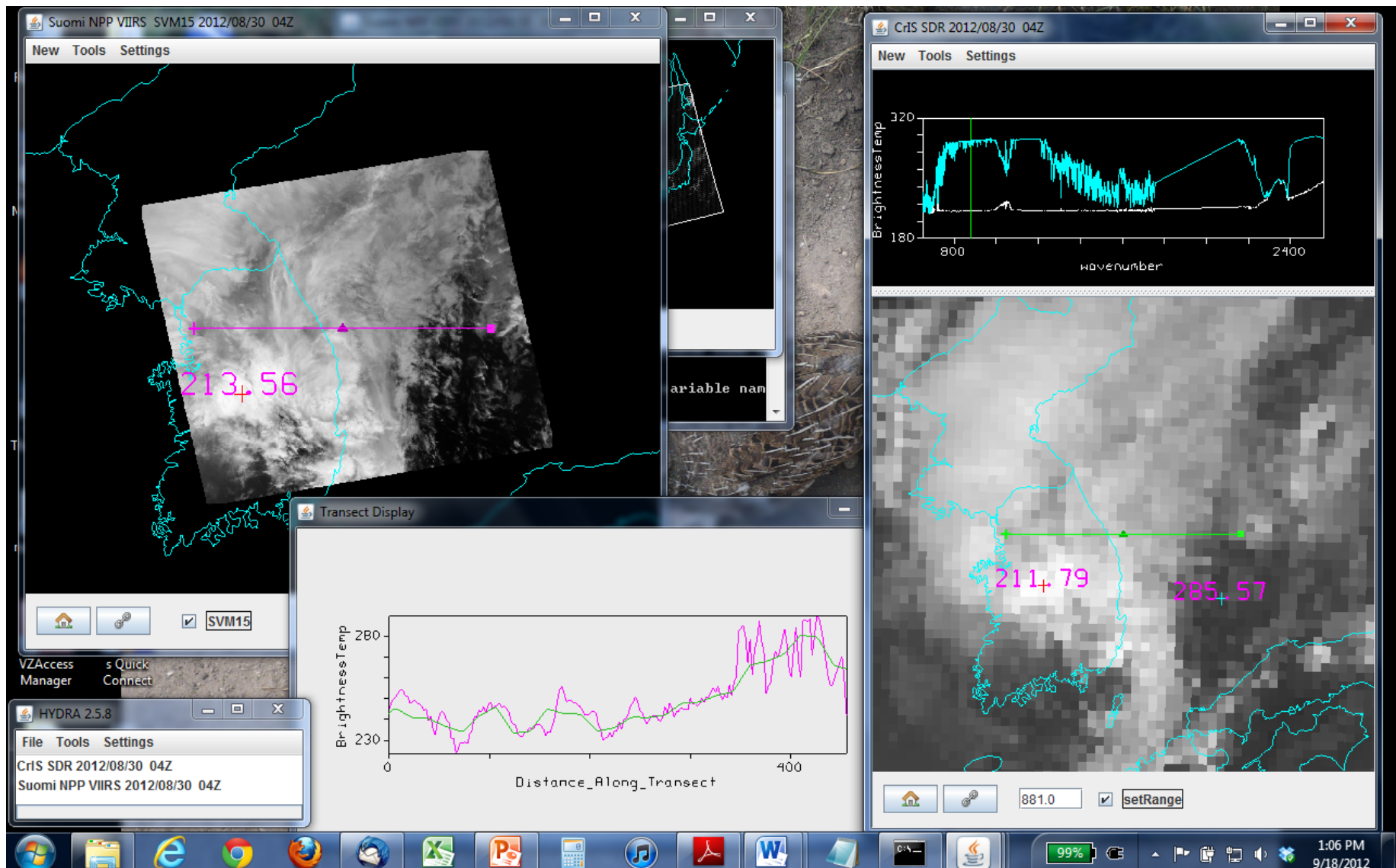
So

$$\Delta T_b = -\varepsilon_s \sigma_m T_s + \sigma_m T_m + \sigma_m (1 - \varepsilon_s) (1 - \sigma_m) T_m$$

For $\varepsilon_s \sim 0.5$ and $T_s \sim T_m$ this is always positive for $0 < \sigma_m < 1$

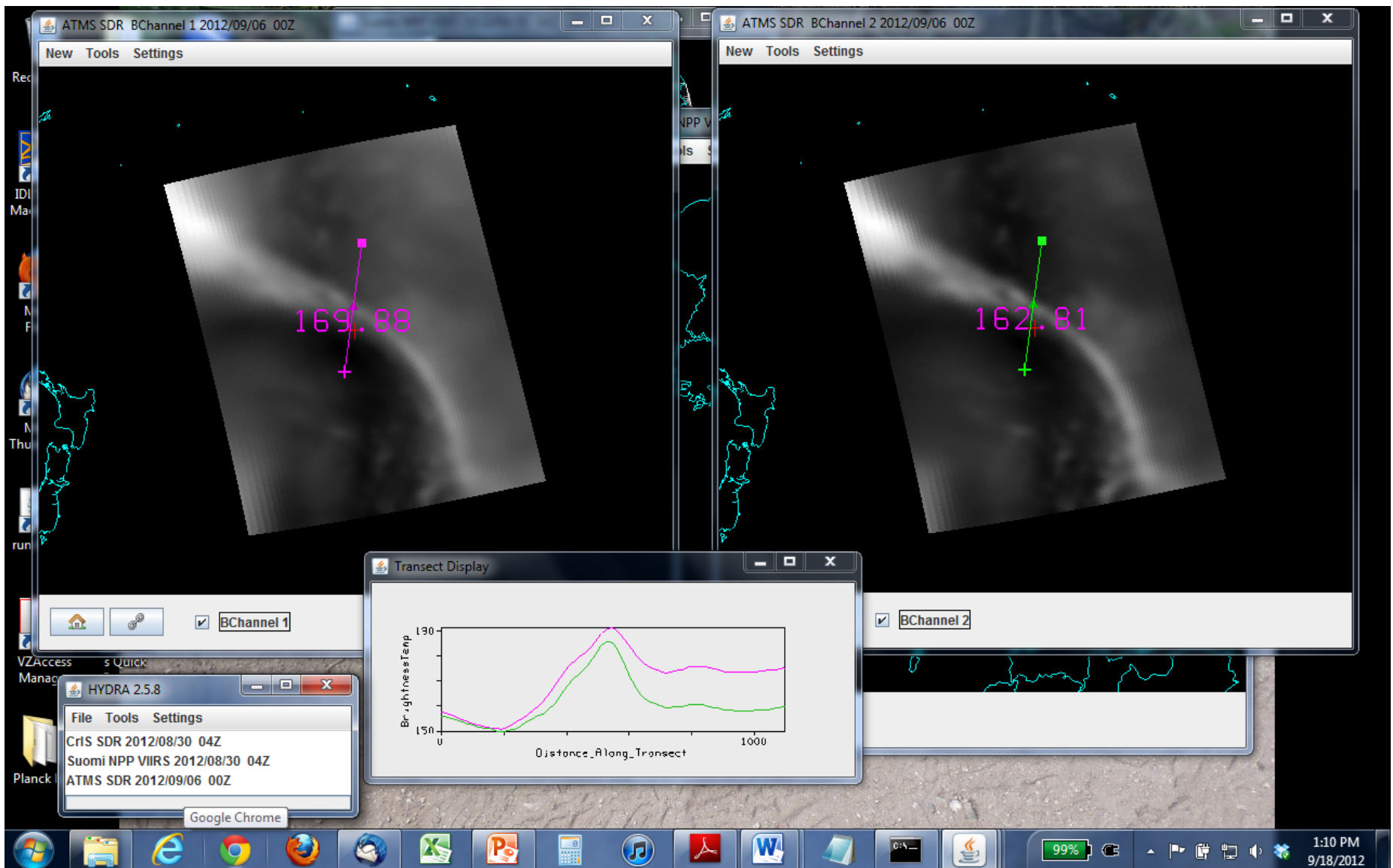


Comparing SNPP sensor measurements



VIIIRS and CrIS

ATMS Ch1 vs Ch2



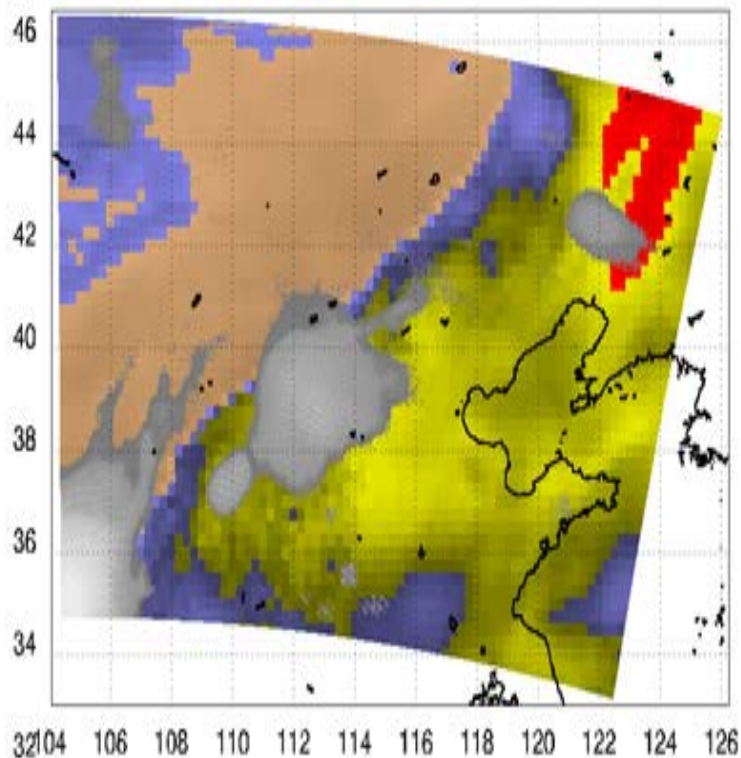
AIRS, CrIS, and 2 IASIs

Multiple overpasses per day

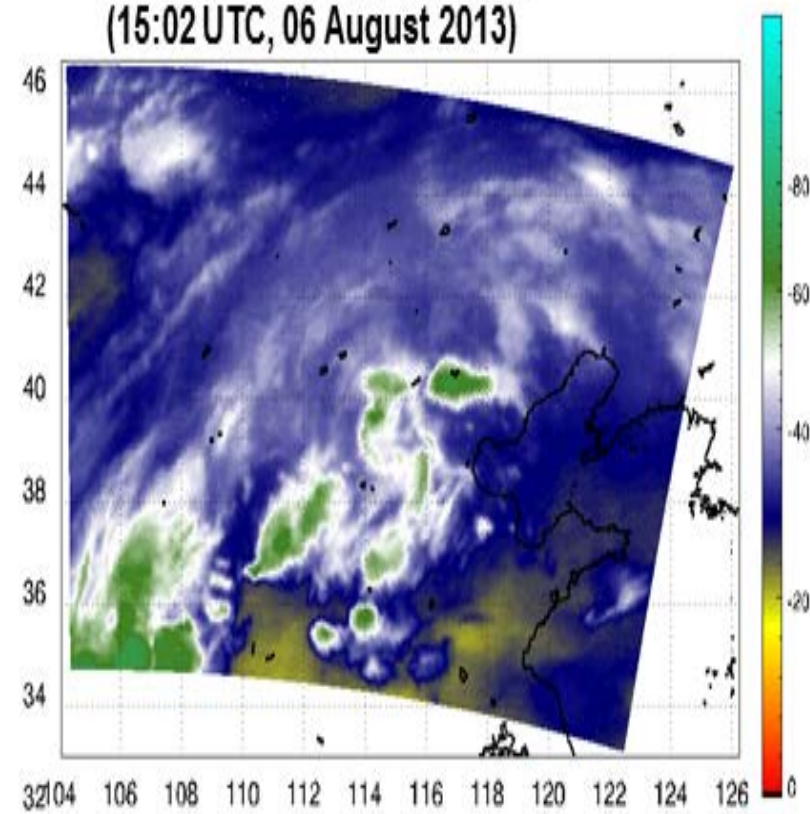
- often more than ten for mid-lats
- enables trending of atm and sfc trends

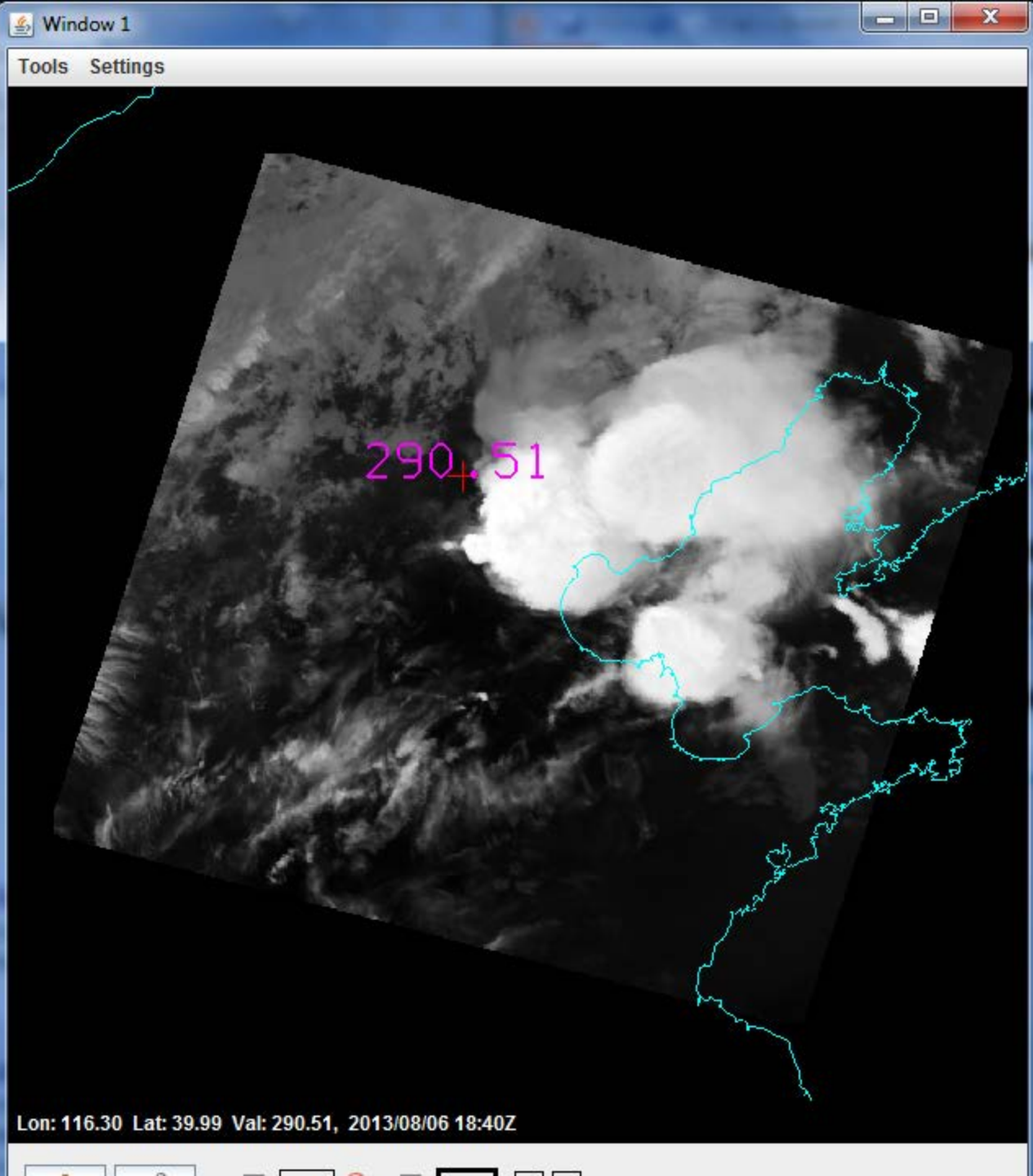
06 Aug 2013 Beijing Storm

Simulated FY-4A INVAS derived Lifted Index
(12:00 UTC, 06 August 2013)



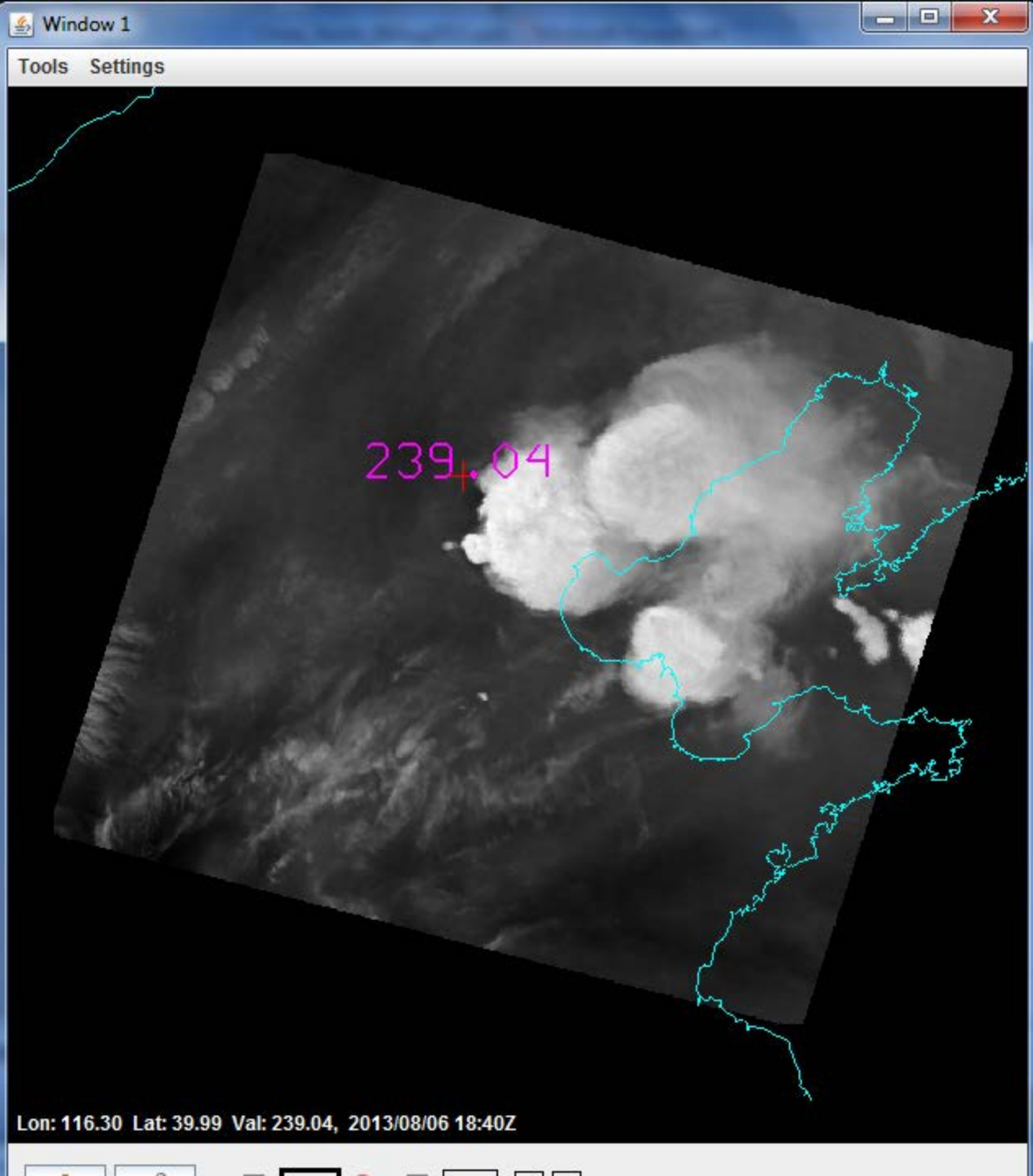
FY-2E 6.8 μm BT observation
(15:02 UTC, 06 August 2013)





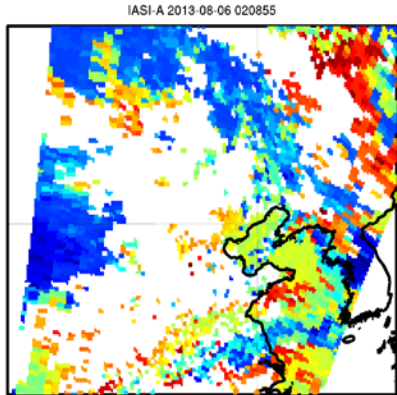
MODIS IRW

1700 UTC
6 Aug 2013

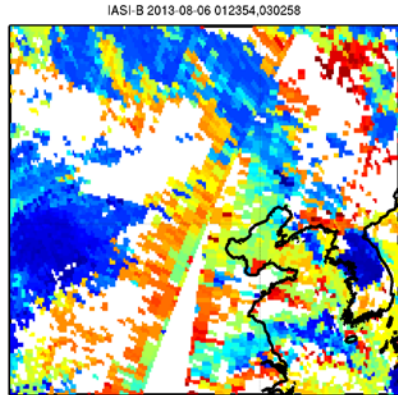


CTOP 6 Aug 2013

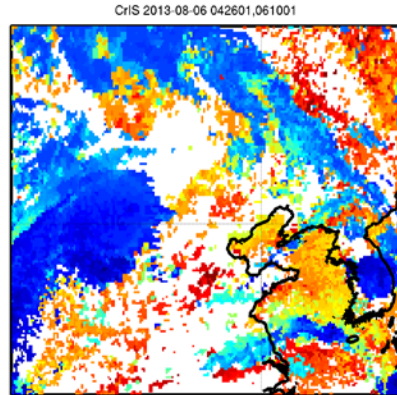
IASI-A



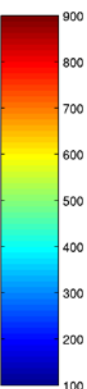
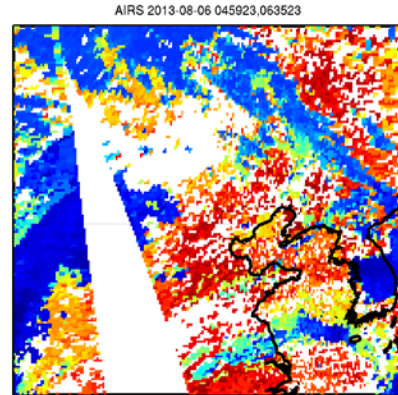
IASI-B



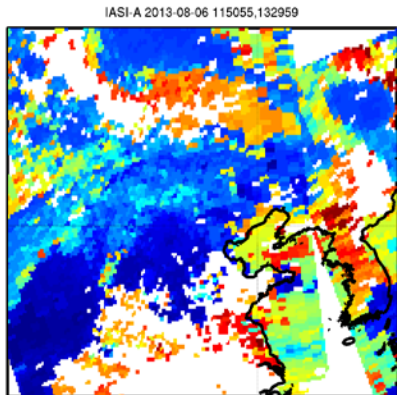
CrIS



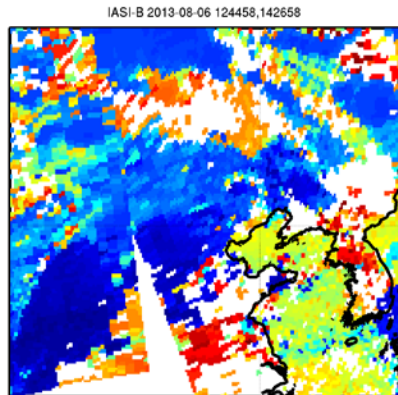
AIRS



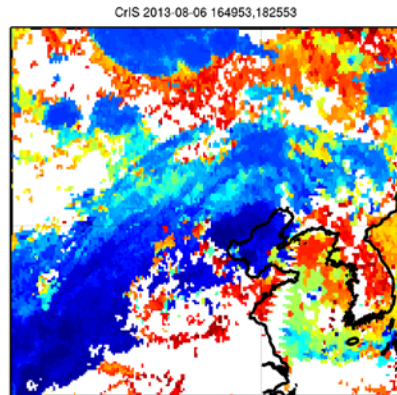
IASI-A



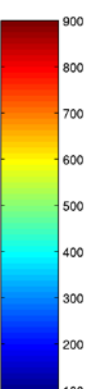
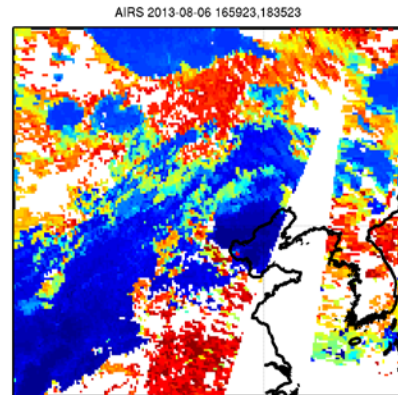
IASI-B



CrIS

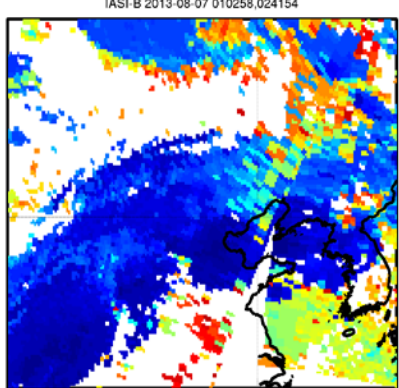


AIRS

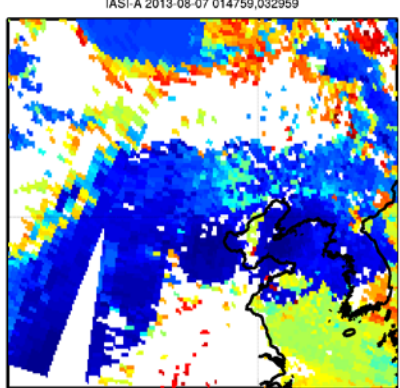


CTOP 7 Aug 2013

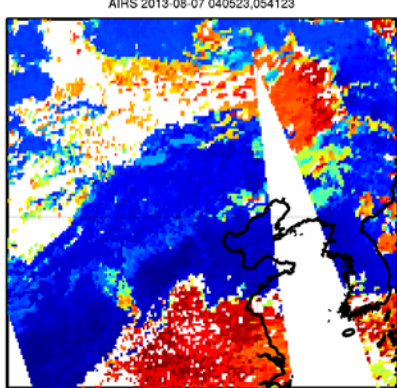
IASI-B



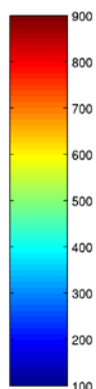
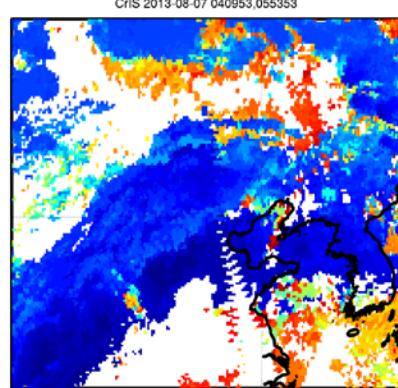
IASI-A



AIRS



CrIS



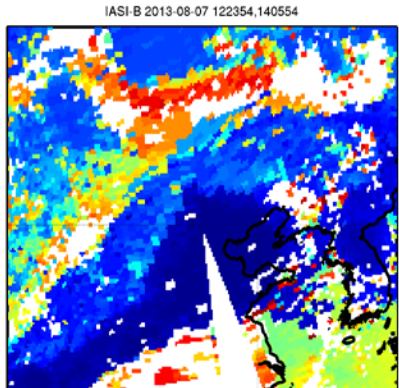
0103&0242

0148&0330

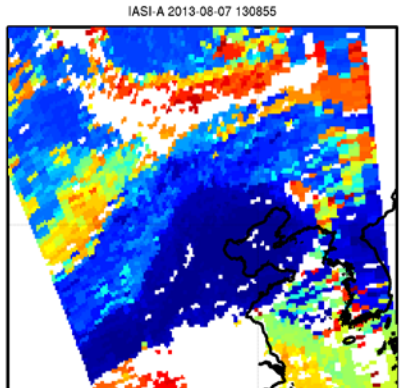
0405&0541

0410&0554 GMT

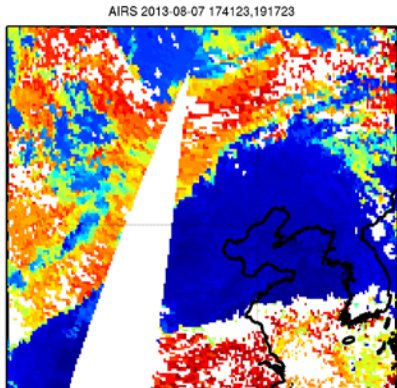
IASI-B



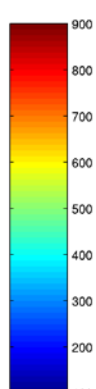
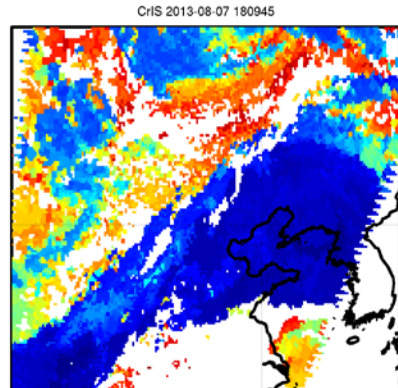
IASI-A



AIRS



CrIS



1224&1406

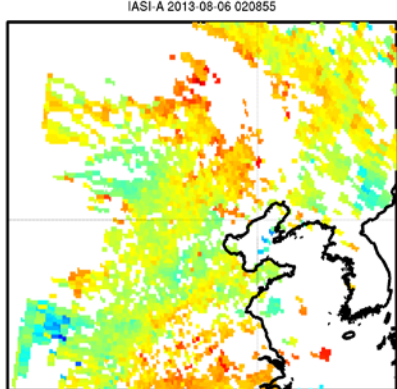
1309

1741&1917

1810 GMT

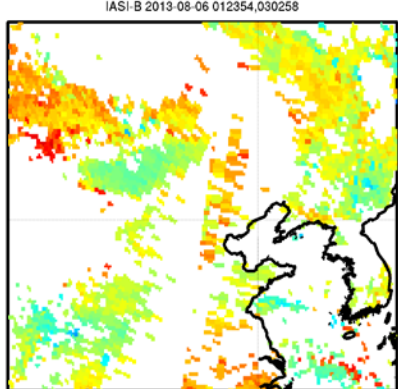
Lifted Index 6 Aug 2013

IASI-A



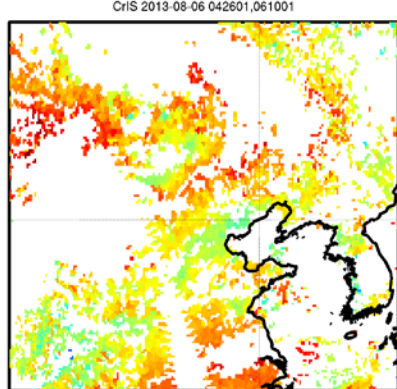
0209

IASI-B

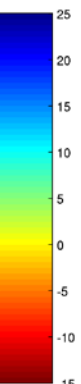
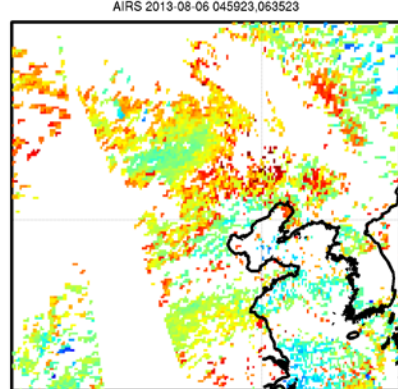


0124&0303

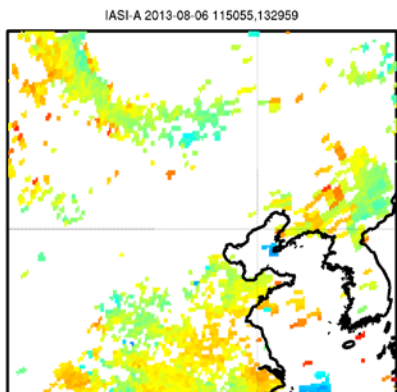
CrIS



AIRS

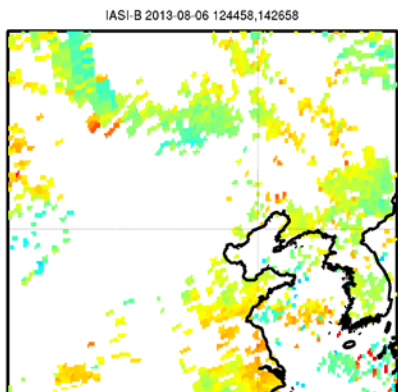


IASI-A



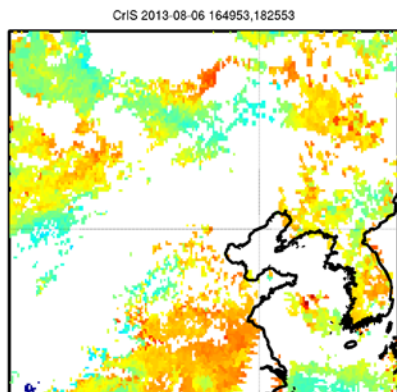
1151&1330

IASI-B



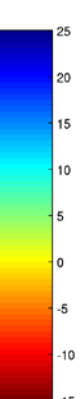
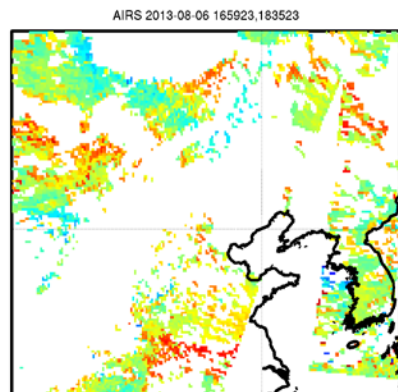
1245&1427

CrIS



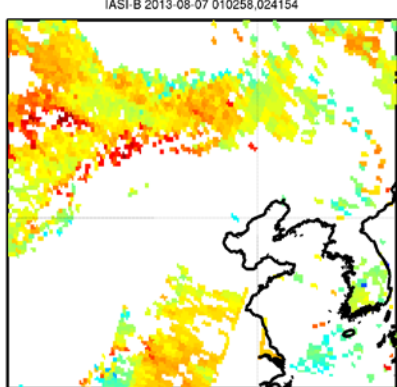
1650&1826

AIRS

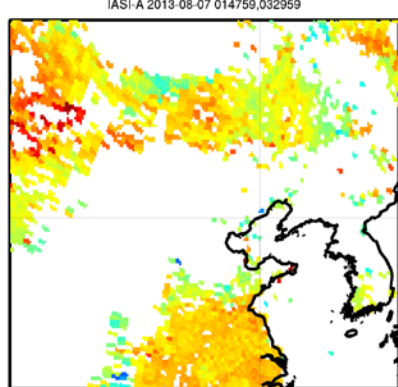


Lifted Index 7 Aug 2013

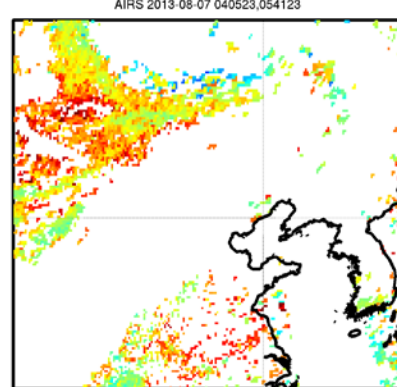
IASI-B



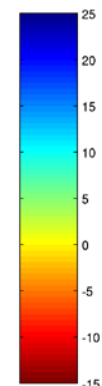
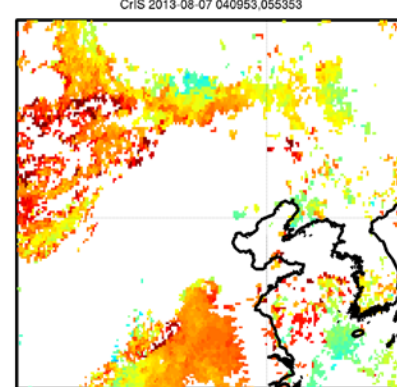
IASI-A



AIRS



CrIS



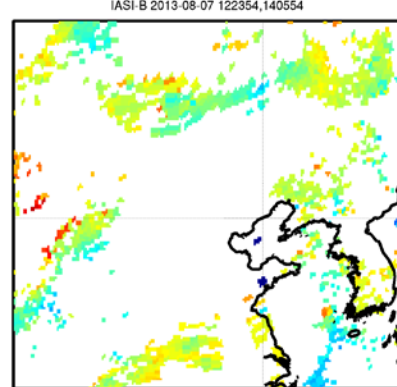
0103&0242

0148&0330

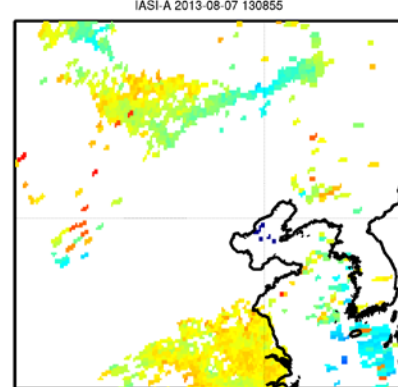
0405&0541

0410&0554 GMT

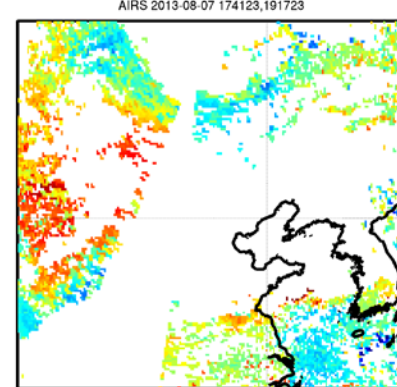
IASI-B



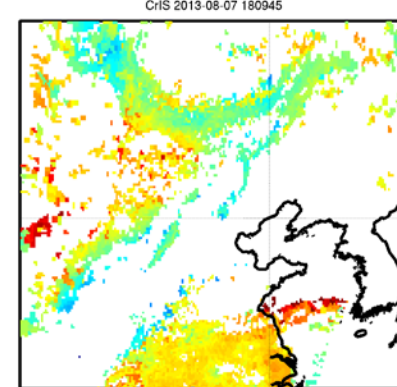
IASI-A



AIRS



CrIS



1224&1406

1309

1741&1917

1810 GMT

LST = GMT + 8

Access to visualization tools and data

For HYDRA2 <ftp://ftp.ssec.wisc.edu/rink/hydra2/>

For MODIS data <http://ladsweb.nascom.nasa.gov/>

For AIRS data <http://daac.gsfc.nasa.gov/>

For IASI, connect with EUMETSAT archive

[http://www.eumetsat.int/website/home/Data/DataDelivery/
OnlineDataAccess/index.html](http://www.eumetsat.int/website/home/Data/DataDelivery/OnlineDataAccess/index.html)

For VIIRS, CrIS, and ATMS data, orbit tracks, guide

<http://www.nsof.class.noaa.gov>

<http://www.ssec.wisc.edu/datacenter/npp/>

http://www.class.ncdc.noaa.gov/notification/faq_npp.htm

See tutorial "How do I order NPP data in CLASS (11/28/11)"

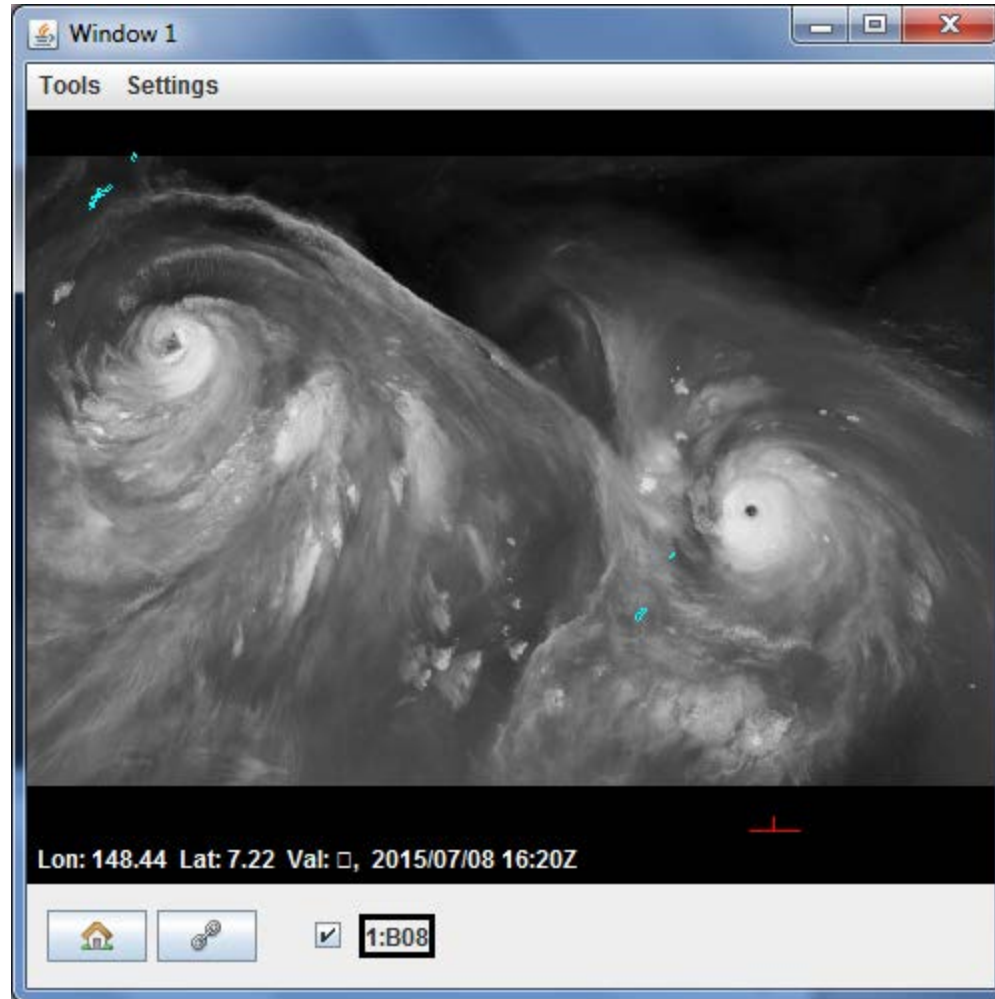
For AHI data

Contact rink@ssec.wisc.edu with request to convert file to NetCDF

AHI Example

Chan-hom
8 Jul 2015

Nangka



AHI	Band	Bandwidth	SNR	Res	Objectives
1	455 nm	50 nm	≤ 300 @ 100 % albedo	1.0 km	Daytime aerosol over land, coastal water mapping
2	510 nm	20 nm	≤ 300 @ 100 % albedo	1.0 km	Green band – to produce color composite imagery
3	645 nm	30 nm	≤ 300 @ 100 % albedo	0.5 km	Daytime vegetation/burn scar and aerosols over water, winds
4	860 nm	20 nm	≤ 300 @ 100 % albedo	1.0 km	Daytime cirrus cloud
5	1610 nm	20 nm	≤ 300 @ 100 % albedo	2.0 km	Daytime cloud-top phase and particle size, snow
6	2260 nm	20 nm	≤ 300 @ 100 % albedo	2.0 km	Daytime land/cloud properties, particle size, vegetation, snow
7	3.85 µm	0.22 µm	≤ 0.16 @ 300 K	2.0 km	Surface and cloud, fog at night, fire, winds
8	6.25 µm	0.37 µm	≤ 0.40 @ 240 K	2.0 km	High-level atmospheric water vapor, winds, rainfall
9	6.95 µm	0.12 µm	≤ 0.10 @ 300 K	2.0 km	Mid-level atmospheric water vapor, winds, rainfall
10	7.35 µm	0.17 µm	≤ 0.32 @ 240 K	2.0 km	Lower-level water vapor, winds and SO ₂
11	8.60 µm	0.32 µm	≤ 0.10 @ 300 K	2.0 km	Total water for stability, cloud phase, dust, SO ₂ , rainfall
12	9.63 µm	0.18 µm	≤ 0.10 @ 300 K	2.0 km	Total ozone, turbulence, winds
13	10.45 µm	0.30 µm	≤ 0.10 @ 300 K	2.0 km	Surface and cloud
14	11.20 µm	0.20 µm	≤ 0.10 @ 300 K	2.0 km	Imagery, SST, clouds, rainfall
15	12.35 µm	0.30 µm	≤ 0.10 @ 300 K	2.0 km	Total water, ash, SST
16	13.30 µm	0.20 µm	≤ 0.30 @ 300 K	2.0 km	Air temperature, cloud heights and amounts

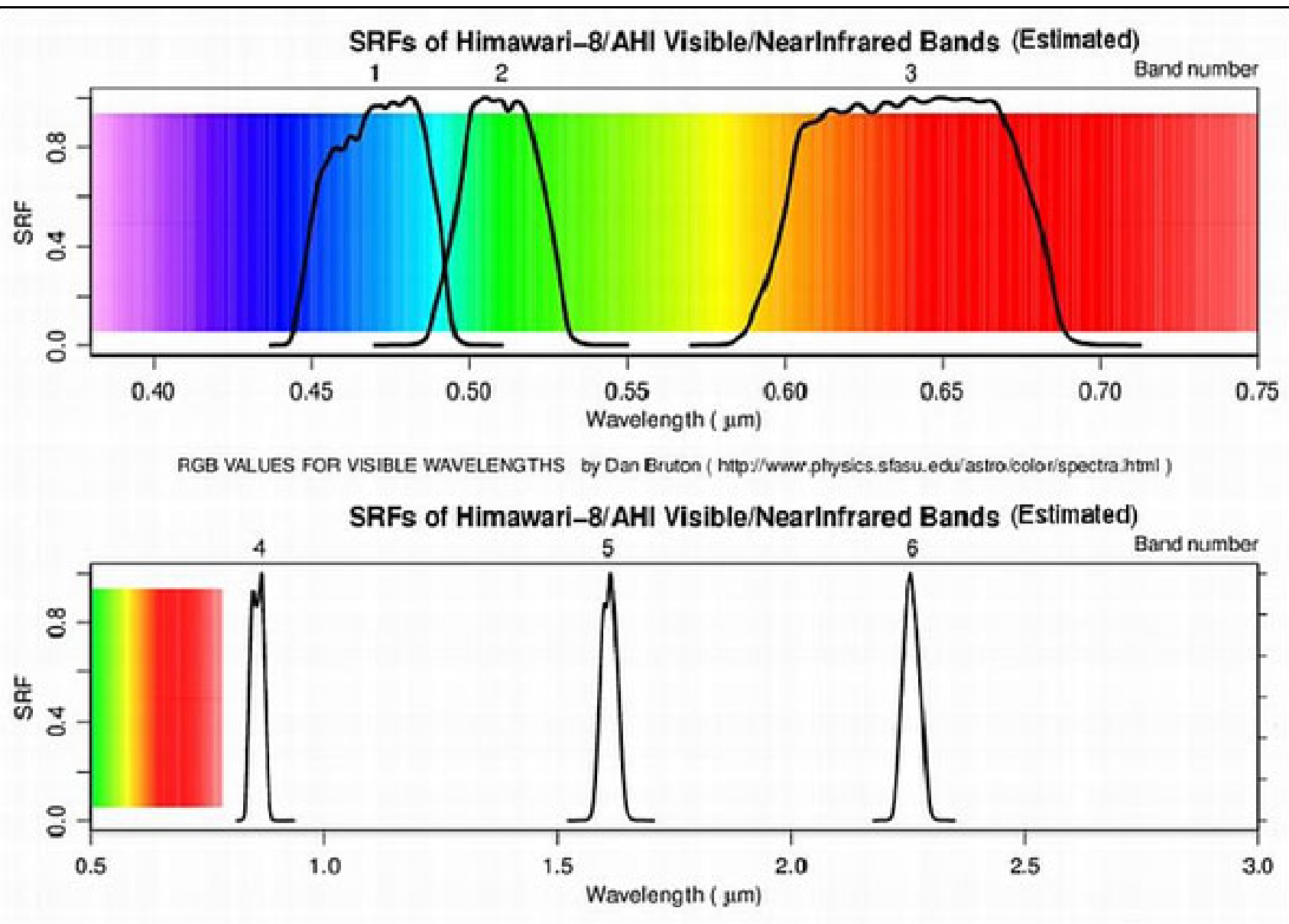


Figure 7: SRF (Spectral Response Functions) of AHI in the VNIR bands (image credit: JMA)

SRFs of Himawari-8/AHI Infrared Bands (Estimated)

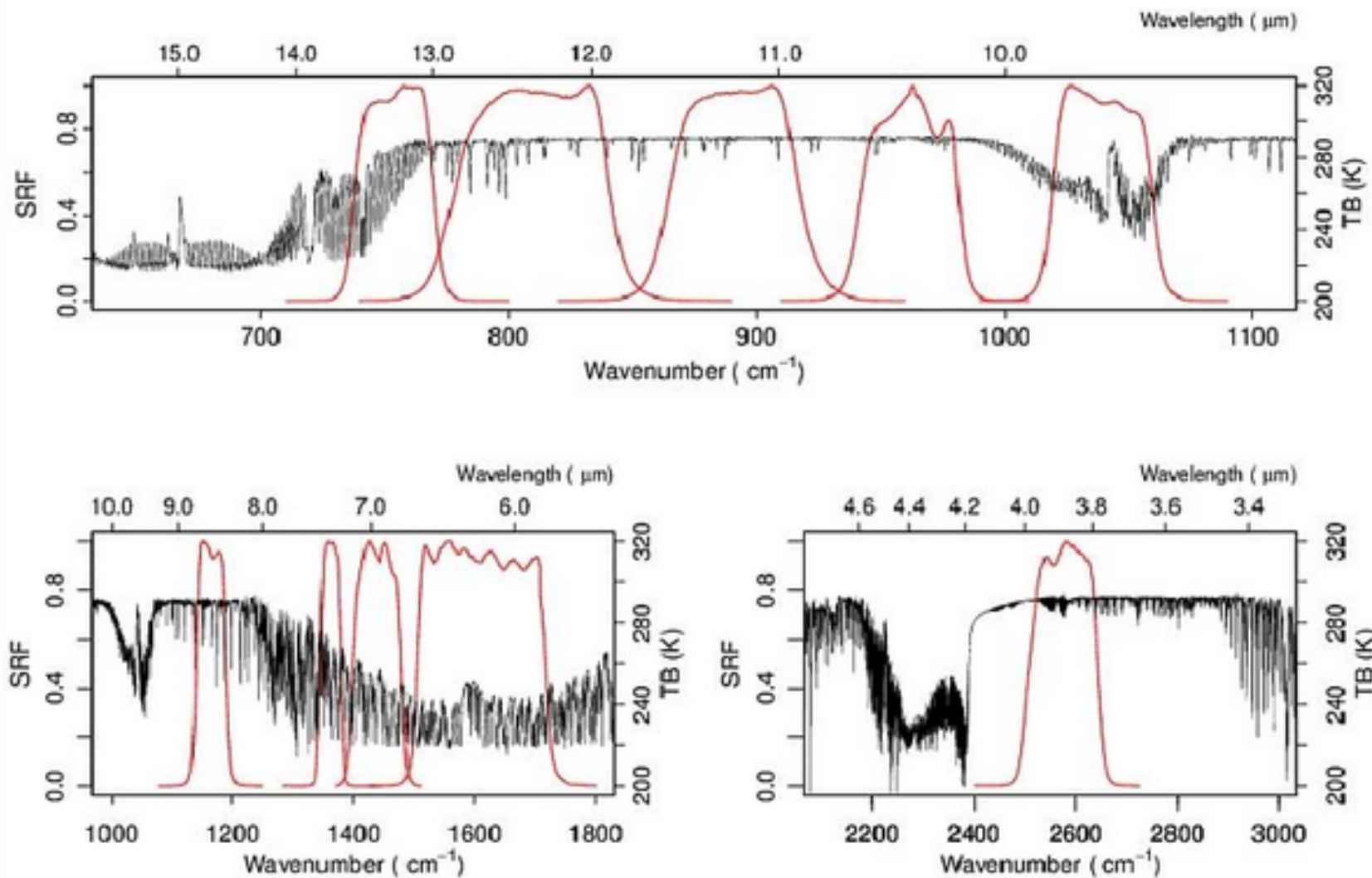


Figure 8: SRF (Spectral Response Functions) of AHI in the IR bands (image credit: JMA)

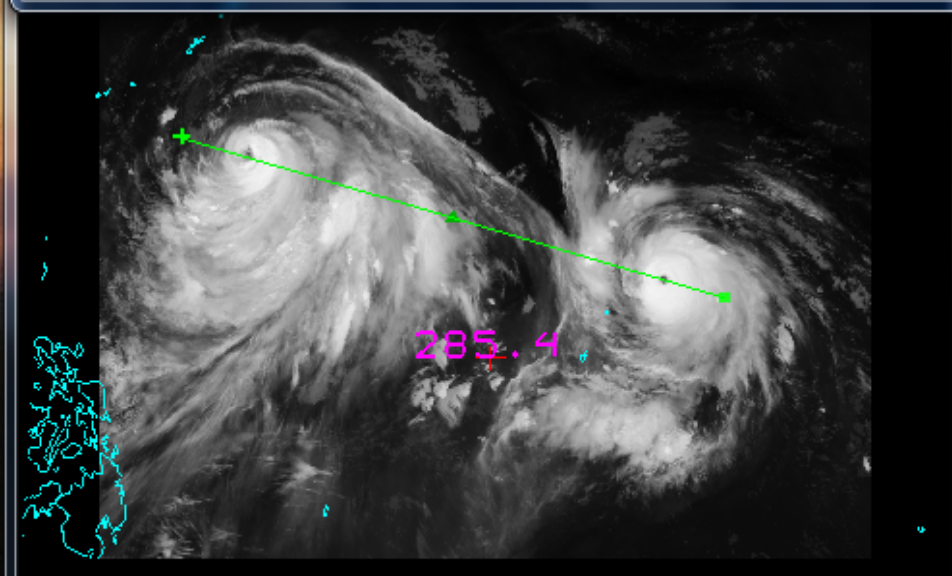
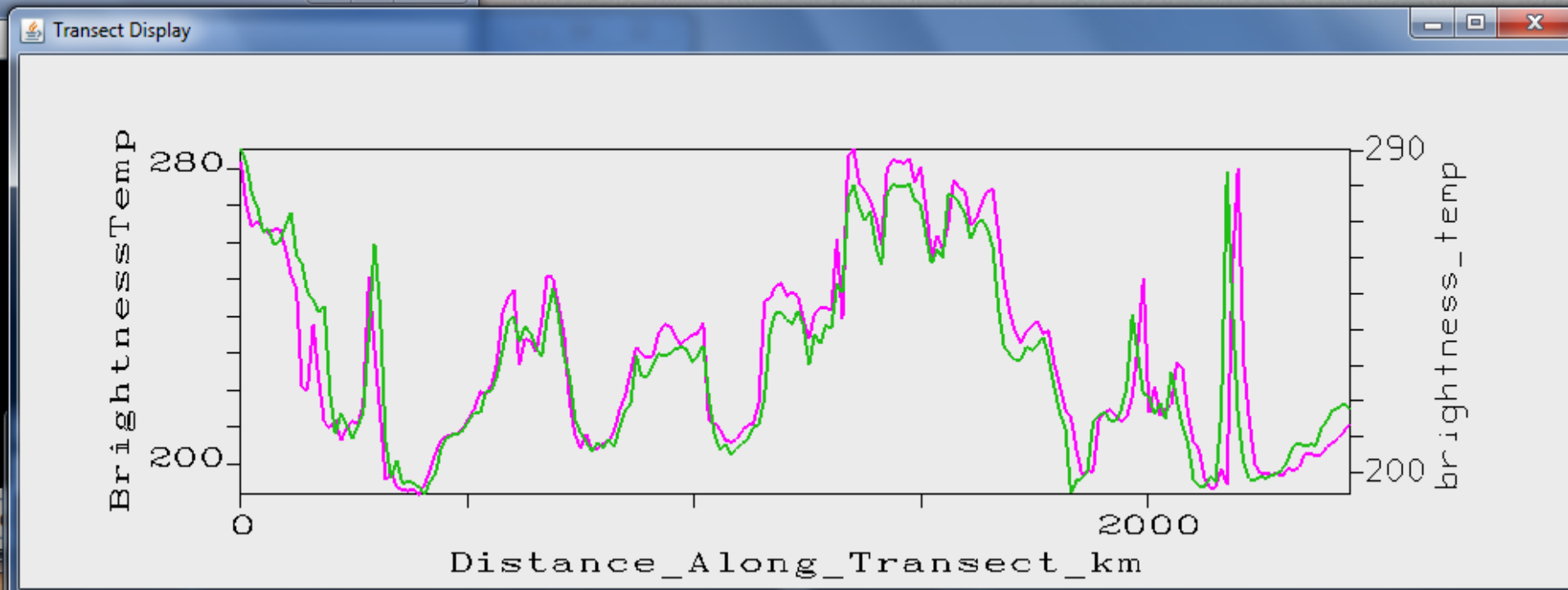
VIIRS bands and bandwidths

VIIRS Band	Central Wavelength (μm)	Bandwidth (μm)	Wavelength Range (μm)	Band Explanation	Spatial Resolution (m) @ nadir
M1	0.412	0.02	0.402 - 0.422	Visible/ Reflective	750 m
M2	0.445	0.018	0.436 - 0.454		
M3	0.488	0.02	0.478 - 0.488		
M4	0.555	0.02	0.545 - 0.565		
M5 (B)	0.672	0.02	0.662 - 0.682	Near IR	750 m
M6	0.746	0.015	0.739 - 0.754		
M7 (G)	0.865	0.039	0.846 - 0.885		
M8	1.240	0.020	1.23 - 1.25	Shortwave IR	750 m
M9	1.378	0.015	1.371 - 1.386		
M10 (R)	1.61	0.06	1.58 - 1.64		
M11	2.25	0.05	2.23 - 2.28	Medium-wave IR	750 m
M12	3.7	0.18	3.61 - 3.79		
M13	4.05	0.155	3.97 - 4.13		
M14	8.55	0.3	8.4 - 8.7	Longwave IR	750 m across full scan
M15	10.763	1.0	10.26 - 11.26		
M16	12.013	0.95	11.54 - 12.49		
DNB	0.7	0.4	0.5 - 0.9	Visible/ Reflective	750 m across full scan
I1 (B)	0.64	0.08	0.6 - 0.68	Visible/ Reflective	375 m
I2 (G)	0.865	0.039	0.85 - 0.88	Near IR	
I3 (R)	1.61	0.06	1.58 - 1.64	Shortwave IR	
I4	3.74	0.38	3.55 - 3.93	Medium-wave IR	
I5	11.45	1.9	10.5 - 12.4	Longwave IR	

M = Moderate (750 m) resolution bands

I = Imagery (375 m) resolution bands

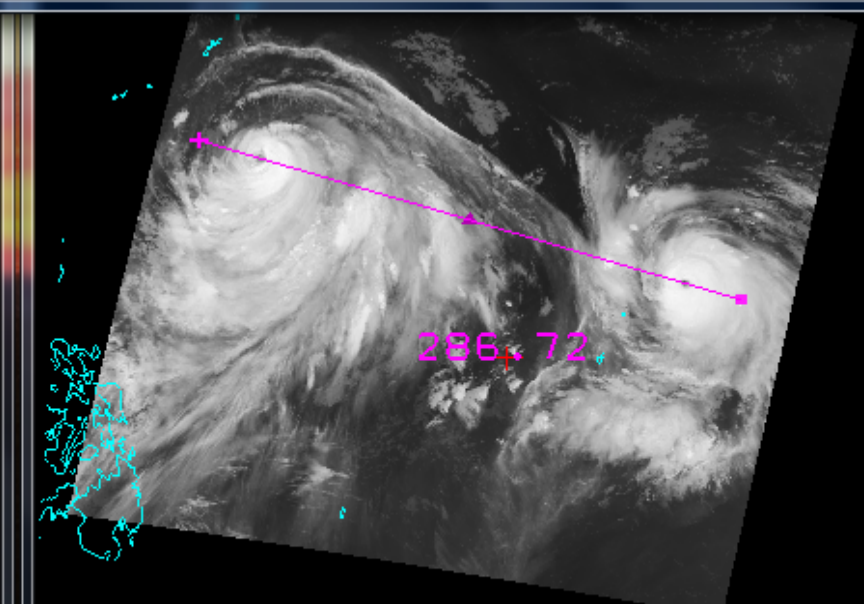
DNB = Day-Night Band (or Near Constant Contrast (NCC) band)



Lon: 141.06 Lat: 13.44 Val: 285.40, 2015/07/08 16:20Z



1:B14

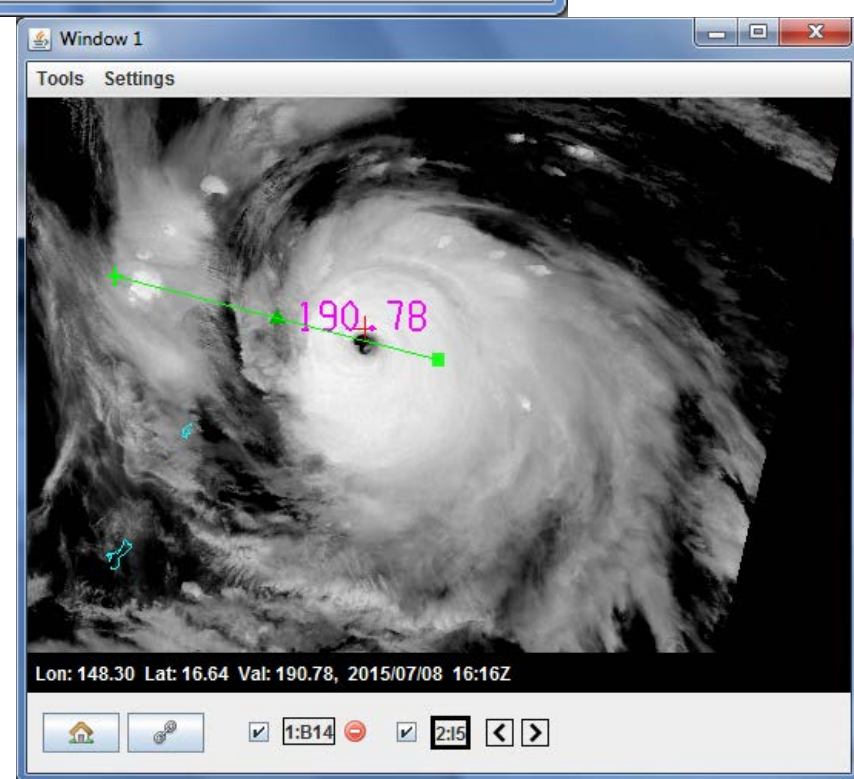
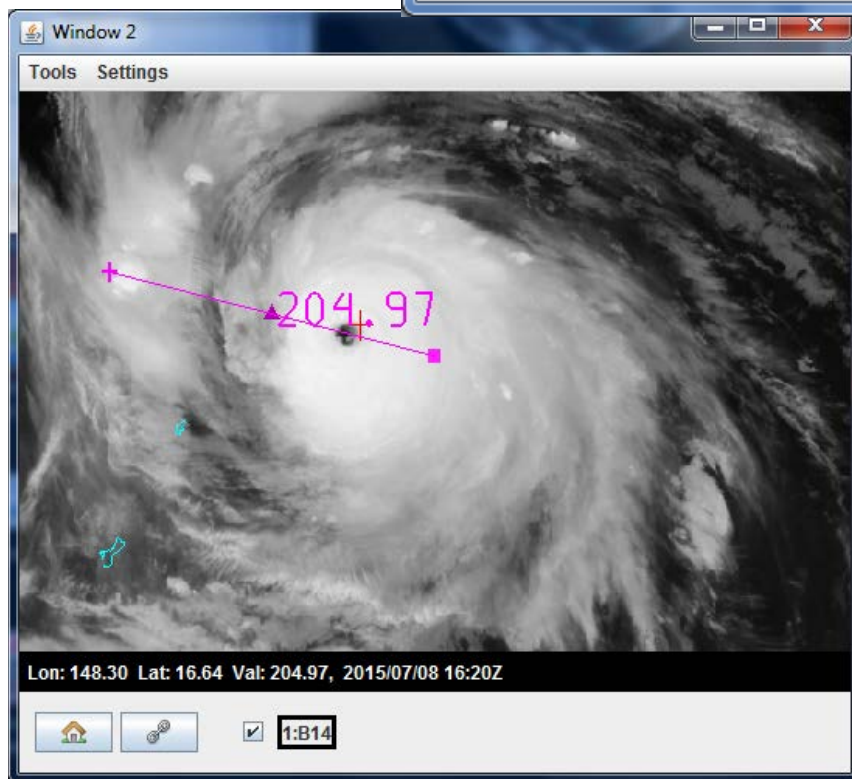
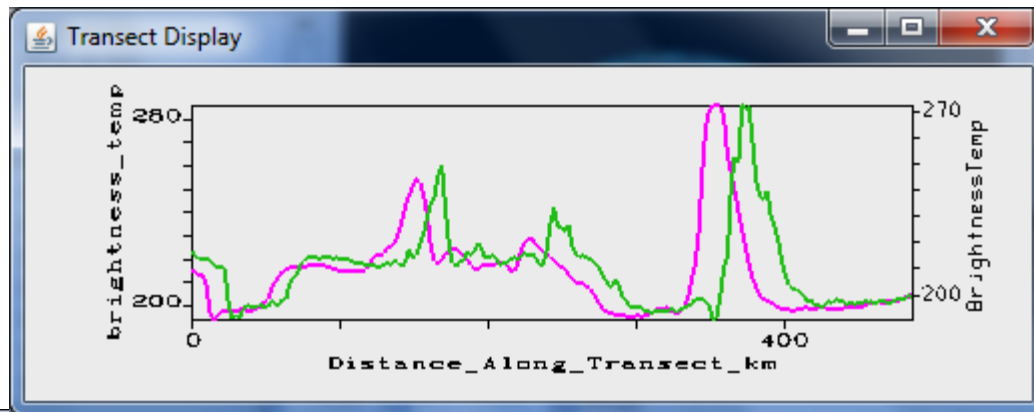


Lon: 141.06 Lat: 13.44 Val: 286.72, 2015/07/08 16:16Z

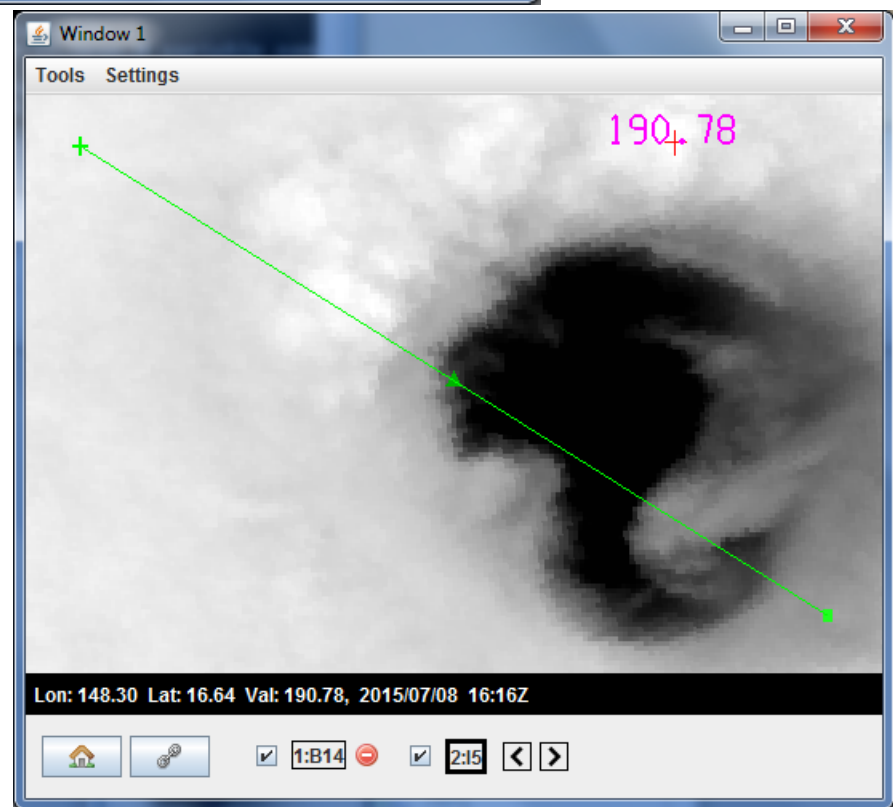
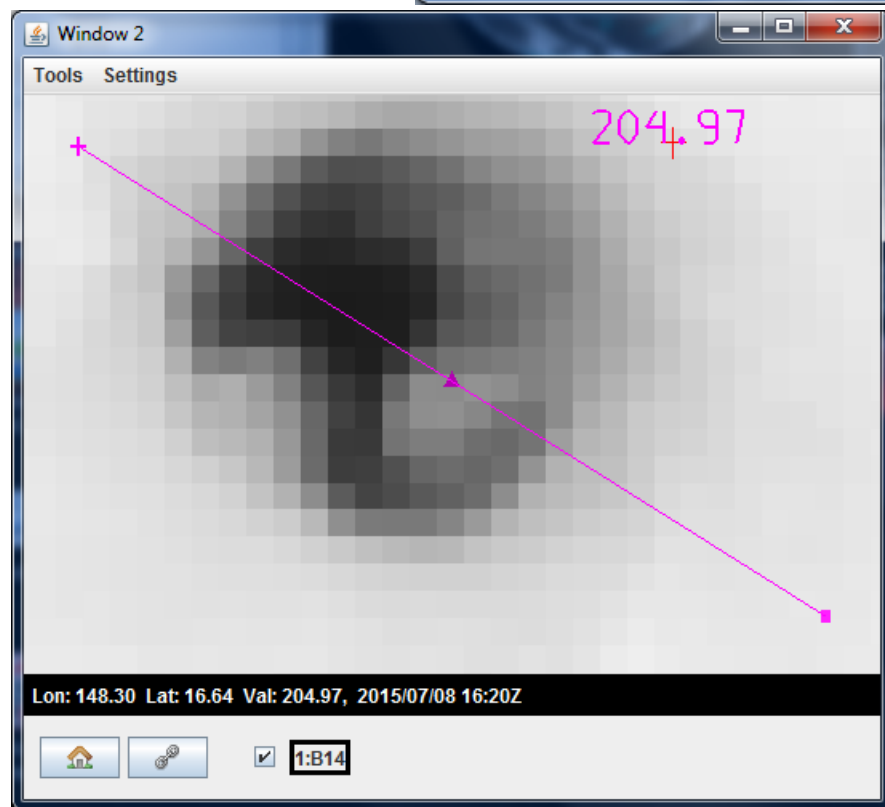
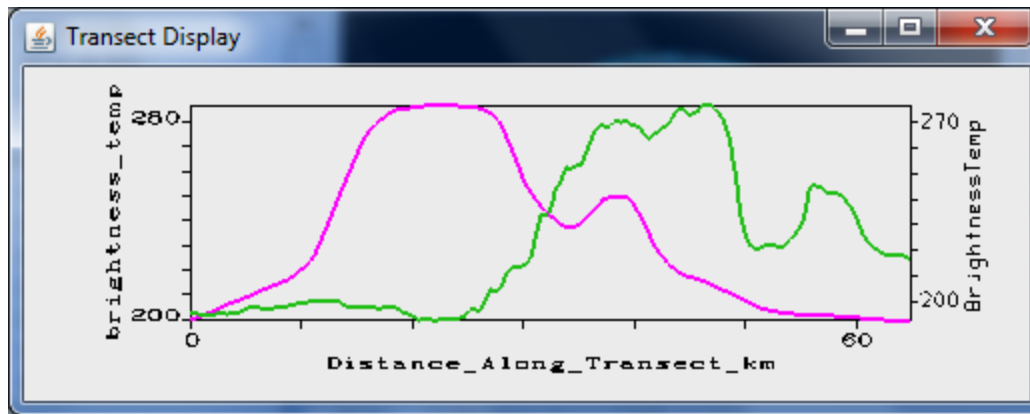


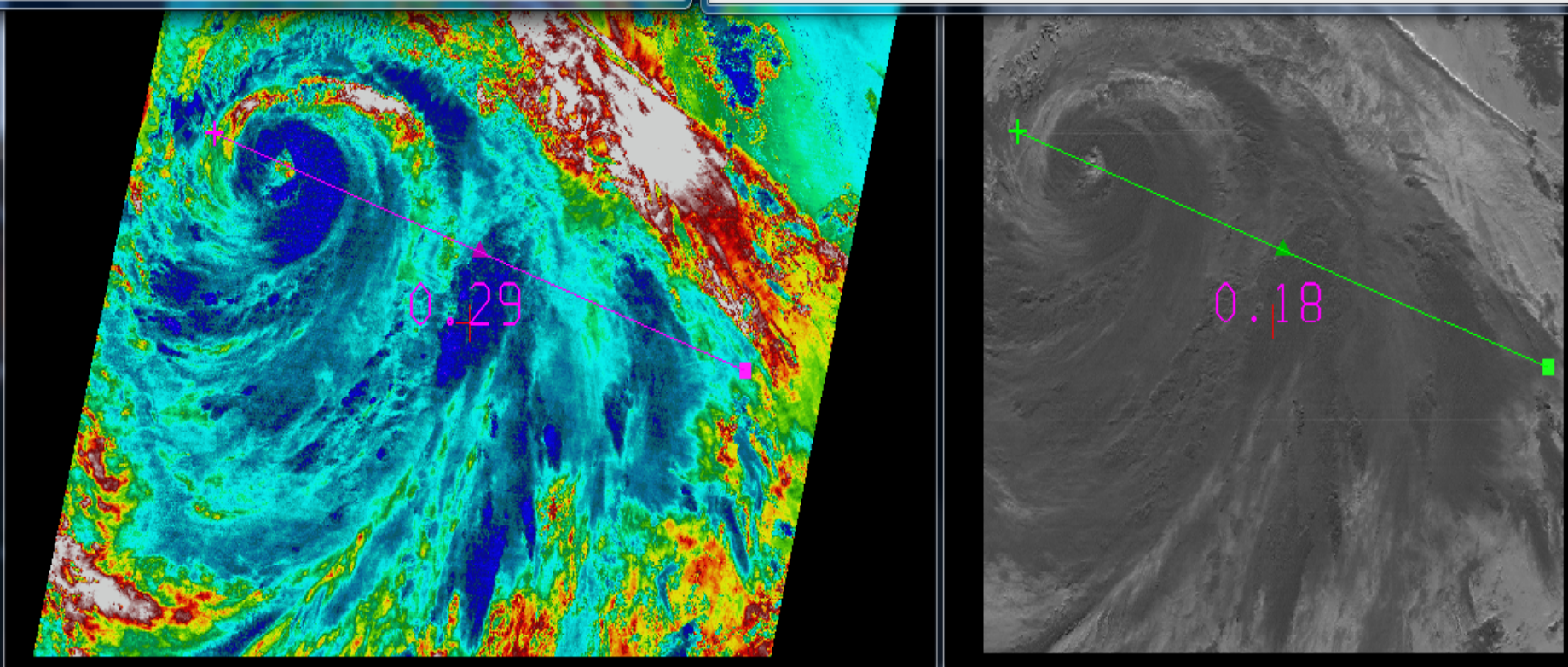
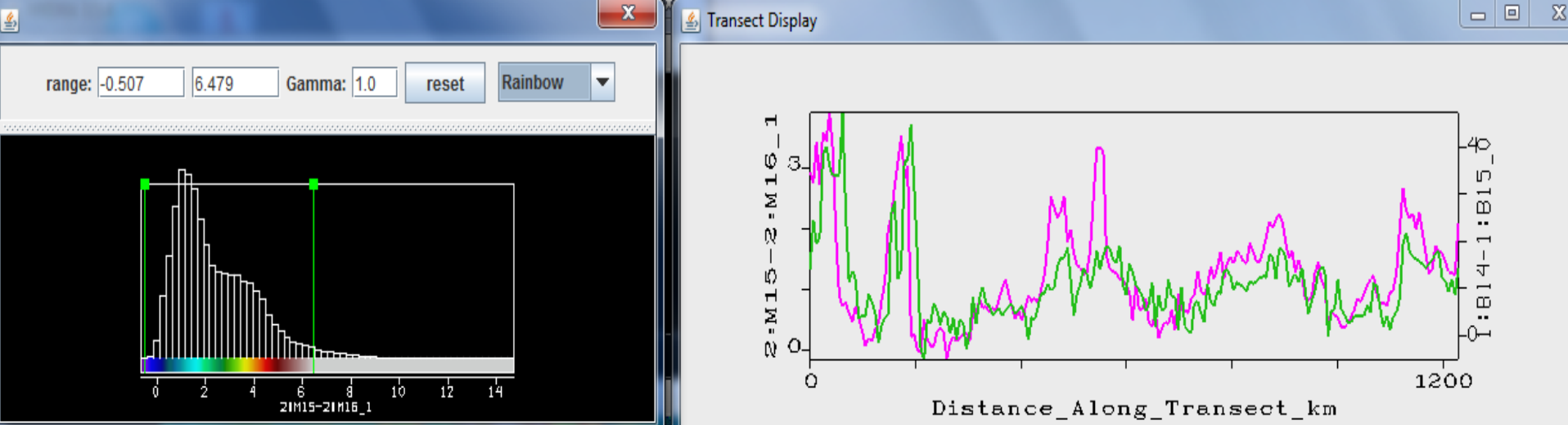
2:M15

IRW AHI (left) & VIIRS (right)

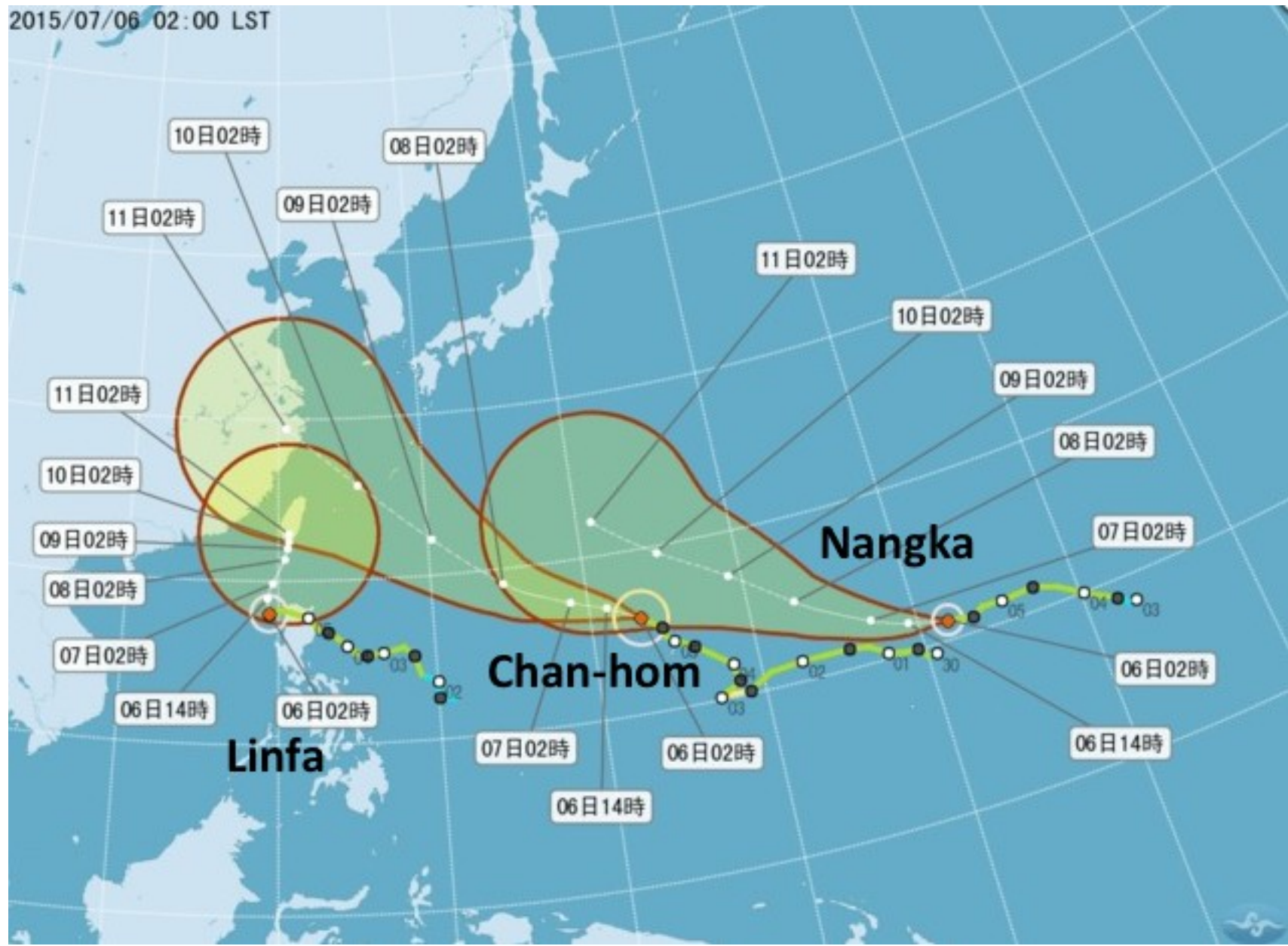


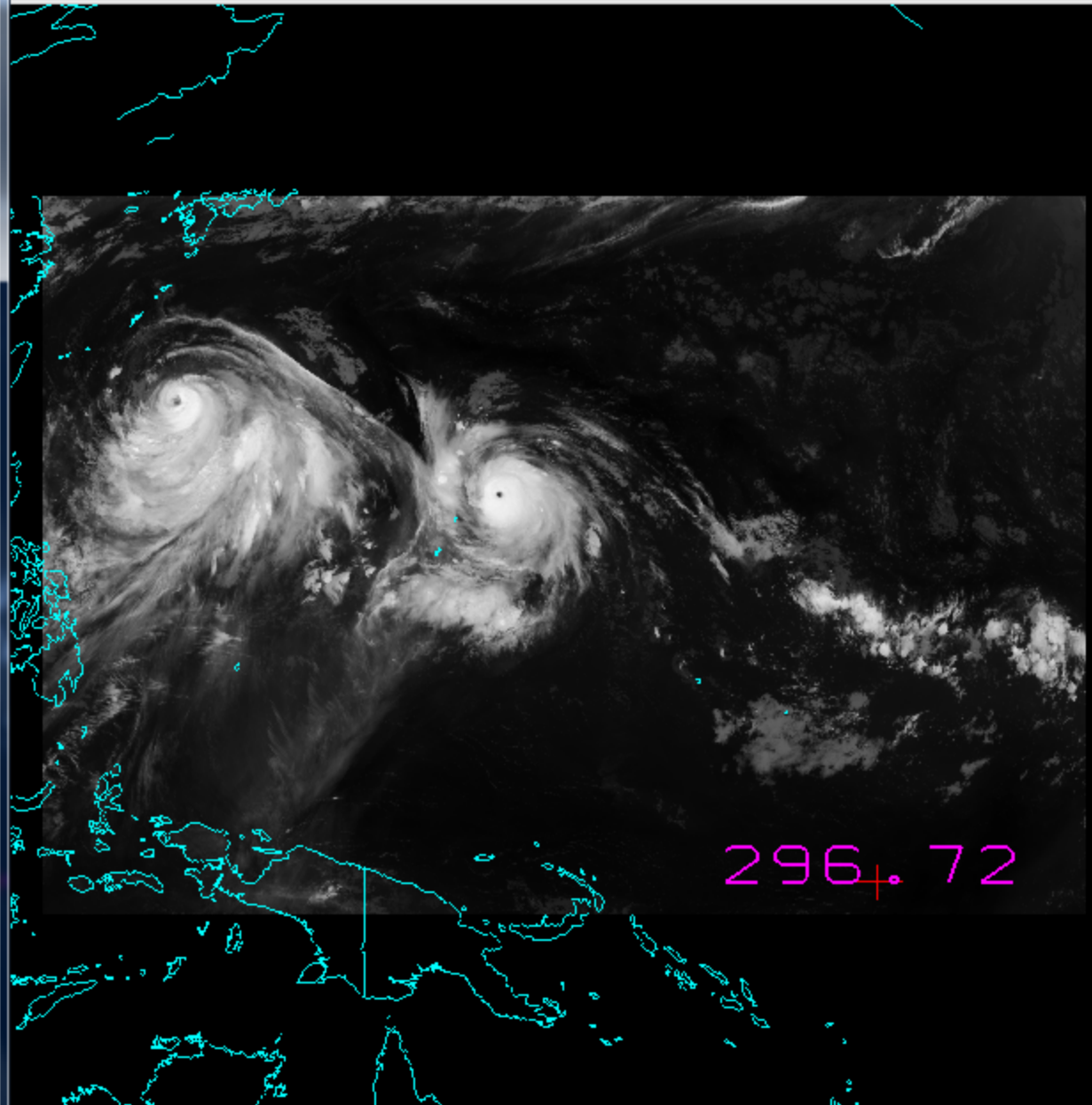
IRW AHI (left) & VIIRS (right)





2015/07/06 02:00 LST





Lon: 168.27 Lat: -3.40 Val: 296.72, 2015/07/08 16:20Z



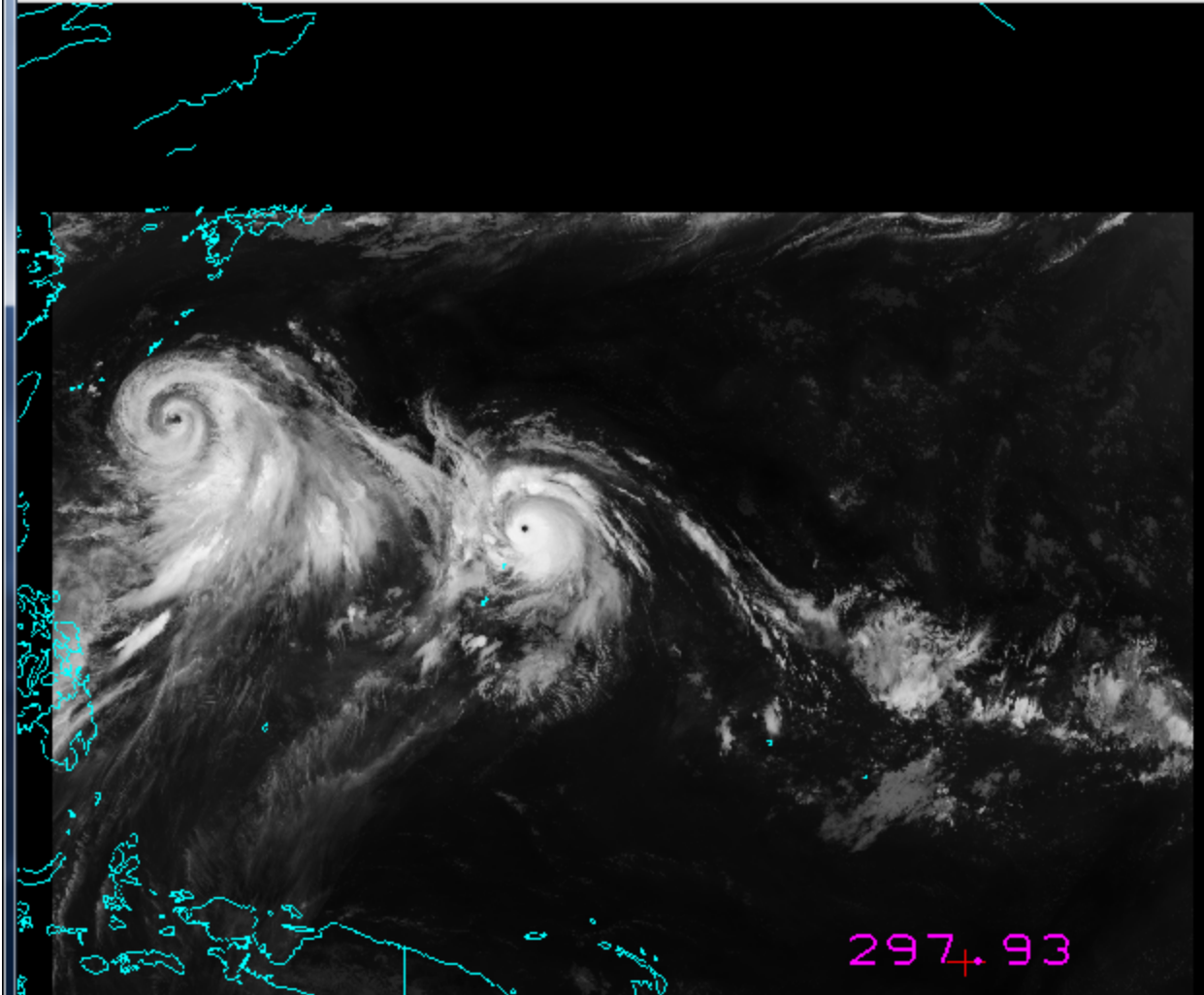
[1:B14+1:B14]-1:B15



1:B14



Tools Settings



Lon: 168.27 Lat: -3.40 Val: 297.93, 2015/07/09 00:00Z



2:B05

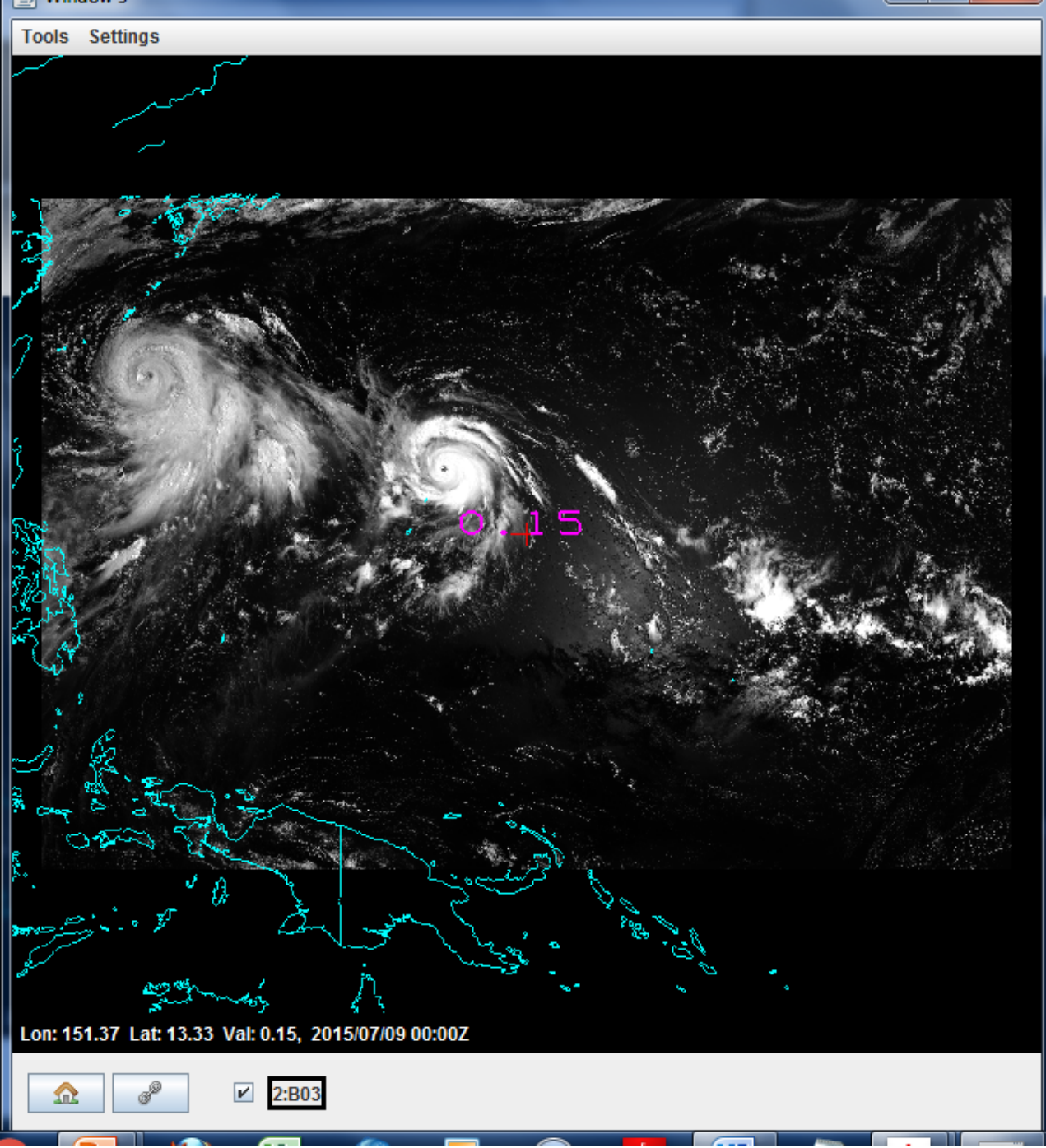


[2:B14+2:B14]-2:B15

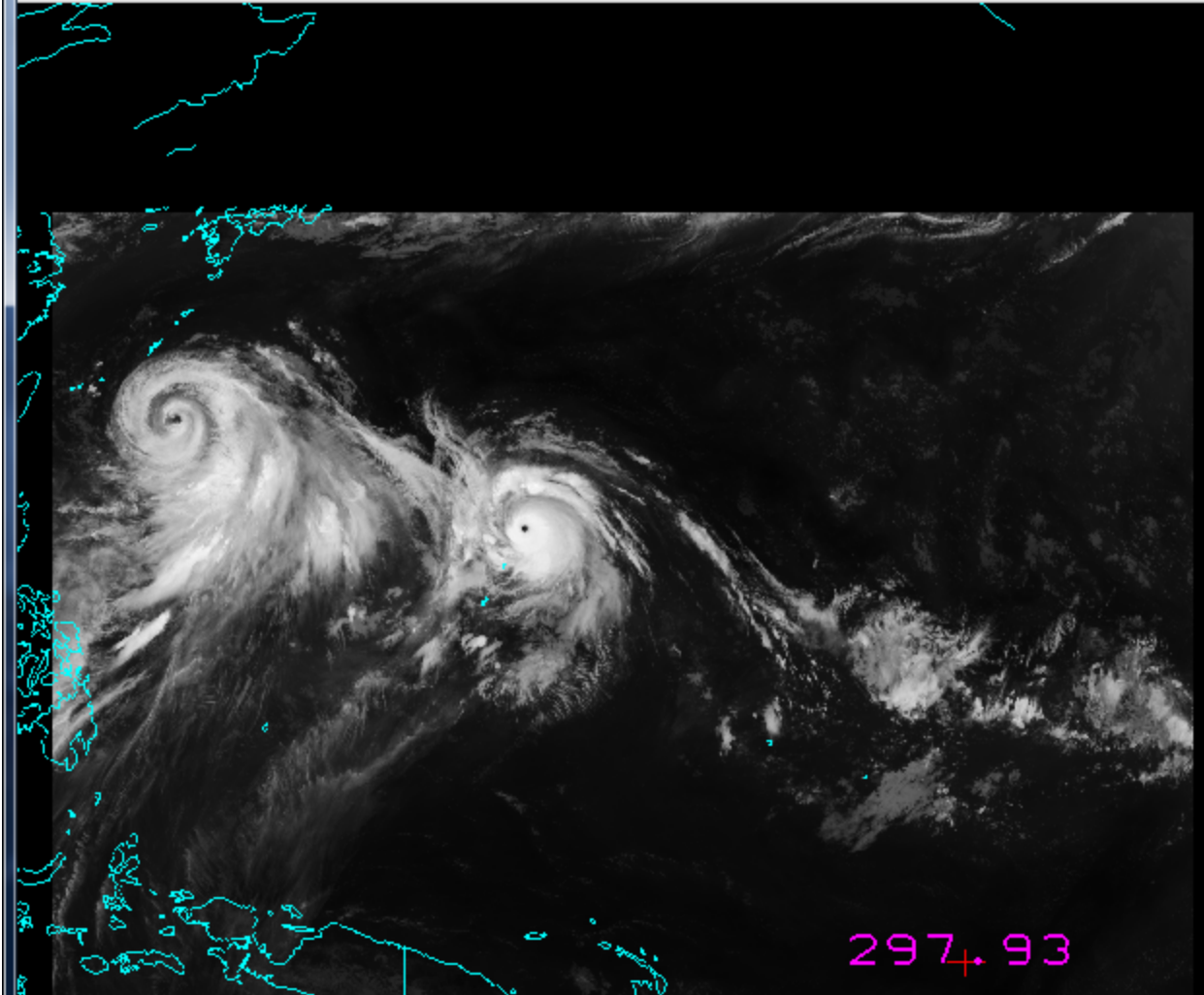


2:B14





Tools Settings



Lon: 168.27 Lat: -3.40 Val: 297.93, 2015/07/09 00:00Z



2:B05



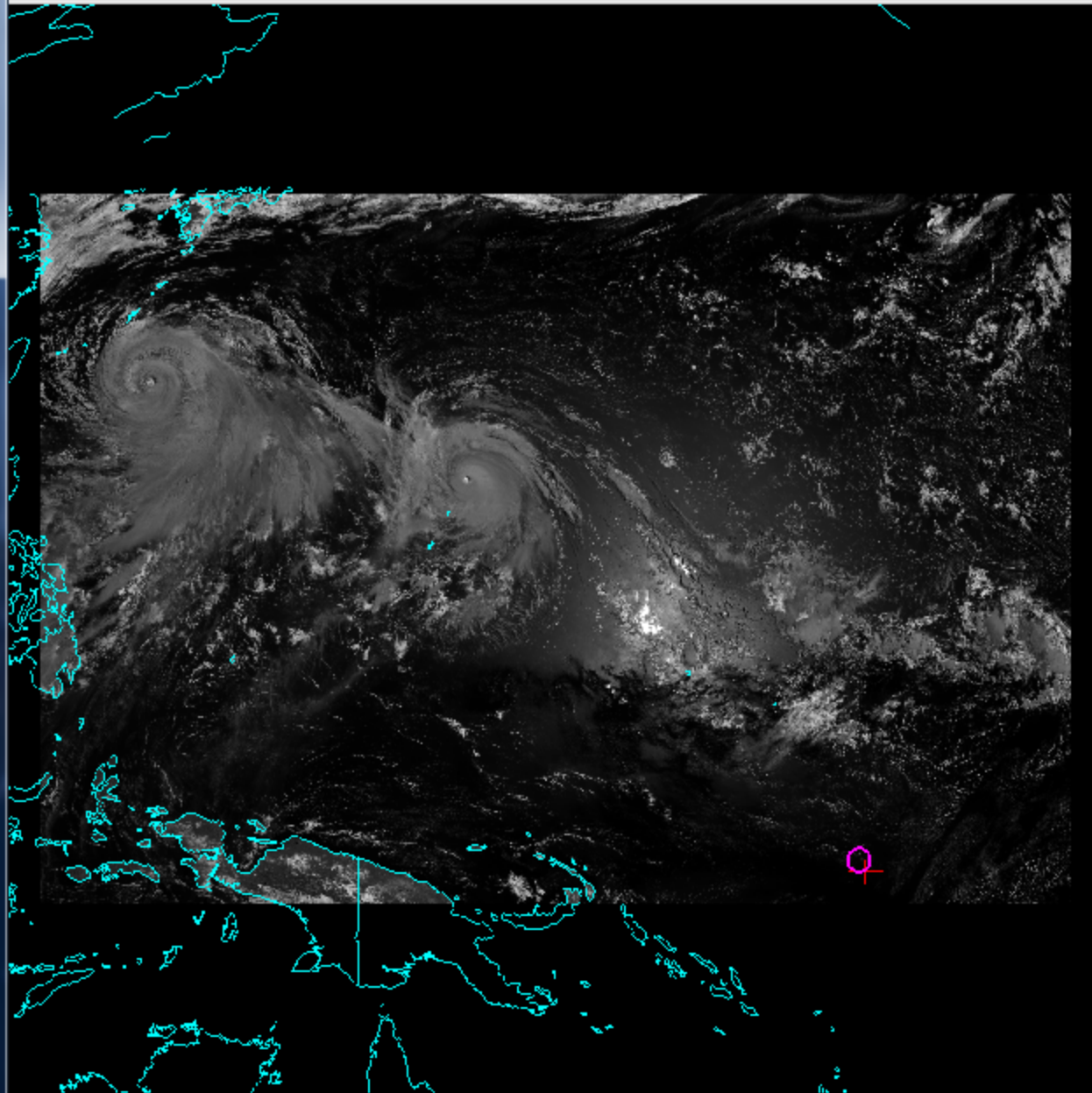
[2:B14+2:B14]-2:B15



2:B14



Tools Settings



Lon: 168.27 Lat: -3.40 Val: 0.00, 2015/07/09 00:00Z



2:B05



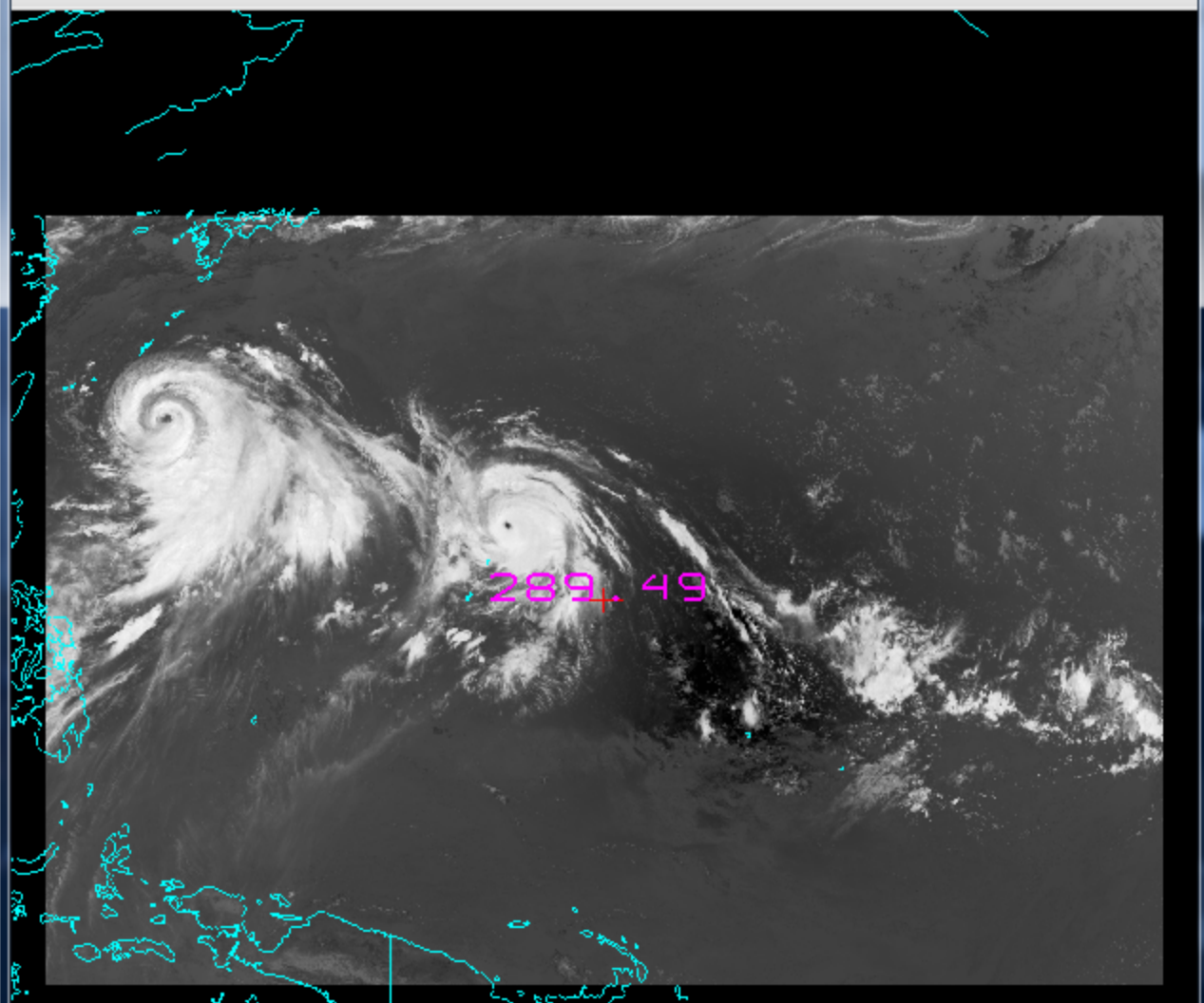
[2:B14+2:B14]-2:B15



2:B14



Tools Settings



289.49

Lon: 151.37 Lat: 13.33 Val: 289.49, 2015/07/09 00:00Z



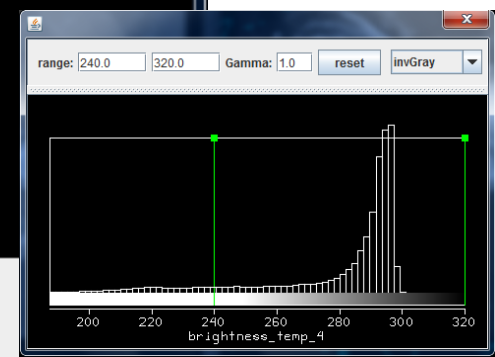
2:B07-2:B14



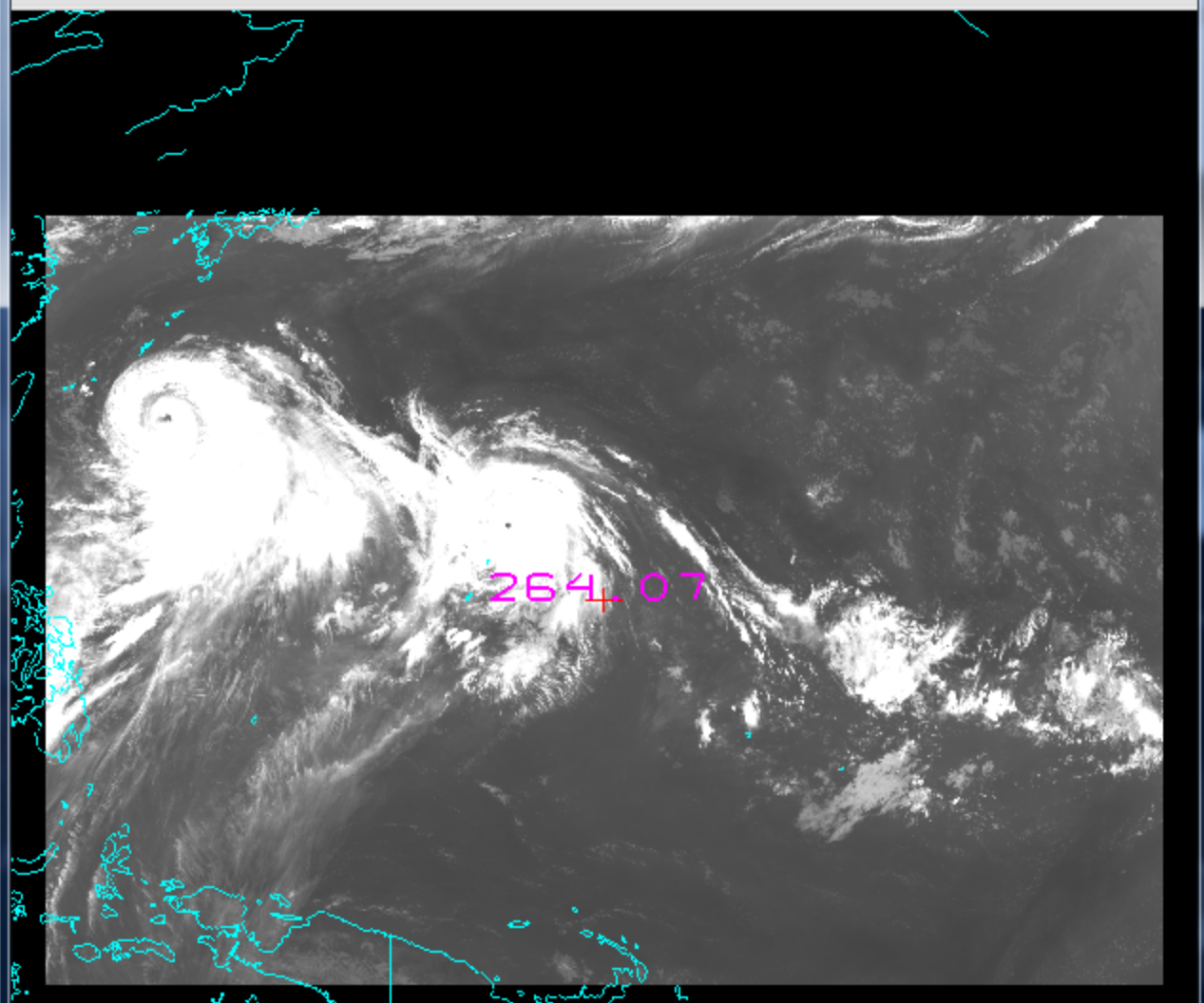
2:B14



2:B07



Tools Settings



Lon: 151.37 Lat: 13.33 Val: 264.07, 2015/07/09 00:00Z



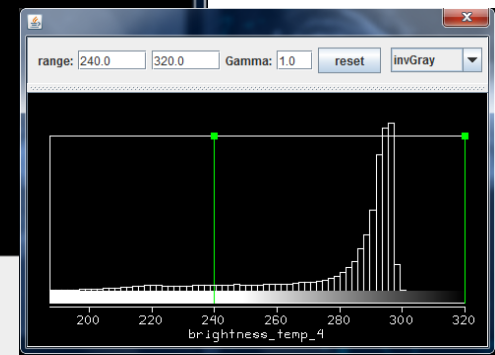
2:B07-2:B14



2:B14

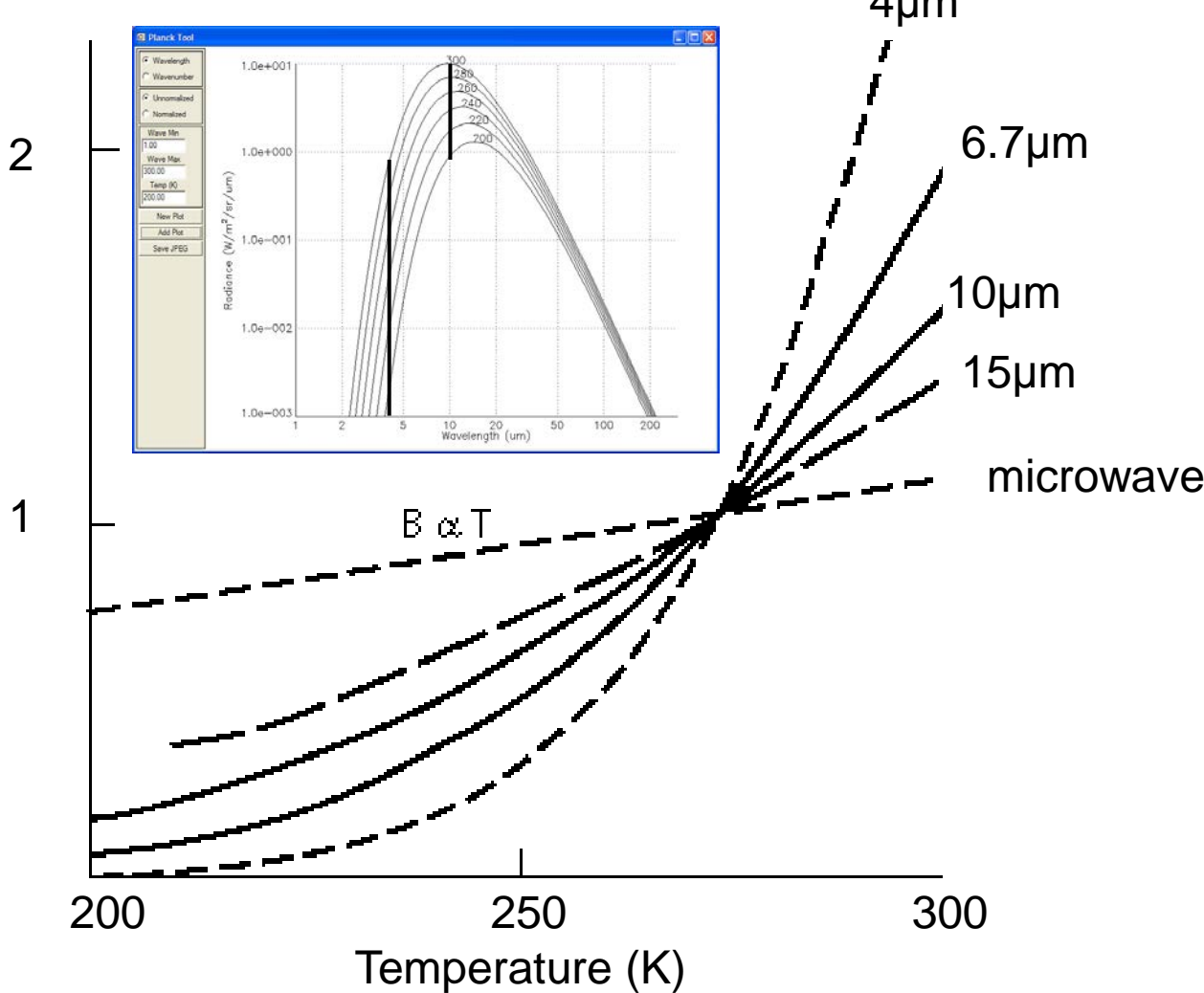


2:B07

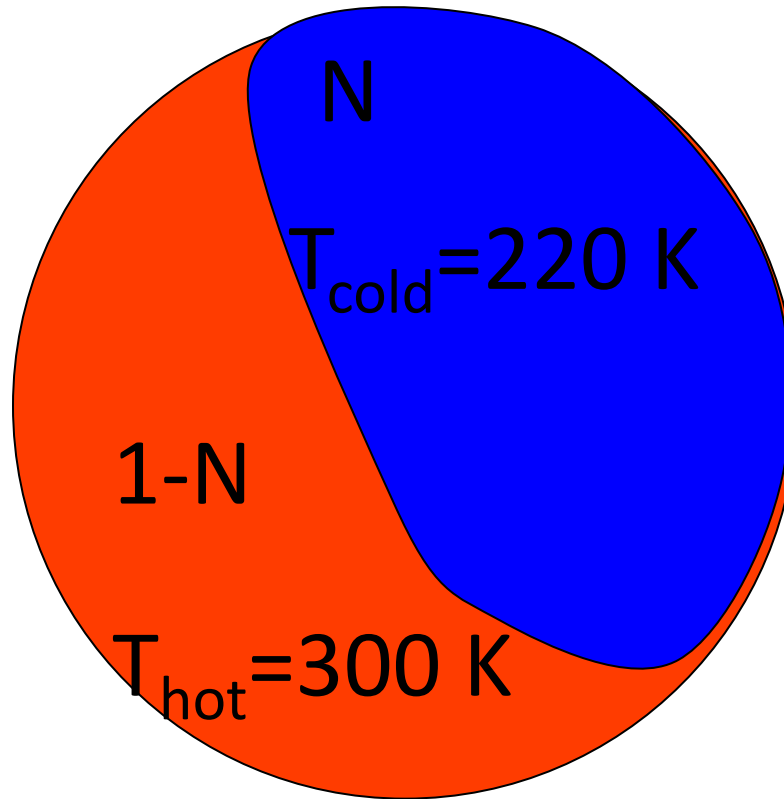


Temperature Sensitivity of $B(\lambda, T)$ for typical earth temperatures

$B(\lambda, T) / B(\lambda, 273K)$

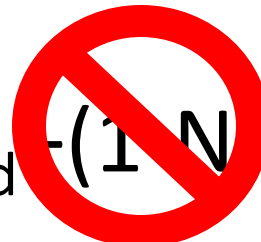


Non-Homogeneous FOV

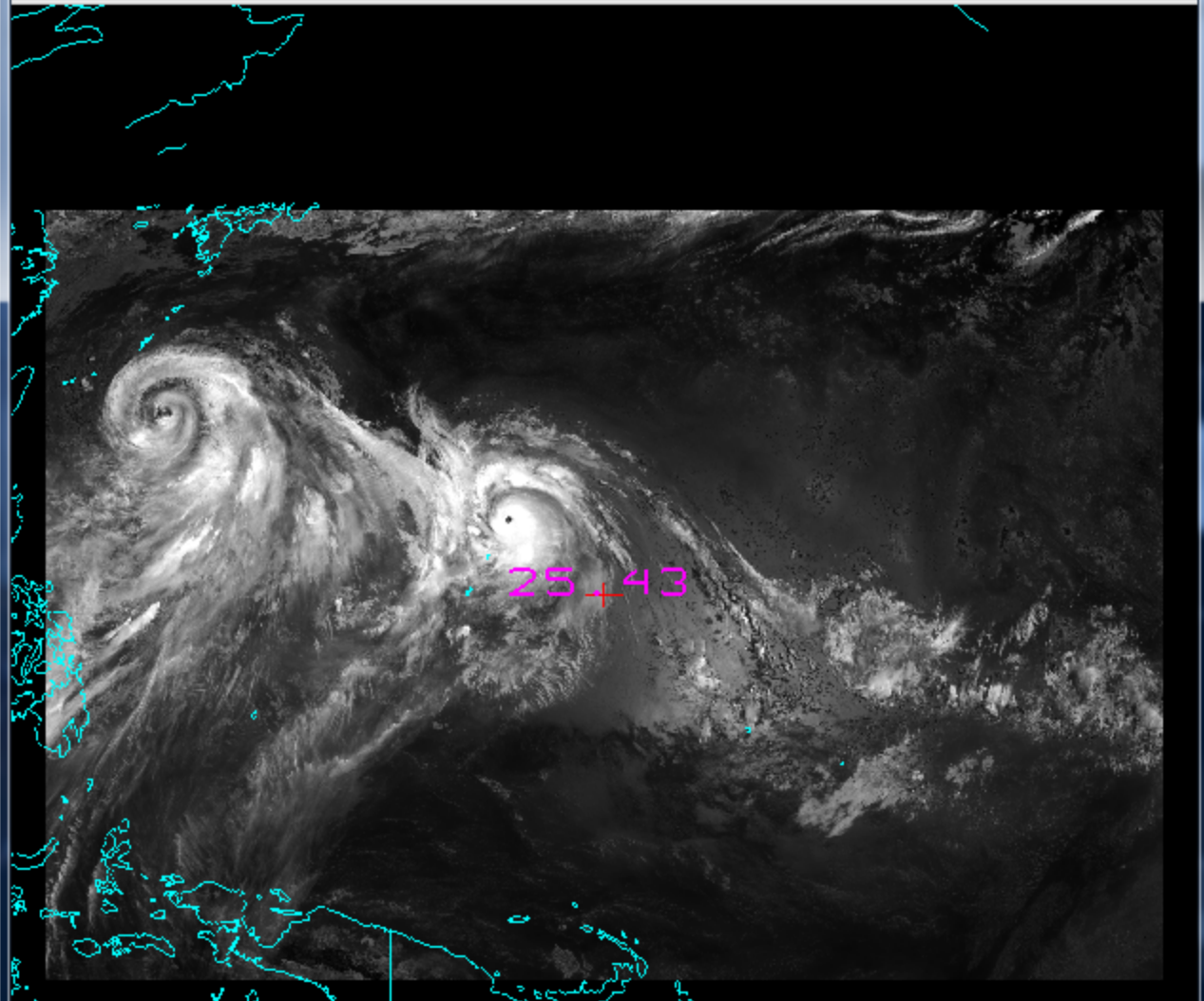


$$B=N \cdot B(T_{\text{cold}}) + (1-N) \cdot B(T_{\text{hot}})$$

$$BT=N \cdot T_{\text{cold}} - (1-N) \cdot T_{\text{hot}}$$



Tools Settings



Lon: 151.37 Lat: 13.33 Val: 25.43, 2015/07/09 00:00Z



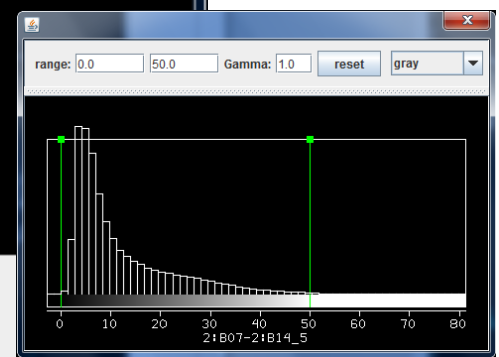
2:B07-2:B14



2:B14



2:B07



BT11=265K and BT4=290K.

What fraction of R4 is due to reflected solar radiance?

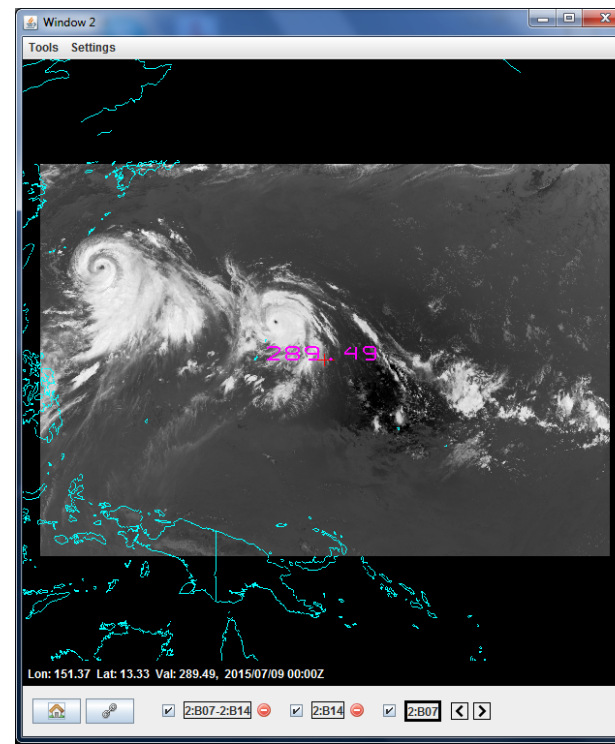
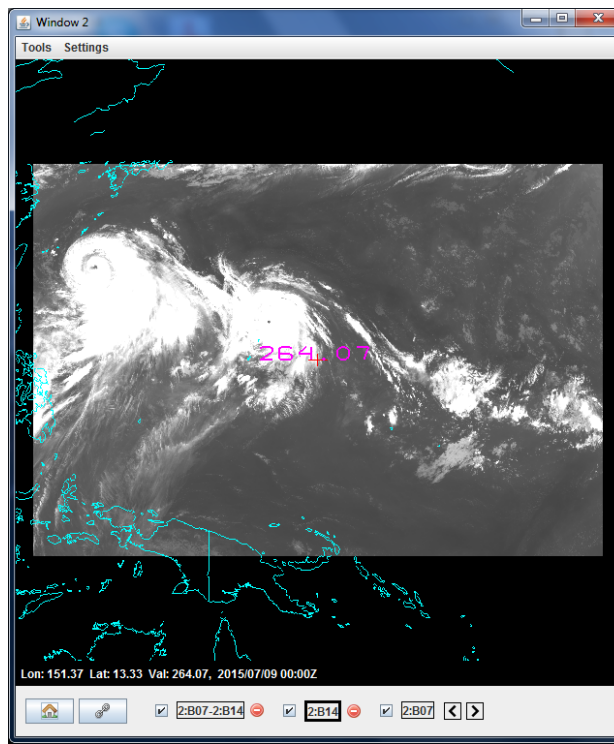
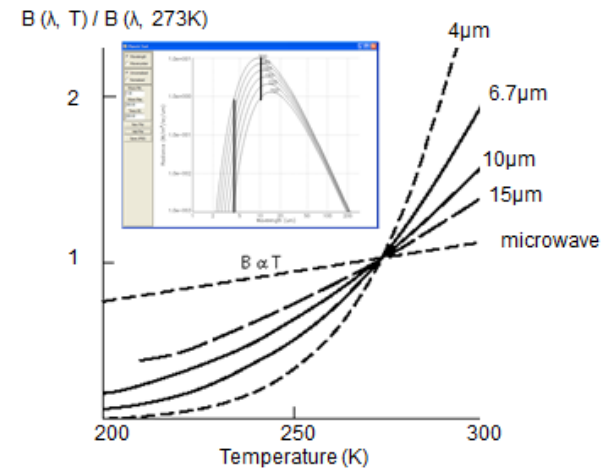
$$R_4 = R_4 \text{ refl} + R_4 \text{ emiss}$$

$$BT4 \text{ emiss} = BT11$$

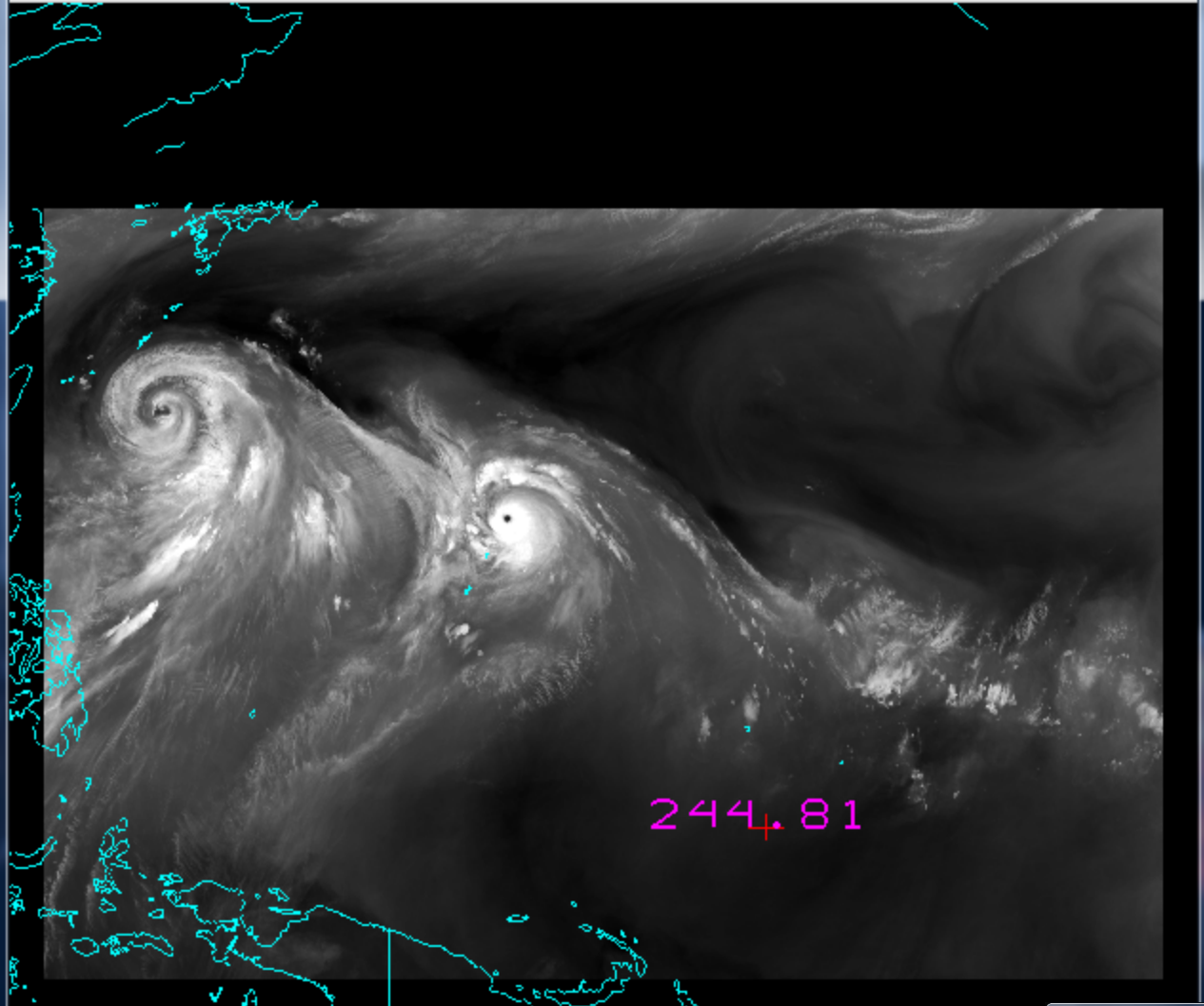
$$R_4 \sim T^{**12}$$

$$\text{Fraction} = [290^{12} - 265^{12}] / 290^{12} \sim .66$$

Temperature Sensitivity of $B(\lambda, T)$ for typical earth temperatures



Tools Settings



Lon: 158.94 Lat: 2.21 Val: 244.81, 2015/07/09 00:00Z



2:B08



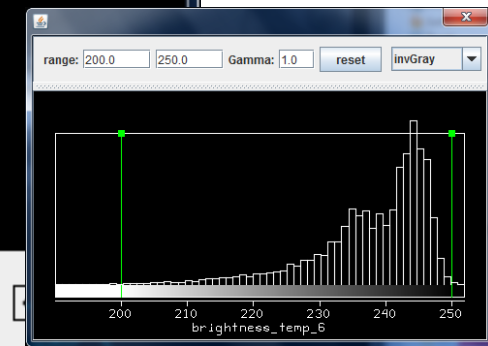
2:B07-2:B14



2:B14



2:B07



$$I_\lambda = \varepsilon_\lambda^{\text{sfc}} B_\lambda(T_{\text{sfc}}) \tau_\lambda(\text{sfc} - \text{top}) + \sum_{\text{layers}} \varepsilon_\lambda^{\text{layer}} B_\lambda(T_{\text{layer}}) \tau_\lambda(\text{layer} - \text{top})$$

The emission of an infinitesimal layer of the atmosphere at pressure p is equal to the absorption (1 - transmission). So,

$$\varepsilon_\lambda(\text{layer}) \tau_\lambda(\text{layer to top}) = [1 - \tau_\lambda(\text{layer})] \tau_\lambda(\text{layer to top})$$

Since transmission is multiplicative

$$\tau_\lambda(\text{layer to top}) - \tau_\lambda(\text{layer}) \tau_\lambda(\text{layer to top}) = -\Delta\tau_\lambda(\text{layer to top})$$

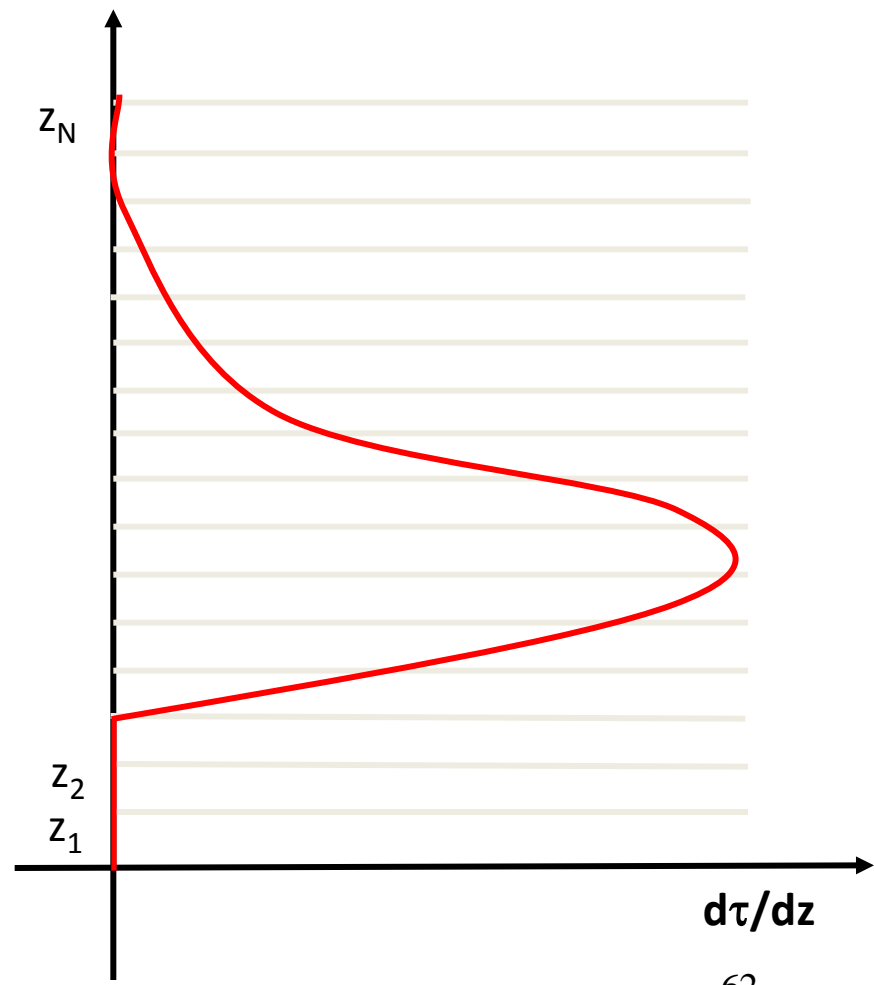
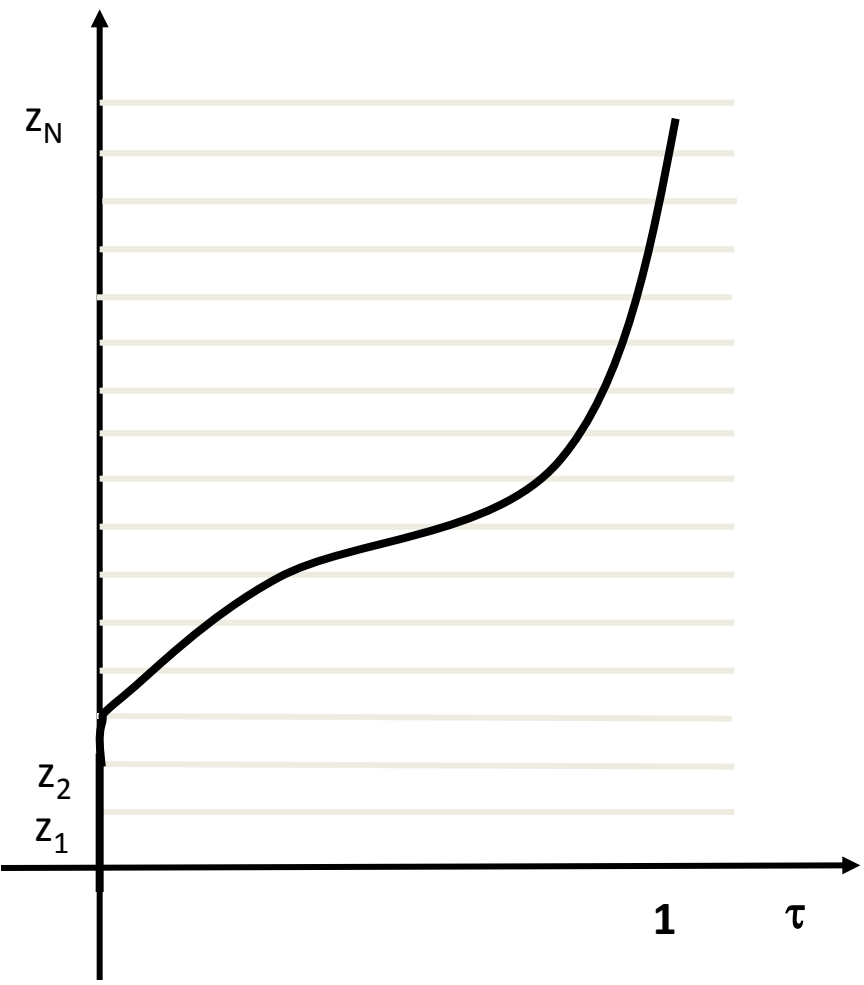
So we can write

$$I_\lambda = \varepsilon_\lambda^{\text{sfc}} B_\lambda(T(p_s)) \tau_\lambda(p_s) - \sum_p B_\lambda(T(p)) \Delta\tau_\lambda(p).$$

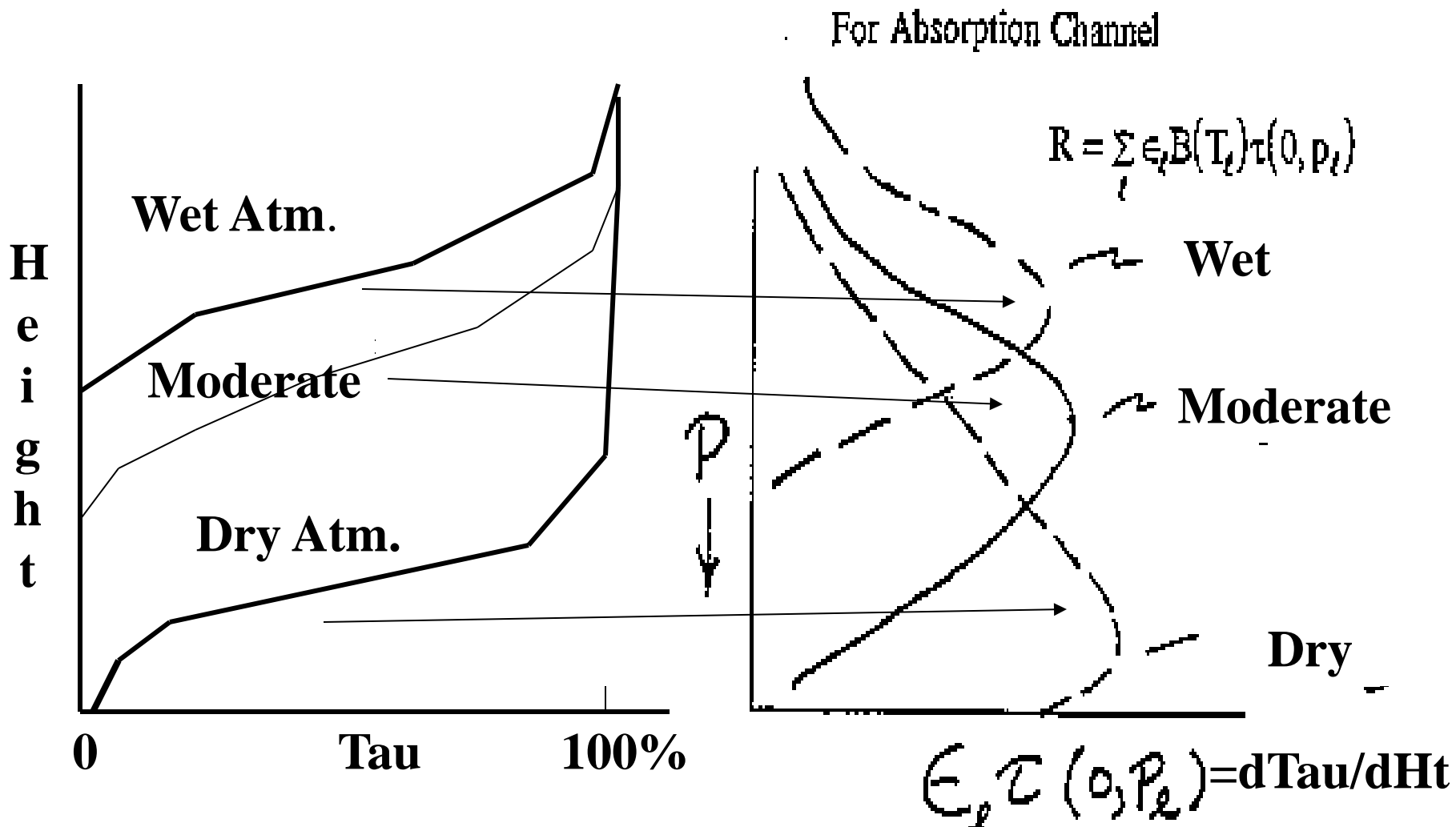
which when written in integral form reads

$$I_\lambda = \varepsilon_\lambda^{\text{sfc}} B_\lambda(T(p_s)) \tau_\lambda(p_s) - \int_0^{p_s} B_\lambda(T(p)) [d\tau_\lambda(p) / dp] dp.$$

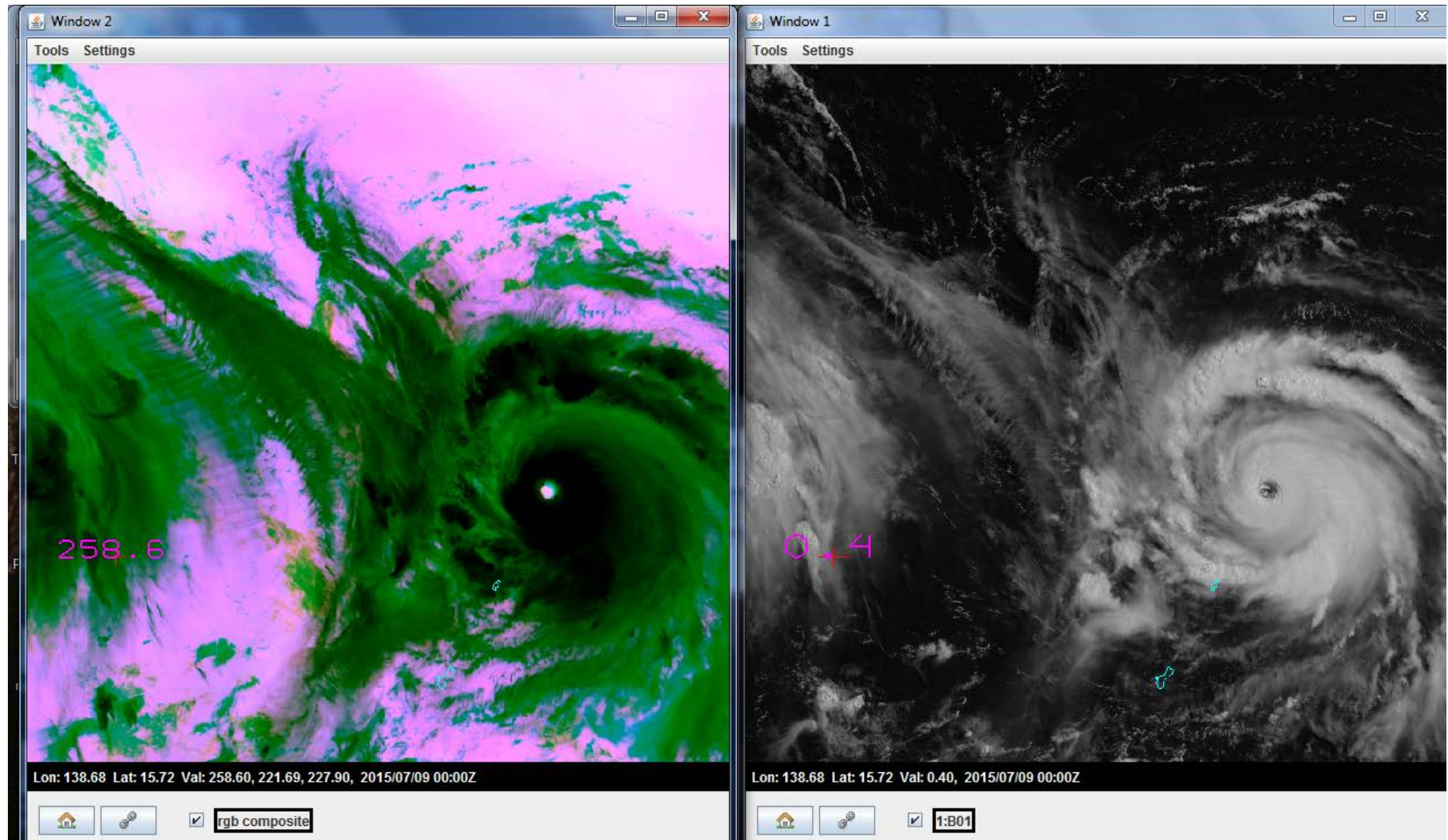
Weighting Functions



For a given water vapor spectral channel the weighting function depends on the amount of water vapor in the atmospheric column

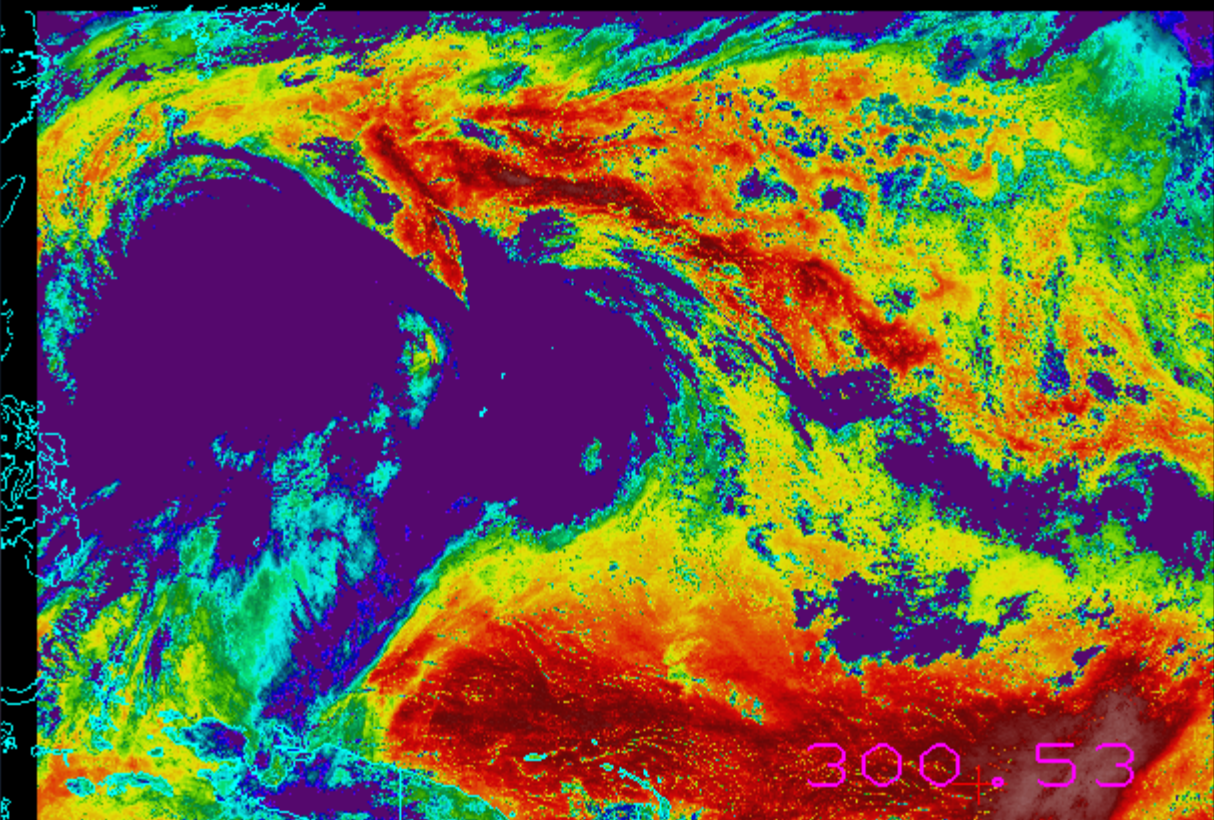


CO₂ is about the same everywhere, the weighting function for a given CO₂₆₃ spectral channel is the same everywhere



R-SWIRW, G-WV, B-LWIRW

Tools Settings



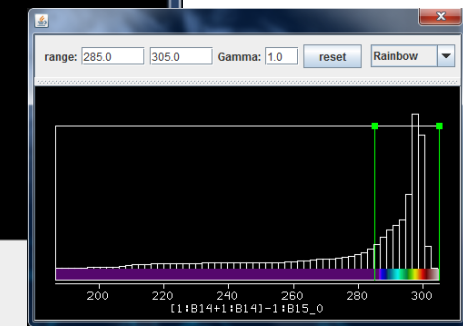
Lon: 168.27 Lat: -3.40 Val: 300.53, 2015/07/08 16:20Z



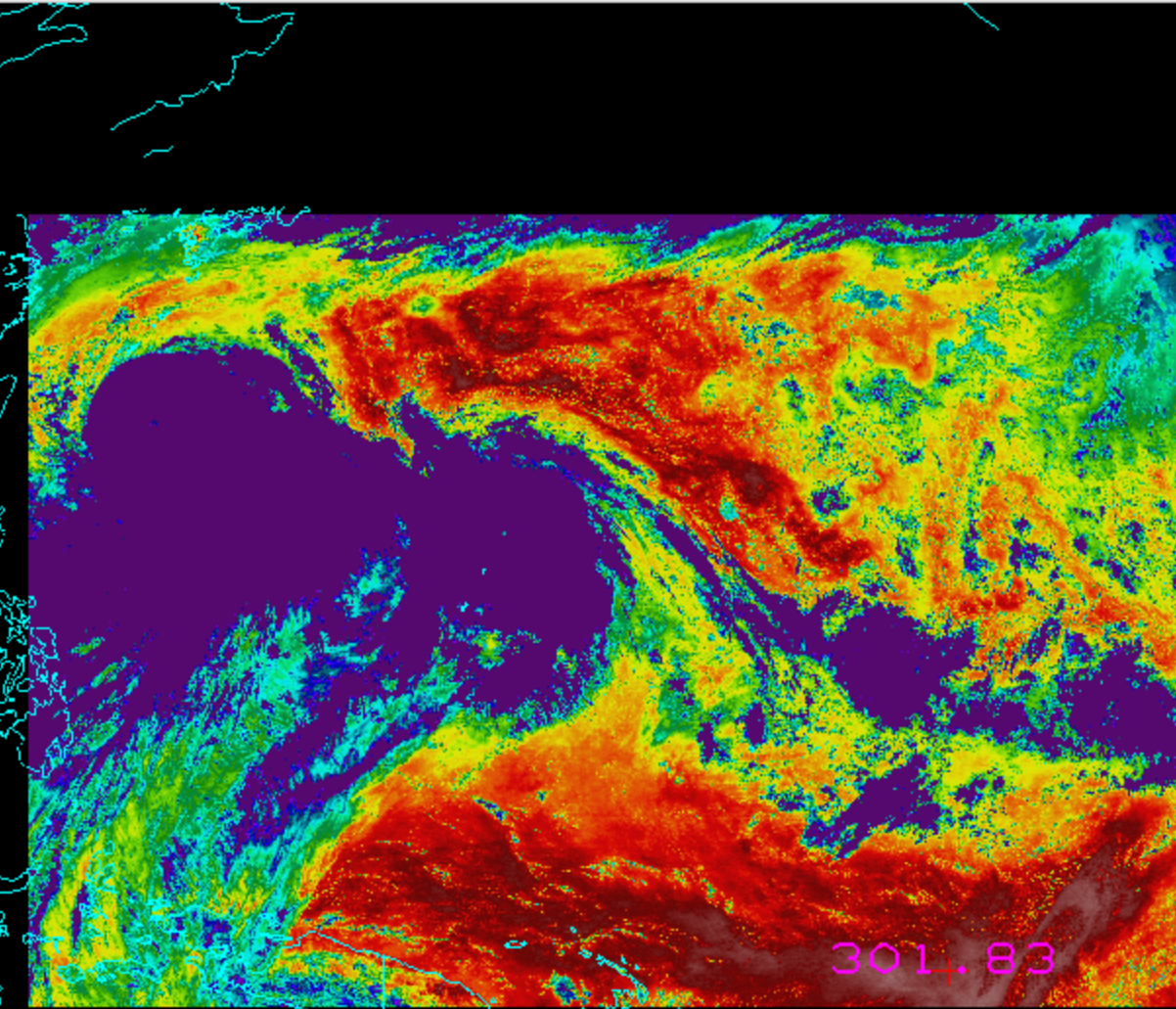
[1:B14+1:B14]-1:B15



1:B14



Tools Settings



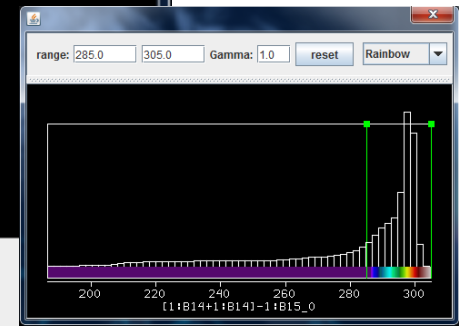
Lon: 168.27 Lat: -3.40 Val: 301.83, 2015/07/09 00:00Z



[2:B14+2:B14]-2:B15



2:B14



First Order Estimation of SST

Moisture attenuation in atmospheric windows varies linearly with optical depth.

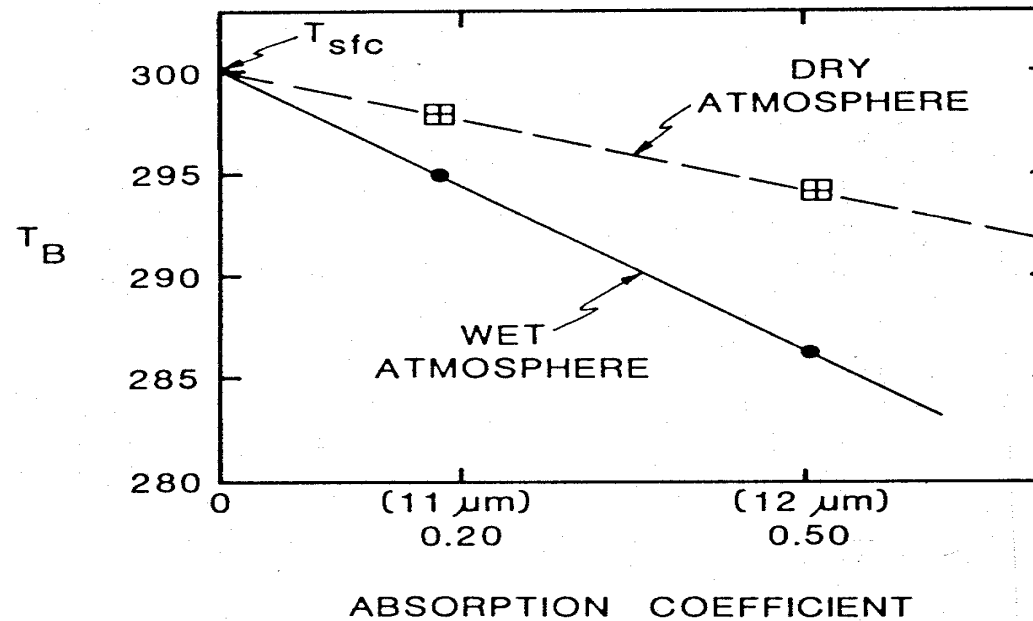
$$- k_\lambda u$$

$$\tau_\lambda = e^{-k_\lambda u} = 1 - k_\lambda u$$

For same atmosphere, deviation of brightness temperature from surface temperature is a linear function of absorbing power. Thus moisture corrected SST can inferred by using split window measurements and extrapolating to zero k_λ

$$T_s = T_{bw1} + [k_{w1} / (k_{w2} - k_{w1})] [T_{bw1} - T_{bw2}] = a_0 + a_1 T_{bw1} + a_2 T_{bw2} .$$

Moisture content of atmosphere can be inferred from slope of linear relation.



**REMOTE SENSING APPLICATIONS
WITH
METEOROLOGICAL SATELLITES**

by

W. Paul Menzel

**University of Wisconsin
Madison, WI**

November 2012

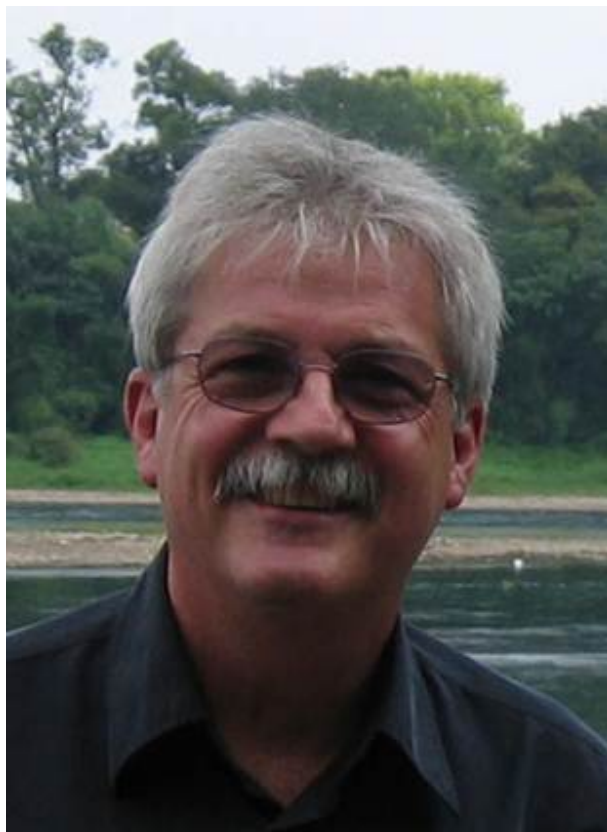
© 2012 W. Paul Menzel

TABLE OF CONTENTS

	Page
CHAPTER 1 - EVOLUTION OF SATELLITE METEOROLOGY	
1.1 Before Satellites	8
1.2 Evolution of the Polar Orbiting Satellites	8
1.3 The Geostationary Program	14
1.4 Data Processing Capability	17
1.5 Impact of Satellite Data on NWP	18
1.6 Summary	19
CHAPTER 2 - NATURE OF RADIATION	
2.1 Remote Sensing of Radiation	26
2.2 Basic Units	26
2.3 Definitions of Radiation	27
2.4 Historical Development of Planck's Radiation Law	29
2.5 Related Derivations	31
2.5.1 Wien's Displacement Law	31
2.5.2 Rayleigh-Jeans Radiation Law	32
2.5.3 Wien's Radiation Law	33
2.5.4 Stefan-Boltzmann Law	33
2.5.5 Brightness Temperature	34
CHAPTER 3 - ABSORPTION, EMISSION, REFLECTION, AND SCATTERING	
3.1 Absorption and Emission	41
3.2 Conservation of Energy	41
3.3 Planetary Albedo	42
3.4 Selective Absorption and Emission	42
3.5 Absorption (Emission) Line Formation	44
3.6 Vibrational and Rotational Spectra	46
3.7 Summary of Interactions between Radiation and Matter	47
3.8 Beer's Law and Schwarzschild's Equation	48
3.9 Atmospheric Scattering	51
3.10 The Solar Spectrum	52
3.11 Composition of the Earth's Atmosphere	53
3.12 Atmospheric Absorption and Emission of Solar Radiation	53
3.13 Atmospheric Absorption and Emission of Thermal Radiation	54
3.14 Atmospheric Absorption Bands in the IR Spectrum	55
3.15 Atmospheric Absorption Bands in the Microwave Spectrum	56
3.16 Remote Sensing Regions	56
CHAPTER 4 - THE RADIATION BUDGET	
4.1 The Mean Global Energy Balance	67
4.2 The First Satellite Experiment to Measure Net Radiation	67
4.3 The Radiation Budget	69
4.4 Distribution of Solar Energy Intercepted by the Earth	70
4.5 Solar Heating Rates	71
4.6 Infrared Cooling Rates	71
4.7 Radiative Equilibrium in a Gray Atmosphere	72
CHAPTER 5 - THE RADIATIVE TRANSFER EQUATION (RTE)	
5.1 Derivation of RTE	78
5.2 Temperature Profile Inversion	82
5.3 Transmittance Determinations	83
5.4 Fredholm Form of RTE and Direct Linear Inversion	84
5.5 Linearization of the RTE	86
5.6 Statistical Solutions for the Inversion of the RTE	87
5.6.1 Statistical Least Squares Regression	87
5.6.2 Constrained Linear Inversion of RTE	87
5.6.3 Statistical Regularization	89
5.6.4 Minimum Information	90
5.6.5 Empirical Orthogonal Functions	90
5.7 Numerical Solutions for the Inversion of the RTE	95
5.7.1 Chahine Relaxation Method	95
5.7.2 Example Problem Using Relaxation Method	97
5.7.3 Smith's Iteration	99
5.7.4 Example Problem Using Smith's Iteration	100
5.7.5 Comparison of Chahine & Smith Iteration Solution	102
5.8 Direct Physical Solution	103
5.8.1 Solving Linear RTE Direct	103
5.8.2 Simultaneous Direct Physical Solution of the RTE	104
5.9 Water Vapor Profile Solutions	107
5.10 Microwave Form of RTE	108
CHAPTER 6 - DETECTING CLOUDS	
6.1 RTE in Cloudy Conditions	113
6.2 Inferring Clear Sky Radiances in Cloudy Conditions	114
6.3 Finding Clouds	116
6.3.1 Threshold Tests for Finding Cloud	116
6.3.2 Spatial Uniformity Tests to Find Cloud	122
6.4 The Cloud Mask Algorithm	123
6.4.1 Thick High Clouds	124
6.4.2 Thin Clouds	124
6.4.3 Low Clouds	124
6.4.4 Thin High Clouds	125
6.4.5 Ancillary Data Requirements	125
6.4.6 Implementing the Cloud Mask Algorithms	126
6.4.7 Clear Sky Composite Maps	127
6.5 Cloud Properties Derived in a MODIS Granule	127
6.5.1 Cloud Masking	127
6.5.2 Cloud Thermodynamic Phase	128
6.5.3 Cloud Top Pressure and Effective Cloud Amount	129
6.5.4 Detection of UT/LS Clouds	129
6.5.5 Cloud Optical and Microphysical Properties	131
6.5.6 Detection of Multi-layered Clouds	131
6.5.7 Global Gridded Products	132

<ftp://ssec.wisc.edu/pub/menzel>

Arigatō



paulm@ssec.wisc.edu